LIDAR PLACEMENT OPTIMIZATION USING A MULTI-CRITERIA APPROACH

by

Zainab Abidemi Saka

A Thesis

Submitted to the Faculty of Purdue University

In Partial Fulfillment of the Requirements for the degree of

Master of Science in Civil Engineering

Lyles School of Civil Engineering

West Lafayette, Indiana

December 2023

THE PURDUE UNIVERSITY GRADUATE SCHOOL
STATEMENT OF COMMITTEE APPROVAL

Dr. Samuel Labi, Chair
Lyles School of Civil Engineering

Dr. Yiheng Feng
Lyles School of Civil Engineering

Dr. Joseph Sinfield
Lyles School of Civil Engineering

Approved by:
Dr. Dulcy Abraham

Dedicated to my parents, Mr. Muritala Saka and Mrs. Idayat Saka, whose prayers have reflected consistently in my life journey.

ACKNOWLEDGMENTS

I begin by returning all praise and adoration to Almighty Allah for the grace bestowed upon me even when I had the smallest faith.

I extend my heartfelt appreciation to my supervisor, Professor Samuel Labi, for his unwavering guidance, support, and invaluable insights, which have not only advanced my research but have also been instrumental in shaping my entire journey through graduate school. His kindness has played a significant role in my professional growth, academic success, and overall experience.

My gratitude also extends to the members of my thesis committee, Dr. Yiheng Feng, and Dr. Joseph Sinfield, for their feedback, and helpful suggestions. Their expertise and scholarly input have greatly enhanced the quality of this research.

Special thanks are due to the members of the Black and Gold Autonomous Racing, Digital Photogrammetry Research Group, my colleagues in Geomatics and Transportation, and my family and friends, especially Light and Khadijah. Their unwavering support, encouragement, and steadfast belief in my abilities have served as pillars of strength through the highs and lows of my graduate school journey. Each of you has left an indelible mark, and I am profoundly grateful for your enduring presence in my life.

Furthermore, I extend my heartfelt appreciation to the Center for Connected and Automated Transportation (CCAT) at Purdue. The generous funding provided by CCAT, under Grant No. 69A3551747105 from the U.S. Department of Transportation, Office of the Assistant Secretary for Research and Technology (OST-R), through the University Transportation Centers Program, has been instrumental in facilitating this research. I am also grateful to the Purdue Lyles School of Civil Engineering for the Ross Fellowship, which significantly eased the pursuit of my academic endeavors.

In conclusion, this thesis would not have come to fruition without the collective support, encouragement, and contributions of individuals who served as a source of strength for me, at various points of my graduate school journey. Thank you all. *E seun, modupe* (Thank you, I am grateful). I understand that this journey would not have been possible without the grace of Almighty Allah. Alhamdulillah.

TABLE OF CONTENTS

LIST OF TABLES

LIST OF FIGURES

LIST OF ABBREVIATIONS

2D LiDAR:	Two-dimensional LiDAR sensor
3D LiDAR:	Three-dimensional LiDAR sensor
ADAS:	Advanced Driver Assistance Systems
AHP:	Analytical Hierarchy Process
AV:	Autonomous Vehicle
CARLA:	Car Learning to Act
CILOS:	Criterion Impact Loss
DM:	Decision Maker
DR:	Direct Rating
ELECTRE:	ELimination Et Choix Traduisant la REalité
GNSS:	Global Navigation Satellite System
GPS:	Global Positioning System
IMU:	Inertial Measurement Unit
LiDAR:	Light Detection and Ranging
LOB:	Local Occupancy Board
LOG:	Local Occupancy Grid
MAUT:	Multi-attribute Utility Theory
MCDA:	Multi Criteria Decision Analysis
MCDM:	Multi Criteria Decision Making
MOO:	Multi-Objective Optimization
NHTSA:	National Highway Traffic Safety Administration
PA:	Point Allocation
POG:	Probabilistic Occupancy Grid

Python API:	Python Application Programming Interface
RADAR:	Radio Detection and Ranging
ROI:	Region of Interest
SIMOS:	Structured Importance-Performance Multi-Objective Screening
SONAR:	Sound Navigation and Ranging
TOF:	Time of Flight
TOPSIS:	Technique for Order Preference by Similarity to Ideal Solution
V2I:	Vehicle-to-Infrastructure
WSM:	Weighted Sum Method
WPM:	Weighted Product Method

LIST OF COMMONLY USED TERMS

Amalgamation: The combining or integration, for each design alternative, of multiple evaluation factors or criteria (each duly weighted) to form a unified evaluation outcome.

Blindspot Region: The area around a vehicle or sensor where objects or obstacles are not directly visible or detectable, posing a potential hazard due to limited visibility.

Decision Maker: An individual, group, or system responsible for making choices or decisions, often based on specified criteria or objectives.

Ego Vehicle: In autonomous vehicle terminology, it refers to the vehicle itself—often used as a reference point or perspective in sensing and decision-making within the vehicle's environment.

LiDAR Placement Design: The strategic positioning or arrangement of LiDAR sensors on a vehicle or within an environment to optimize data collection or detection capabilities.

Multi-Criteria Decision Analysis: A decision-making methodology involving the systematic evaluation of multiple criteria or factors to support complex decision-making processes.

Point Density: Refers to the number of data points or measurements collected within a given area by sensors like LiDAR, indicating the level of detail or resolution in capturing information about the environment.

Scaling: The process of transforming or adjusting values within a specific range or proportion to facilitate comparisons or integration of diverse factors or criteria.

Sensing Target: The object or entity being detected, observed, or measured by sensors, such as LiDAR, in the surrounding environment.

Value Function: A mathematical or conceptual representation used to assess or quantify the value or utility of different alternatives or criteria in decision-making processes.

Weighting: Assigning relative importance or significance to different factors or criteria in a decision-making process, influencing their impact on the overall outcome.

ABSTRACT

Most road fatalities are caused by human error. To help mitigate this issue and enhance overall transportation safety, companies are turning to advanced driver assistance systems and autonomous vehicle development. Perception, a key module of these systems, mostly uses light detection and ranging (LiDAR) sensors and enables object detection and environmental mapping. Extensive research on the use of LiDAR for autonomous driving has been documented in the literature. Yet still, several researchers and practitioners have advocated continued investigation of LiDAR placement on autonomous vehicles. To address this research need, this thesis begins with a comprehensive review of sensor technologies – camera, radio detection and ranging, global positioning system, and inertial measurement units – and exploring their strengths and limitations. Next, the thesis developed a methodological multiple criteria framework and implemented it in LiDAR placement optimization. Given the numerous criteria and placement alternatives associated with LiDAR placement, multi-criteria decision analysis (MCDA) was identified as an effective tool for LiDAR placement. MCDA has been applied to some extent in decision making regarding autonomous vehicle development. However, its application in LiDAR placement optimization remains unexplored. In evaluating the LiDAR placement alternatives, the research first established the placement alternatives and then developed a diverse set of criteria – point density, blind spot regions, sensor cost, power consumption, sensor redundancy, ease of installation, and aesthetics. The data collection methods included CARLA simulator, sensor datasheets, and questionnaire surveys. The relative importance among the evaluation criteria was established using weighting approaches such as respondent-assigned weighting, equal weighting, and randomly generated weighting. Then, to standardize the different measurement units, scaling was carried out. Finally, the weighted and scaled criteria measures were amalgamated to obtain the overall evaluation score for each alternative LiDAR placement design. This enabled ranking of the placement designs and identification of the best and worst performing designs. Hence, the optimization method used is the enumeration technique. The findings of this study serve as a reference for future similar efforts that seek to optimize LiDAR placements based on select criteria. Further, it is expected that the thesis's framework will contribute to enhanced understanding of the overall impact of LiDAR placement on autonomous vehicles, thus, enabling the cost-effective design of their placement and, ultimately, improving AV operational outcomes including traffic safety.

CHAPTER 1. INTRODUCTION

1.1 Study Background

Safety is an essential aspect of any transportation system and continues to be a critical issue in current times. Road traffic accidents lead to significant loss of life and cause injuries to millions of people annually. According to a recent technical report published by the National Highway Traffic Safety Administration (NHTSA), the number of people killed in traffic accidents involving motor vehicles in 2021 was 10.5% higher than the number recorded in 2020. The vast majority of fatalities are caused by human error such as excessive speeding, drinking, and driving, and failing to wear seat belts (NHTSA, 2021).

In addition to safety concerns, transportation systems globally face significant challenges related to congestion. Rapid urbanization and increasing populations have led to a surge in the number of vehicles on the roads, which has resulted in traffic congestion predominantly in urban areas (USDOT, 2022). Such congestion not only causes commuter delays and frustration but also contributes to increased fuel consumption and air pollution (FHWA, 2005).

As travel amounts increase, the existing infrastructure often struggles to cope with this increase in demand. It is often the case that existing roads were designed to accommodate contemporaneous traffic volumes. This leads to insufficient capacity, which hinders efficient transportation operations and increases the risk of accidents (US EPA, 2022).

Transportation is also a major contributor to greenhouse gas emissions, air pollution, and climate change. Fossil fuel-powered vehicles emit carbon dioxide and other harmful pollutants that have a significant impact on air quality and contribute to global warming. The need to reduce the transportation sector's environmental footprint is a pressing concern for both policymakers and the public (US EPA, 2015).

Nonetheless, access to reliable and efficient transportation is crucial for socioeconomic development and individual well-being. However, certain populations, such as low-income communities and people with disabilities, often face challenges accessing transportation services. Lack of transportation options can limit access to education, employment, healthcare, and essential goods and services, thus exacerbating existing social and economic disparities (Morency et al., 2012).

As a result, transportation engineers, stakeholders, and policy makers continue to seek solutions to persistent problems concerning road safety, congestion, environmental sustainability, and equity. They might also pave the way for a more inclusive and equitable transportation system, ensuring that all individuals, regardless of their backgrounds or abilities, have access to vital services and opportunities.

1.2 Study Motivation

The automotive industry, an important stakeholder in transportation development, has been working on a variety of advanced driver assistance systems (ADAS) to address transportation safety and mobility concerns. ADAS integrates diverse subsystems within a vehicle to facilitate driver assistance through the implementation of various functions. Contemporary automotive technology has allowed the integration of particular features (such as blind spot recognition, lane departure warnings, adaptive cruise control, and automatic emergency braking) into operational vehicles. Common sensor types used in ADAS include cameras, light detection and ranging (LiDAR), radar, and ultrasonic sensors. ADAS continue to advance and are expected to direct the eventual realization of autonomous driving.

As defined by the Society for Automotive Engineers (SAE), vehicles that have no ADAS are considered level 0 vehicles, whereas vehicles that have some form of driver assistance are considered to be level 1 vehicles (SAE, 2021; Figure 1.1).

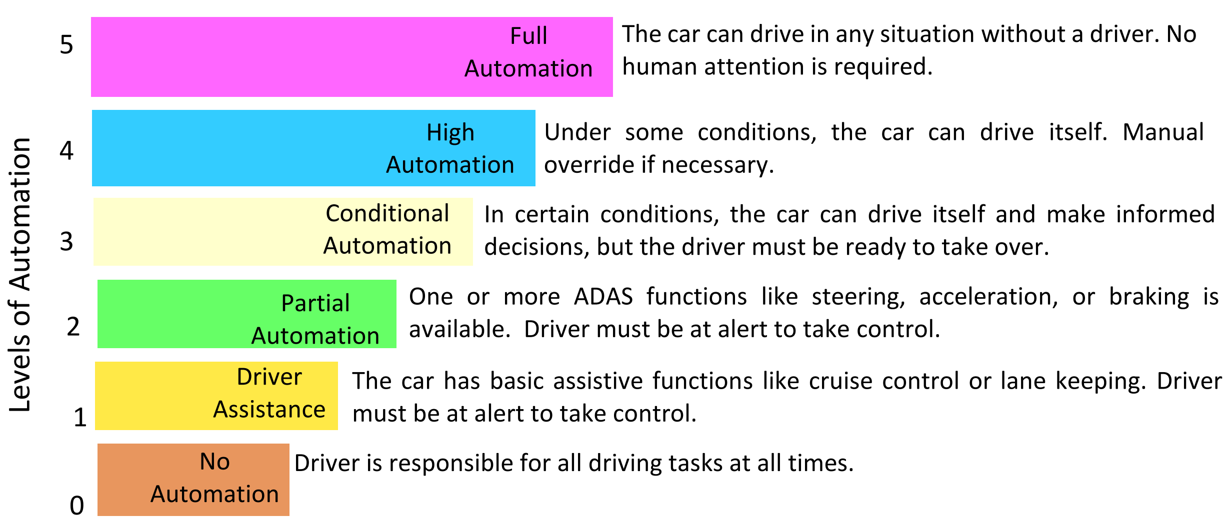

Figure 1.1: Autonomous Driving Levels according to SAE (SAE, 2021)

Accordingly, the progression from one level of autonomy to the next necessitates additional study and development in a variety of fields, including sensor technologies (Kukkala et al., 2018). LiDAR is an important sensor in ADAS and is crucial for the development of autonomous driving systems and pedestrian and passenger safety. The vehicle's onboard computer uses data from the LiDAR sensor to make real-time judgments to safely navigate the roadway. Any error or malfunction in the LiDAR sensors could result in hazardous situations, thus, underscoring the importance of research that improves LiDAR technology.

As the development of autonomous vehicles (AVs) progresses, considerable difficulties in the technology and regulations related to testing and deployment have yet to be overcome. Even though AVs have the potential to improve road safety by eliminating human driving error (Curto et al., 2021; Guo et al., 2021; Shetty et al., 2021), it is extremely important to ensure that they are thoroughly tested and validated before such vehicles are allowed on public roads. This testing also includes evaluating the performance of the various sensors that provide the vehicle with some level of autonomy.

To this end, this thesis is motivated by the potential benefits that AVs could contribute to road users and society in general. First, AVs could transform transportation by drastically reducing the number of accidents and fatalities that occur on the roads. Combs et al. (2019) confirmed that AVs could minimize the number of pedestrian deaths and injuries. Human error has been identified as one of the leading causes of accidents (NHTSA, 2020), and AVs can remove or reduce the element of human error (NHTSA, 2021), thus, significantly impacting the number of traffic accidents. In addition to enhancing safety, AVs also reduce fuel consumption and carbon emissions and other environmental threats (Szűcs & Hézer, 2022).

Furthermore, AVs could yield significant benefits for a broad spectrum of travelers and road users in terms of health and overall quality of life. AVs facilitate travel for people who are unable to drive a car for reasons such as old age or physical disability. In addition, passengers in AVs are also able to engage in other activities during travel, adding to the convenience and enjoyment of their journeys. As a result, AVs will have a beneficial impact on the overall quality of life of many people (Russell, 2015; Sundararajan et al., 2019).

Equally, the value of travel time may change in the prospective era of AVs. Zhong et al. (2020) investigated how consumers valued their journey time when traveling in AVs and sharing AVs compared to traditional automobiles. According to their findings, AVs and sharing AVs potentially lowered the value of commuting travel time less when compared to human-driven vehicles (HDVs). The impact on passengers was shown to be less substantial than the impact on drivers. The study also found that the effect on the value of travel time for drivers differed between cities, suburbs, and rural areas, with the most significant drop occurring in the suburbs.

Finally, overall, AVs could provide significant advantages and economic benefits for the U.S. economy of up to approximately US$450 billion per year (Fagnant & Kockelman, 2015). This immense expected benefit will be attributable to a reduction in the number of accidents, a reduction in the amount of parking space required (Aria et al., 2016; Milakis et al., 2017; Wu et al., 2021), a reduction in traffic congestion, and increased passenger and freight mobility. Figure 1.2 presents the possibilities of AVs in terms of their potential benefits to society, road users, and travelers.

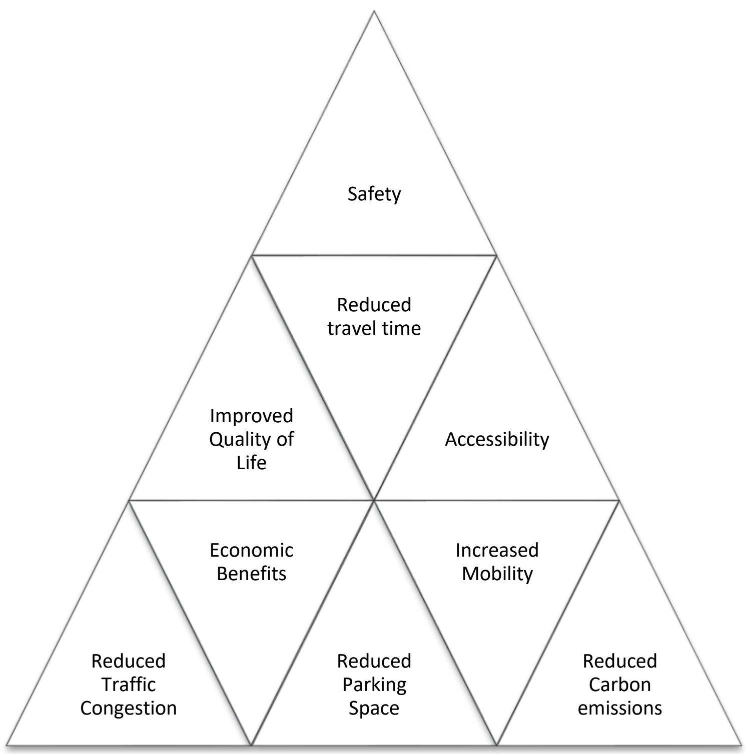

Figure 1.2: Promises of AVs

Although AVs are expected to yield all these potential benefits, there are still many issues that need to be resolved before they reach full deployment. One of the most critical problems is to ensure that the AV sensing technology (such as LiDAR) is reliable. Other obstacles include inadequate infrastructure, lack of user trust, immature or untested automated driving technology, uncertain demand, and lagging policy and regulations (Labi & Sinha, 2022). However, irrespective of these difficulties, the future of AVs appears promising. In the coming years, AV technology is expected to continue improving. If this improvement occurs, it may expedite the deployment of AVs on public roads.

1.3 Study Objectives

The continued development and operational success of Autonomous Vehicles (AVs) will depend on their ability to perform efficiently and safely. Despite significant progress in research towards improving various aspects of AV development, there still remain critical issues that need to be addressed. Therefore, further research is required to identify and tackle these issues, with the ultimate goal of enhancing AV performance.

One critical component for the development of AVs is obstacle detection and mapping of the roadway environment. Companies use different approaches for this, including placement of LiDAR sensors on their AVs. However, the impact of these placements on AV perception is not well understood. This inadequate insight poses a significant challenge to the development of AVs and ultimately, impairs safe deployment of AVs on roads.

For that reason, this research focuses on LiDAR placement optimization using a multi-criteria decision analysis approach. As such, the objectives of this thesis consist of the following:

1) To conduct a comprehensive review of different sensor technologies for AVs, including LiDAR, radar, and cameras. This review is expected to facilitate identification of the strengths and weaknesses of each technology and their potential for improving AV performance.
2) To perform an MCDA to systematically evaluate and compare the performance of alternative LiDAR placement configurations.
3) To investigate the effects of different weights on the analysis outcome.

The findings of this study are expected to contribute to a better understanding of the impacts of AV LiDAR placement. This knowledge will prove invaluable in the development of more reliable AVs and ultimately contribute to increased road safety.

This research will also help enhance vehicle reliability and provide engineers with the information needed to design more robust LiDAR systems or develop robust algorithms to ensure the reliable operation and better performance of AVs. Doing so will ultimately pave the way for the widespread adoption of AVs, making transportation safer, more efficient, and more convenient for all.

1.4 Scope of the Study

1) Sensor type: In contrast to the array of sensors used in AVs, including cameras, radar, inertial measurement units (IMUs), ultrasonic sensors, and GPS. However, this thesis focuses on LiDAR technology. The rationale for this focus lies in the unique capabilities and advantages offered by LiDAR in terms of high-precision 3D mapping, environmental perception, and obstacle detection.
2) Simulation environment: To facilitate the collection of pertinent data and streamline the evaluation process, the research leverages the Car Learning to Act (CARLA) simulation environment. CARLA provides a virtual platform that is invaluable for assessing LiDAR placement. This approach offers several advantages, including cost-effectiveness and lower resource demands.
3) Placement location and number: Of all the candidate locations for LiDAR sensor placement and the number of sensors that can be used, this thesis focuses on the vehicle roof of the vehicle as a key area for the sensor deployment and a maximum number of four sensors.

CHAPTER 2. LITERATURE REVIEW

2.1 AV Sensor Types and Characteristics

Sensor technology enables AVs to sense and understand their surroundings, thus, enabling safe roadway navigation and decision-making. A variety of unique sensor types (Figure 2.1), each with a unique set of abilities and functions, are used by AVs.

Figure 2.1: Camera, Ultrasonic Sensor, LiDAR, and Radar Sensor (Du, 2023)

AVs rely on sensing technologies to acquire essential information on the driving environment, ensuring safe navigation, obstacle detection, and response. Sensors are devices that play a fundamental role in detecting events or alterations in their environment and subsequently translating these observations into measurable digital signals. They can be broadly categorized into active and passive sensors (Javaid et al., 2021). Active sensors necessitate an external power source for their operation, whereas passive sensors function independently without external power input (Patel et al., 2020). Examples of active sensors include GPS, LiDAR, sonar and radar. Passive sensors include thermal sensors, electric field sensors, passive infrared sensors, acoustic sensors, and metal detectors (Ignatious et al., 2022; Javaid et al., 2021; Vargas et al., 2021).

Sensors can be further classified based on their underlying detection mechanisms, encompassing diverse fields such as electrical, biological, chemical, and radioactive detection methods. This categorization extends to conversion phenomena, including thermoelectrical, photoelectrical, electrochemical, electromagnetic, and thermo-optic processes (Sinha, 2017).

Additionally, sensors can be categorized as exteroceptive or proprioceptive (Figure 2.2). Exteroceptive sensors primarily focus on environmental perception and range determination, while proprioceptive sensors are specifically engineered for internal measurements, such as assessing forces, angular rates, and other internal dynamics (Woo et al., 2018). Essentially, exteroceptive sensors are analogous to the eyes and ears of a vehicle, allowing it to gather information from the external environment. These sensors detect various stimuli such as distance, light, sound, and objects such as pedestrians or other vehicles. They enable vehicles to interpret this information to create a comprehensive understanding of their surroundings and informing decisions based on the data received (Ortiz et al., 2023).

In contrast, proprioceptive sensors more closely resemble the vehicle's internal senses. They actively monitor and assess changes occurring within the vehicle's internal systems, including motor performance, battery status, and other vital components. These sensors play a critical role in providing essential data for determining fluid levels and acceleration and are able to measure internal dynamics such as vehicle rotation, individual wheel speeds, and lateral acceleration. This detailed information contributes significantly to understanding the vehicle's movements within its environment, thereby enhancing its overall operational intelligence, which is crucial for the vehicle's intelligent functionality (Kelly & Sukhatme, 2014; Ortiz et al., 2023).

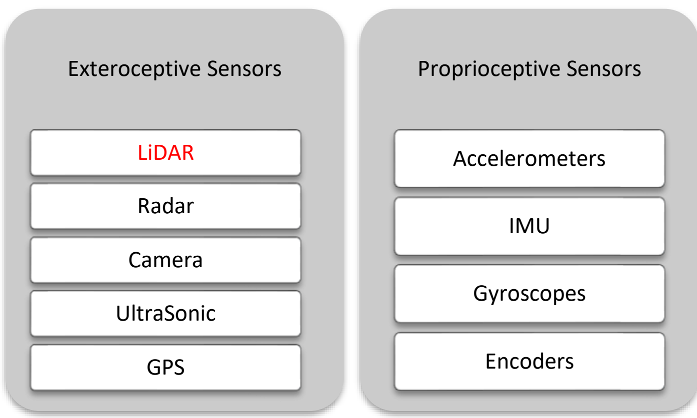

Figure 2.2: Sensors used in Autonomous Driving (adapted from Woo et al., (2018)).

2.1.1 Cameras

Cameras play a vital role in AV sensing. They are classified as passive sensors because they do not emit energy actively. Rather, they rely on naturally occurring electromagnetic radiation (such as light) to operate. Therefore, they operate in the same spectrum as human sight, making it easy for the vehicle to interpret visual information in its environment that helps in making decisions (Yeong et al., 2021). Cameras are useful for detecting and classifying road obstacles. Cameras can also be equipped with image recognition algorithms to track and identify objects such as pedestrians, road markings, and other obstacles (Campbell et al., 2018).

Different types of cameras are currently being used in AV deployment. RGB cameras, which are commonly used for day-to-day image acquisition and videotaping, are mounted on vehicles to capture a 360° view of the road environment (Cazzato et al., 2020). These cameras provide information that can be used with information from radar and LiDAR to identify detected objects. Cameras also provide depth information (Gross & Webster, 2021) when they are strategically installed in conjunction with other cameras. Such strategies include stereo vision or structure from motion to obtain the distance of a vehicle relative to other objects in the scene. This information can be used to make informed decisions regarding the vehicle's trajectory and obstacle avoidance. However, limitations exist in camera sensing efficacy in inclement weather and low-light conditions (Y. Zhang et al., 2023).

Other camera types, such as infrared cameras (also known as thermal cameras) have superior effectiveness compared to RGB cameras. They excel in low-light conditions (Parekh et al., 2022), as they can detect heat signatures that RGB cameras are unable to capture. Infrared cameras also offer several benefits including in-depth estimation, object identification, cost-effectiveness compared to other sensors, and optimal performance when used in conjunction with other sensor technologies. Hence, infrared cameras are a valuable addition to sensing systems for a wide range of applications, providing enhanced capabilities in scenarios characterized by low-light conditions and where heat detection and cost-effective performance are important.

2.1.2 LiDAR

2.1.2 (a) Description

LiDAR sensors are considered active sensors. They emit energy in the form of laser light and then measure the time that it takes for the light to bounce back from the sensing target to the sensor (Nobis et al., 2019). This process helps measure the distance between the sensor and the object, which allows the vehicle to understand its surroundings and thus make informed operational decisions as it builds up a 3D detailed map of the environment (Arikumar et al., 2022).

LiDAR is a key sensor for perceiving the environment and detecting road boundaries and lane markings (Khayyam et al., 2020); hence, it has been critical in autonomous driving development. As previously mentioned, the price of LiDAR has depreciated over the years, which has opened up more opportunities for research. For example, in 2005, Velodyne, a leading LiDAR manufacturer, introduced its first high resolution LiDAR sensor known as the HDL-64E, which cost around US$75,000. In 2012, the company released another LiDAR, the HDL-32E version, which was smaller and lighter than the HDL-64E and cost US$30,000. In comparison to the HDL-64E, the HDL-32E was a spinning 3D laser scanner that had fewer laser beams. It was designed for use in smaller vehicles. In 2016, the company released another version of the sensor, the VLP-16, a solid-state sensor that uses a single laser emitter to generate a 360-degree view of its surrounding area. It was priced at approximately US$8,000, making it even more affordable. Currently, the VLP Puck costs approximately half the price of the 2016 model. In 2018, the LiDAR price fell further when Velodyne released a solid-state LiDAR According to a 2020 press release by Velodyne LiDAR (Velodyne Lidar, 2020), the solid-state LiDAR-Vellaray H800 costs less than US$500 for high volume orders.

The LiDAR industry has experienced tremendous adjustments and advances over time. Many newer versions of sensors have been introduced with upgraded features and capabilities to suit specific applications. For example, some sensors are designed for use in specific environments such as urban areas, while others are intended for mapping, surveying, security purposes, and other related applications. With advances in technology, the sensors are becoming more compact, lightweight, and efficient while also becoming more affordable.

2.1.2 (b) Specifications Criteria

LiDAR sensors can be selected based on specifications (Figure 2.3) that depend on the application context. Specification criteria include point density, scan pattern and rate, accuracy and precision, field of view, range, and resolution. These criteria are further described in the following figure:

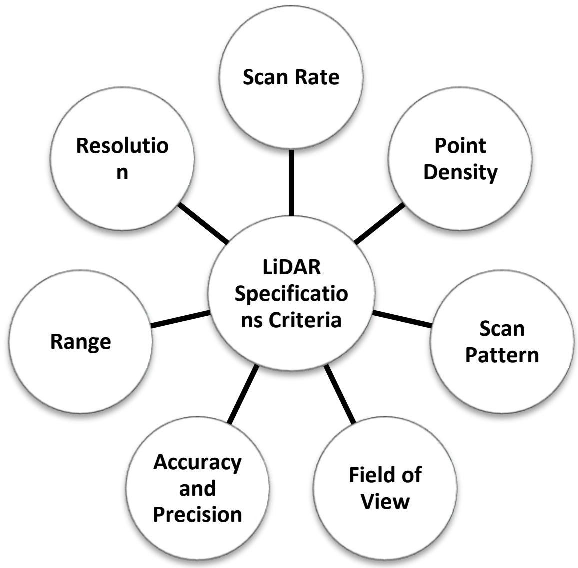

Figure 2.3: LiDAR Sensor Specifications Criteria.

2.1.2 (b.1) Point Cloud Density

Point cloud density refers to the number of laser points measured per unit area or volume within a specified region (Yoo et al., 2010). The sensor performance can be evaluated depending on the density of the point clouds as compared to another sensor with different specifications. The higher the density, the more detailed the representation of the scanned object. However, a disadvantage may be the large file storage requirements and the excessive processing time this method requires. In addition, in some applications such as aerial laser scanning, noise (due to, for example, adverse weather and atmospheric conditions) is introduced into the point cloud, thereby increasing the density (Lin et al., 2022). This noise can be removed using methods such as ground point filtering (Serifoglu Yilmaz & Gungor, 2018).

2.1.2 (b.2) Scan Pattern

Scan patterns represent the distinctive ways in which sensors emit pulses to measure the surrounding area. Different LiDAR sensors have different scanning patterns, which vary depending on the specific application or requirement (Raj et al., 2020). For example, some LiDAR sensors use a rotating prism or mirror to scan the laser beams in both vertical and horizontal directions, creating a 3D point cloud of the environment (Choi & Kim, 2020). Other sensors may use multiple fixed beams or a combination of rotating and fixed beams to create a more detailed 3D map (Yeong et al., 2021). The scanning patterns used by LiDAR sensors vary widely depending on their design and intended use. LiDAR sensors can be customized to use specific scanning patterns to meet the needs of different applications, such as robotics, AVs, and industrial automation (Li et al., 2022).

2.1.2 (b.3) Field of View (FOV)

FOV is the maximum angular range within which the sensor can see and measure objects in its surroundings. In the case of 2D LiDAR, the FOV is confined to the horizontal plane alone, while it encompasses both the horizontal and vertical planes for 3D scanners (Raj et al., 2020). The FOV of a LiDAR sensor depends on the number of beams emitted and the physical design of the sensor (Kibii et al., 2022). For example, Velodyne LiDAR provides sensors with different numbers of beams, such as Velodyne 16, 32, and 128, whereby the number of beams corresponds to the number of laser emitters on the sensor. The higher the number of beams, the higher the resolution and level of detail that can be captured (Yang et al., 2023).

2.1.2 (b.4) Accuracy and Precision

Accuracy and precision indicate the proximity of the obtained LiDAR measurement to the ground truth (Kim et al., 2022). Ground truth is the actual measurements or observations of a phenomenon that serves as a benchmark for evaluating the accuracy of data obtained from other sources (Yan et al., 2018). Accuracy can be in terms of the range, the angles or in a 3D space. Precision refers to the closeness of repeated measurements and can be evaluated in terms of the range, angle, or spatial precision.

Figure 2.4 illustrates the accuracy-precision relationship. The first circle shows tightly clustered points centered around the target, thus, demonstrating high accuracy and precision. Conversely, the second circle displays scattered points, neither close to the target nor tightly grouped, thereby indicating low accuracy and precision. In the third circle, tightly clustered points, though not centered around the target, signify high precision but low accuracy. Finally, the fourth circle depicts widely dispersed yet centered points, thus, portraying high accuracy despite low precision.

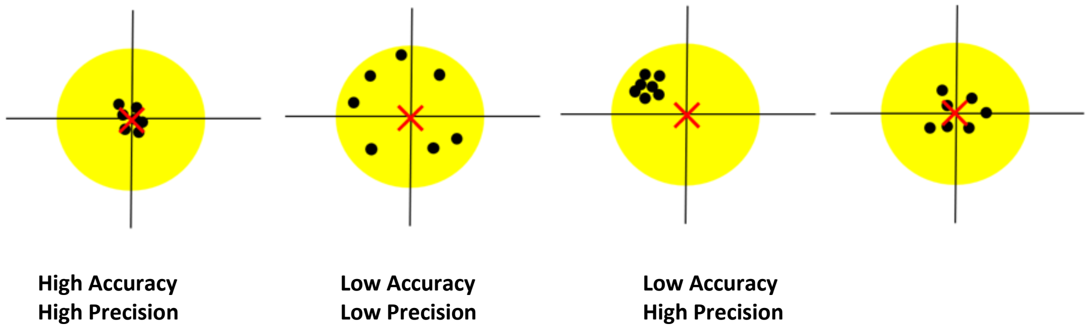

Figure 2.4: Accuracy and Precision

2.1.2 (b.5) Range

The range of a LiDAR sensor is the distance to which it can sense an object (Choi, 2016). This varies depending on the application of the sensor, such as for self-driving cars or mapping. LiDAR sensors can be classified as short-range and long-range sensors. Long-range LiDAR sensors can detect, locate, and identify objects as far from the vehicle as 250 meters or more (Campbell et al., 2018). They are ideal for identifying pedestrians, emergency braking, and other situations. Short-range LiDAR, in contrast, are better suited to monitoring the vehicle's immediate surroundings (Rablau, 2019).

2.1.2 (b.6) Resolution

Resolution refers to the level of detail that can be perceived in the point cloud (Anderson et al., 2006). This level can be impacted by factors such as the number of laser pulses that are emitted in a unit area, the wavelength of the light, or the angular FOV. The resolution of a LiDAR sensor has an effect on the way it measures distances to objects. A higher resolution is more reliable, as it produces a more detailed and finer representation of objects (Azim & Aycard, 2012; Imad et al., 2021). There is a distinctive price difference between the price of lower resolution LiDAR and its higher resolution counterpart (Bai et al., 2022): the cost of a low-resolution LiDAR is approximately 12.5% of that of its high resolution equivalent.

2.1.2 (b.7) Scan Rate

The scan rate is the frequency at which the LiDAR sensor emits and receives pulses. The scan rate determines the angular resolution of the system (Warren, 2019). The scan rate of a LiDAR sensor varies depending on the sensor's particular design and intended use. Typically, when the scan rate is high, the point cloud density also produces a detailed 3D representation of the target area (Benedek et al., 2021). A higher scan rate is an important specification for AVs because it provides an indication of the extent to which the sensor captures detailed information of the target area, such as the location and movement of other vehicles, pedestrians, and objects in real-time (Raj et al., 2020). This information can then be used by the AV's algorithms to make driving decisions.

2.1.3 Radar

Radar sensors work similarly to LiDAR in that they also emit a signal towards objects and calculate the distance to the object (Bilik, 2023). However, radar uses radio waves and works by emitting radio signals in a distinctive pattern. The time taken for the signal to bounce back from the object is measured and, together with the speed of light, is used to calculate distances. There is some similarity between radar and LiDAR, however, key differences also exist.

Radar has a long operational range (Bilik et al., 2019) and works well even in rain, fog, or snow because it is an all-weather sensor. In addition, the price is significantly lower than LiDAR (Campbell et al., 2018; Kim et al., 2019). Radars can be classified as long, medium, and short range. The long-range radars operate at 77 GHz frequency, while short- to medium-range radar sensors operate at 24 GHZ and 76 GHz frequencies, respectively (Kocić et al., 2018).

2.1.4 Inertial Measurement Unit

The IMU is a key sensor for measuring and estimating an AV’s orientation, acceleration, and angular velocity. The IMUs provide information related to the vehicle’s position and orientation. They typically consist of a combination of accelerometers, magnetometers, and gyroscopes (Kim et al., 2021), which work together to measure aspects of the vehicle’s motion. The gyroscopes measure the angular velocity of the vehicle around each of its three axes, while the accelerometers measure the linear acceleration of the vehicle along each of its three axes (x, y, and z). The IMU can determine the vehicle's orientation (pitch, roll, and yaw), as well as its linear acceleration and angular velocity, by combining the information from the accelerometers and gyroscopes (Vavra, 2022).

2.1.5 Ultrasonic Sensors

An ultrasonic sensor uses sound waves typically in the range of 20K Hz to 40 kHz (Rosique et al., 2019) to calculate distances to objects. It works by transmitting ultrasonic sound waves and using the time they take to return along with the speed of sound waves (331 m/s) to calculate the range to the object (Reddy Cenkeramaddi et al., 2020). Ultrasonic sensors are typically used in conjunction with other sensors for close-range applications, including parking assistance.

2.1.6 Global Positioning System

GPS is a global navigation satellite system that provides positional information. Other such systems include GLONASS, BeiDou, Galileo, QZSS, and NavIC. Of these, GPS is the most commonly used for a variety of applications (Rosique et al., 2019).

GPS was originally developed for military purposes before it was eventually widely adopted for civilian use. Some of the applications include mapping, agriculture, construction, and autonomous driving navigation (Awange & Kiema, 2019). In AV use, GPS plays a critical role in providing information on the position required to navigate the vehicle to its desired destination by using either pre-planned route information or a modified route based on prevailing road conditions such as traffic. However, GPS is susceptible to poor performance in places such as tunnels or areas around tall buildings because the signals are blocked. This introduces errors and inaccuracies in the system but can be managed by merging data from other sensors. Figure 2.5 presents additional information on sensors and their applications in ADAS and autonomous driving (Hussain et al., 2021).

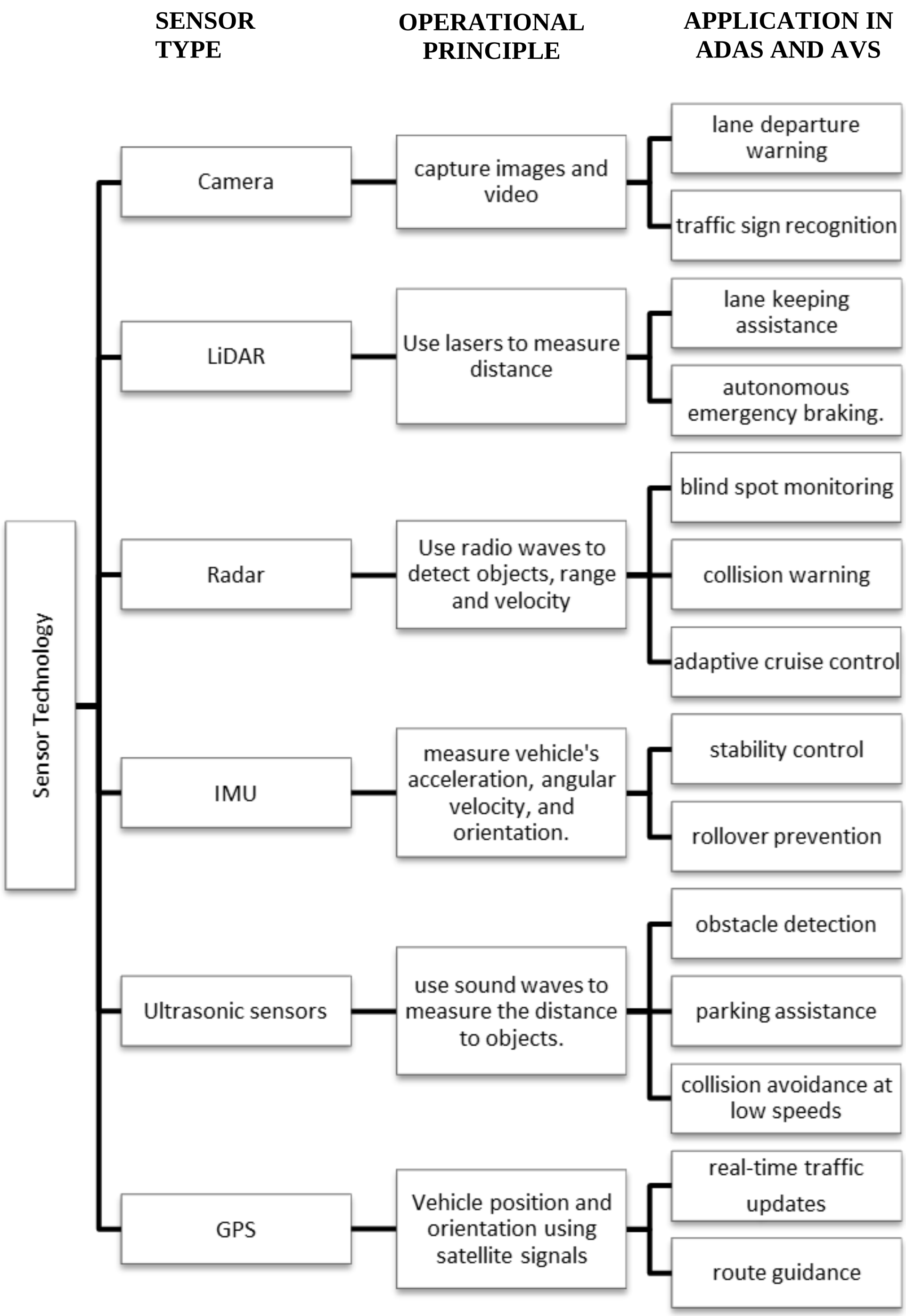

Figure 2.5: Sensor Technology applications in ADAS and Autonomous Driving.

2.2 Improving Perception in AVs Using Sensors

Several criteria have been considered in AV studies and AV enhancement. For example, in addition to sensors that enable the AV to see, one approach also allows the AV hear through an audio classification network based on a deep learning framework (Walden et al., 2022). The results of Walden et al.'s study indicate the potential their approach has to improve safety and operational efficiency in various scenarios. For example, their study suggests that AVs can be made capable of recognizing audio cues, such as the sounds of children playing or essential auditory signals such as horns and idling engines, to reduce the risk of accidents.

Individual sensor types or a combination of sensor types can also be chosen in a way that acknowledges the limitations of specific sensor types in adverse weather conditions. For example, cameras and LiDAR work together very effectively in adverse weather conditions: Cameras excel at capturing visual features, while LiDAR provides precise depth information and excels at detecting speed and distance (Chen et al., 2017; Vargas et al., 2021).

The fusion of radar and cameras also improves perception (Nobis et al., 2019), as the radar sensor's ability to penetrate through fog, snow, or rain compensates for any limitations of the camera sensor (Pavitha et al., 2021). Furthermore, the combination of radar, camera, and LiDAR (Ahrabian et al., 2019) maximizes the strengths and overcomes the limitations of each individual sensor type. Figure 2.6 identifies where the different sensors could be placed and how they could complement each other.

The red areas show the LiDAR coverage, the blue areas indicate where short-/medium-range LiDAR have coverage, the green areas are covered by long-range radar, and the gray areas show the camera coverage.

Vehicle to infrastructure (V2I) communication is another resource that is being leveraged as a source of supplementary data to improve AV perception. This improvement is achieved through the development of an environmental perception framework that relies on point voxel region-based convolutional neural networks to enhance the AV's perception capabilities at road intersections. Information from roadside sensors is transferred to the AV to support its perception capabilities (Duan et al., 2021).

There has also been some progress towards improving AV perception by considering the influence of sensor placement on AVs. It is important that sensors are optimally placed to enable the AV to achieve the best understanding and perception of its surroundings (Dybedal & Hovland, 2017a; Kim & Park, 2020a; Liu et al., 2019)

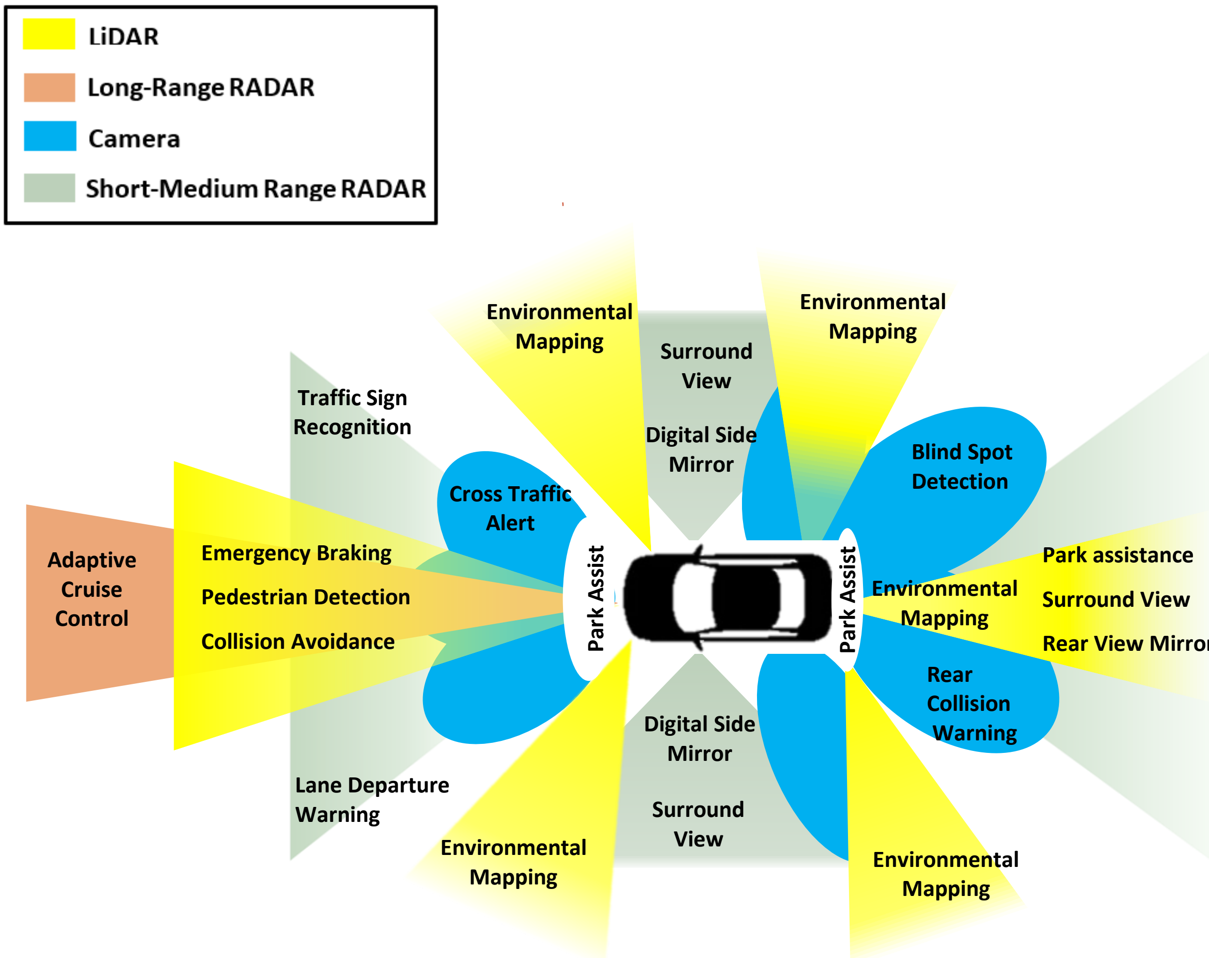

Figure 2.6: Sensor coverage areas (redrawn from Ng (2021)).

2.2.1 Perception as one of Multiple AV Modules

In a manner analogous to human drivers, AVs are equipped with functionalities that enable them to perceive, analyze, and execute tasks. The AV module is conceptually divided into three core components: planning, perception, and control (Claussmann, 2019). The perception component serves as the sensory system of the AV, facilitating environmental awareness, self-localization, and object recognition.

The planning element corresponds to the cognitive component, where the AV processes information obtained from perception to formulate decisions aimed at safely guiding the vehicle to its intended destination while simultaneously navigating around identified obstacles. Finally, the control category represents the facet through which the AV translates these formulated intentions into actions, thus, yielding the desired operational outcomes (Pendleton et al., 2017).

Perception constitutes a pivotal aspect for autonomous driving technology. This component entails the acquisition of data through environmental perception and localization, which represent two distinct subcategories within the field of perception. The gathered information is subsequently processed to enable the AV to comprehend the road conditions, interpret behavioral cues, and discern various obstacles in its immediate vicinity (Emzivat et al., 2018).

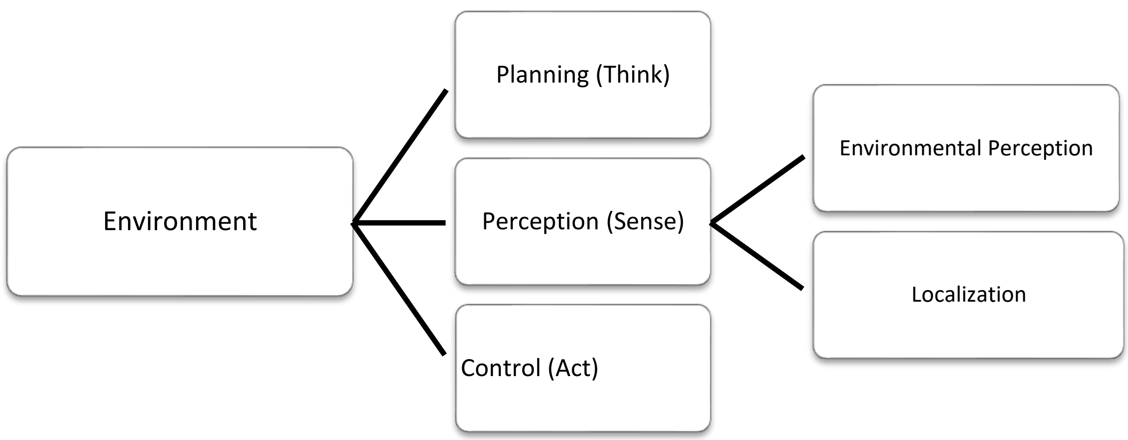

Figure 2.7: Planning, Perception and Control Systems (modified from Claussmann, (2019))

2.2.2 Environmental Perception and Localization

Environmental perception and localization are critical aspects of autonomous driving. Therefore, it is ideal that they are carried out precisely. For this reason, the strengths and limitations of available sensor types must be carefully considered (Pavitha et al., 2021). Environmental perception can be achieved using LiDAR, radar, ultrasonic sensors, cameras, or a combination. First, the AV perceives the environment by acquiring information about the driving scene and identifying the different road obstacles, which include stationary obstacles, such as traffic lights, road signs, streetlights, and movable obstacles, such as pedestrians, cars, bikes, or animals. Then, the information on their speed and behavior is determined to make calculations to predict their movements (Pendleton et al., 2017) and the changing traffic conditions (Duan et al., 2021).

Table 2.1: AV Sensor types: strengths and limitations (Vargas et al., 2021)

Feature	**LiDAR**	**RADAR**	**Camera**	**Ultrasonic**
Primary Technology	Laser beam	Radio wave	Light	Sound wave
Range	~200 m (656.17 ft)	~250 m (820.21 ft)	~200m (656.17 ft)	~5m (16.40 ft)
Resolution	Good	Average	Very good	Poor
Affected by Weather Conditions	Yes	Yes	Yes	Yes
Affected by Light Conditions	No	No	Yes	No
Detects speed	Good	Very good	Poor	Poor
Detects distance	Good	Very good	Poor	Good
Interference susceptibility	Good	Poor	Very good	Good

Localization is another aspect of perception in which the vehicle's location is determined using a global reference (Kuutti et al., 2018). For an AV to operate, it needs to know where it is in the real world, that is, its position and orientation (Elhousni & Huang, 2020). Furthermore, the localization of the AV needs to be carried out as accurately as possible since every other functional operation of the AV, such as planning, control, and even environmental perception, relies on the ability of the AV to know its location in the real world (Kuutti et al., 2018).

The most commonly used sensor for AV localization is GPS, which is easily accessible and less costly compared to other sensor types. However, GPS is prone to errors such as multipath and low accuracy (Awange & Kiema, 2019; Kos et al., 2010). Multipath interference occurs when satellite signals bounce off surfaces before reaching the receiver, causing multiple signal paths and inaccuracies in determining the vehicle's exact position. Therefore, other sensor types such as radar, LiDAR, and cameras are utilized for AV localization.

Figure 2.8 illustrates the concept of perception in AVs. Environmental perception focuses on what the AV senses in its surroundings, while localization pertains to the AV's awareness of its own position. The overlapping area (Perception) signifies the integration of environmental awareness and self-awareness, which is crucial for informed decision-making and safe navigation.

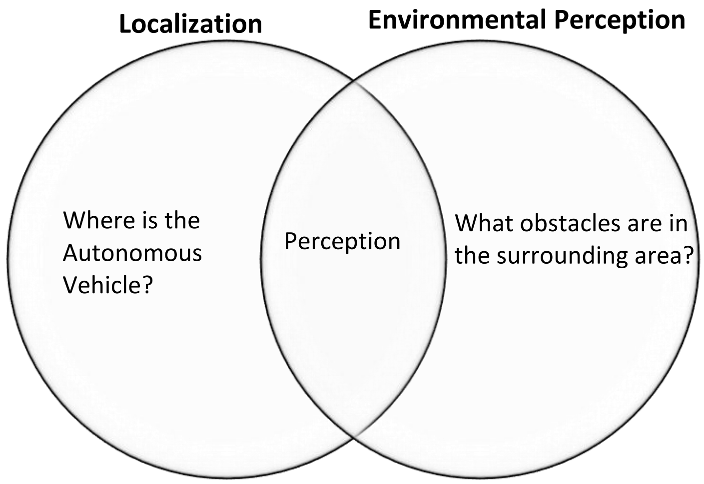

Figure 2.8: Environmental Perception and Localization

2.3 LiDAR Sensor Technology

The time of flight (ToF) principle entails measuring the round-trip travel time of a laser pulse from the LiDAR sensor to a target. This measured time difference, denoted as Δt, is a key parameter for determining the distance between the LiDAR sensor and the target (Liu et al., 2018). This principle is applicable for generating detailed point cloud data that enables AVs to understand and navigate their environments.

The ToF in LiDAR follows a precise sequence of operations to ensure the accurate measurement of distances. Initially, the LiDAR system aligns with the target and emits laser light pulses toward it. The emitted signal serves as the trigger for a counter, commencing the counting of clock pulses. As the target diffusely reflects the echo signal, it traverses through the atmosphere and enters the receiving optical system. Here, a photoelectric detector converts it into an electric pulse. Subsequently, an amplifier intensifies this electric pulse, which in turn functions as the gate-closing signal for the counter, thereby halting the counting process. The number of clock pulses counted during the gate-opening phase is pivotal to determining the precise distance to the target (Maatta & Kostamovaara, 1998).

In Figure 2.9, the underlying concept is visually depicted. It illustrates the generation of a reference light pulse at time (t), which triggers the clock within the timer circuit. A photosensor then converts the returning signal (reflected light) into an electric pulse that stops the timer from counting.

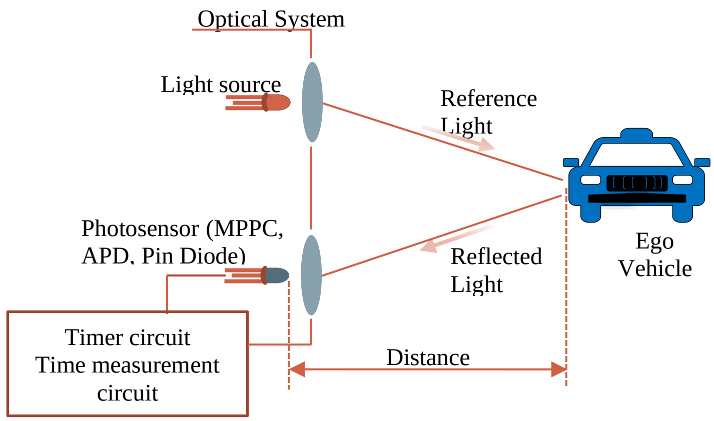

Figure 2.9: Time-of-flight LiDAR system (recreated from Liu et al., (2018))

The time taken for the emitted light (pulse) to reach the target and be sent back (return) to the source is used together with the speed of light to build a 3D representation of the surrounding environment (Campbell et al., 2018) through the ToF principle.

$$R = \frac{c}{2} \times \Delta t,$$

where R is the distance to the object, c is the speed of light ($3 \times 10^8\ m/s$) and Δt is the ToF (Royo & Ballesta-Garcia, 2019; Vargas et al., 2021).

The emissions from LiDAR are in the infrared range of 905 nm and 1550 nm of the electromagnetic spectrum. Initially, LiDAR systems at 905 nm were used for AV applications in the early stages of their development because that was the state of the technology at the time. However, there are eye safety concerns at that wavelength, which is an essential consideration for LiDAR's automotive applications. These restrictions limited the object detection range to approximately 100 m (Vargas et al., 2021; Warren, 2019; Wojtanowski et al., 2014). The human eye is more resistant to wavelengths exceeding 1400 nm (Warren, 2019). Hence, to improve the current detection range, LiDAR sensors are designed at 1550 nm.

Since gaining prominence in 1960, subsequent to Theodore Mainman's groundbreaking invention of the ruby laser, LiDAR has undergone a series of evolutionary phases. Various companies have seized the opportunities and potential this technology offers by investing in LiDAR sensors. For example, at a certain period, LiDAR sensors could record only 1000–2000 points per second (Wang et al., 2020). Currently, LiDAR sensors categorized as long-range sensors can scan up to 200,000 points per second while achieving a 360º horizontal rotation with a 30º vertical FOV (Yeong et al., 2021). In addition, Velodyne LiDAR has a sensor with a 40º vertical FOV (*Velodyne Ultra Puck VLP-32C Long-Range LiDAR Sensor — Clearpath Robotics*, n.d.), while Sense Photonics has a LiDAR with a 75º vertical FOV (Photonics, n.d.). Ouster has an ultra-wide sensor with a 90º FOV but a limited range of up to 35 m (*OS0 Ultra-Wide Field-of-View Lidar Sensor for Autonomous Vehicles and Robotics*, n.d.).

Currently, more startups are emerging in the manufacturing and supply of LiDAR sensors. Table 2.2, modified from Wang et al. (2020), presents vendors of LiDAR products that can be deployed in autonomous driving.

LiDAR technology is used in various domains including forestry, geospatial mapping, robotics, mining, security, and smart infrastructure. However, this thesis focuses on the autonomous driving application. One of the compelling factors driving the selection of LiDAR as the primary perception sensor for AVs is its ability to provide extremely precise and rich depth information pertaining to the vehicle's surroundings (Zhang & Singh, 2014). Furthermore, LiDAR generates densely populated point clouds, which are instrumental in advancing simultaneous localization and mapping capabilities (Saraf et al., 2012).

Table 2.2: Vendors with LiDAR Products for Autonomous Driving.

Company	**Products**	**Year founded**	**Country**
Valeo	Near Field LiDAR	1923	France
Hokuyo	UBG Series, URG Series, UST Series, UGM Series, UXM Series	1946	Japan
SICK	LMS Series, MRS Series, LD- MRS Series	1946	Germany
Ibeo	IbeoNEXT, ibeo LUX	1998	Germany
Velodyne LiDAR	Puck, Ultra Puck, Alpha Prime, HDL-32E	2007	USA
Luminar Technologies	Luminar Iris	2012	USA
Quanergy Systems	M Series, S Series	2012	USA
AEYE	AEye 4Sight Intelligent sensing platform	2013	USA
Hesai	Panda128, QT128	2014	China
Robosense	RS Series	2014	China
Leishen	LS Series, HS Series, CX Series	2015	Austria
Baraja	Spectrum Series	2015	Australia
Ouster	OS Series	2015	USA
Cepton	Vista-P, Sora-P, Vista-X, Nova, Helius	2016	USA
Innoviz	InnovizOne, InnovizTwo, Innoviz360	2016	USA
Neuvition	Titan M1 Series, S2 Series, Titan P1	2016	USA

LiDAR technology continues to improve, and its adoption in AVs appears to have a promising future. This type of sensor varies in terms of specifications and options, including cost, size, scanning pattern, FOV, type, pulse rate, scan rate, and detection range (Roriz et al., 2022). The cost of a standard LiDAR sensor has reduced over the years, from US$75,000 (in 2005) to less than US$5,000 (in 2023), thereby facilitating their widespread deployment in the various application areas (Elhousni & Huang, 2020).

2.4 LiDAR Placement on AVs

The success of AV operations largely depends on their ability to accurately perceive and understand their surroundings. The placement of LiDAR sensors on an AV is a critical factor determining the FOV and the data quality. Proper LiDAR placement ensures effective detection of objects, obstacles, and road hazards, which is essential for safe AV operations (Cai et al., 2023; Kim & Park, 2020; Lucic et al., 2020).

Companies each have their own unique LiDAR placement designs or configurations. However, a strategy for determining the placement of the LiDAR has yet to be established (Mou et al., 2018a). As such, researchers are investigating this issue (Berens et al., 2022; Hu et al., 2022; Jin et al., 2022; Liu et al., 2019; Lucic et al., 2020).

Table 2.3: LiDAR Placement location, count, and type of different AV driving teams (modified from Mou et al., (2018a))

Placement location & count	**LiDAR Type**	**Number**	**AV Driving Team**
2 on each side on top roof	Velodyne-16	4	Ford
2 on each side with 1 on the middle front on top roof	Velodyne-16	5	Cruise
On top center of the roof	Velodyne-64	1	Uber
1 Velodyne-16 at each side and 1 Velodyne-64 on top roof	Velodyne-16/64	2/1	Baidu
6 in front and 6 on the rear of the roof	Velodyne-16	12	Apple
2 Velodyne-16 on each side and 1 Velodyne-64 on the roof	Velodyne-16/64	4/1	UM Perl lab
On the center of the roof	Velodyne-64	1	Stanford Driving Lab
On the top front of the roof	Ouster-64	1	Purdue CART Lab
3 placed on top of the racing car	Luminar Solid State LiDAR	3	Black and Gold Autonomous racing Car

The LiDAR sensor placements described in Table 2.3 may vary depending on the specific AV platform and its use case. The placements listed provide a general indication of how LiDAR sensors are typically positioned on AVs. However, other platforms may use different configurations or sensor types. Furthermore, it is important to recognize that LiDAR sensors are just one component of the complex sensor suite that AVs use. Other components include cameras, radars, and other sensing technologies.

2.4.1 Alternative Approaches for LiDAR Placement on AVs

The strategic placement of LiDAR sensors on AVs is of the utmost importance because it necessitates maximizing the acquisition of driving scene data while minimizing the number of LiDAR sensors used. One of the earliest approaches for LiDAR placement considered the sparsity of the LiDAR points (Mou et al., 2018b). The sparsity of point clouds refers to the distribution and density of points captured by the sensor across a given environment. A sparse point cloud has fewer data points, meaning there are larger gaps or areas with fewer measurements. Mou and his research team emphasized that for LiDAR sensors to excel in their perception capabilities, they must possess the ability to discern even the smallest details within their FOV (Mou et al., 2018a). They defined a “region of interest” (ROI) to encompass the immediate neighborhood of the AV. The ROI is conceptualized as a cubic space defined by specific dimensions, with its x-y plane origin aligned with that of the AV from the top view.

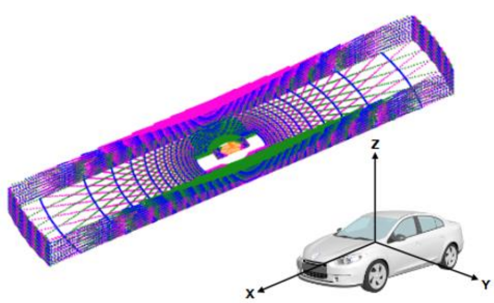

Figure 2.10: Region of Interest for an Autonomous Vehicles with three LiDAR sensors (Mou et al., 2018b)

As a LiDAR sensor rotates, it generates a set of laser beams that define a conical shape. These individual shapes collectively represent the sensor's ROI (Figure 2.11).

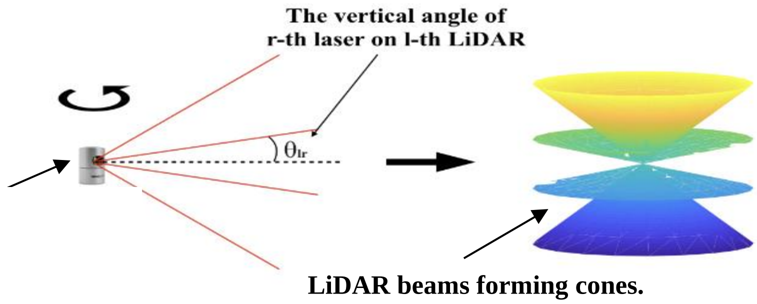

Figure 2.11:LiDAR Beam forming Cones through a 360° Rotation (Mou et al., 2018a)

With a similar concern for sparsity, Kim and Park (2020a) visualized the level of coverage produced by the LiDAR point clouds that result from multiple LiDAR sensor placements on the vehicle. An optimization method was proposed in which a LiDAR Occupancy Board (LOB) was introduced to obtain the occupancy of the LiDAR in each local zone. Occupancy in this context refers to the evaluation and visualization of how well the LiDAR sensor covers or occupies specific areas or zones within its FOV. Kim and Park (2020a) observed that the occupancy was high in places where the point clouds overlapped but low in places with no overlaps in coverage. In addition, the distribution of the points was measured using the concept of a local occupancy grid. The LOB was divided into grids with reference to the number of channels the LiDAR sensor utilized. An algorithm was developed to find a solution to the optimization problem, and this solution was tested using commercial 3D LiDAR sensors. The results of Kim and Park's study confirmed placement is an important factor that influences LiDAR perception performance.

Figure 2.12: LiDAR sensors placed on a Test Vehicle (Kim & Park, 2020b)

Deep learning algorithms have also been developed to process LiDAR data (Deng et al., 2021; Shi et al., 2019). Hu et al. (2022a) approached the problem from the perspective of how the physical design of a LiDAR influences its perception of the target environment. Their approach also considers the area in the vicinity of the AV (which Mou et al. referred to as the ROI). To ensure a proper assessment of LiDAR placement, it is essential to study a consistent pattern of objects in various experiments, which cannot be achieved through real-world scenarios but rather requires simulation.

Simulation offers numerous advantages and disadvantages. Simulation provides flexibility, allowing conditions to be easily modified by adjusting input parameters, thus, aiding in the exploration of various scenarios. Simulations also bypass the limitations of real-world experiments, such as complexity and risks, while ensuring uninterrupted operations during analysis. However, these benefits are also accompanied by limitations. The accuracy of simulation outputs relies heavily on the quality of the input data, meaning that erroneous or limited data lead to incorrect outcomes (Amaran et al., 2016; Labi, 2014; Smith, 1998). In addition, despite their advantages, simulation methods may not always be as efficient as analytical techniques. Nonetheless, simulations remain versatile tools that are particularly invaluable when closed-form analytical solutions for addressing complex problems are unattainable (Labi, 2014).

For example, to test different scenarios using simulation, Hu et al. (2022a) used CARLA, (an open-source simulator for AVs) to test different LiDAR placements. These placements were motivated by those performed in studies from companies such as Toyota, ARGO AI, Cruise, Pony AI, and Ford. The results showed that different target types (vans, cars, box trucks, and cyclists) required different sensor placements.

Additionally, the choice of LiDAR type is essential for improving AV perception. Fang et al. (2018) presented a LiDAR simulation framework that also considered the LiDAR type and placement in 3D LiDAR point cloud production. LiDAR point clouds, which were obtained based on traffic and scenes from the real world, were collected to serve as data for training deep neural networks. The point cloud data was acquired using LiDAR scanners, specifically, the Riegl scanner, which has a resolution of approximately 3 cm within a range of 100 m (Fang et al., 2018). In contrast to previous research (Hu et al., 2022a; Kini, 2020a; Mou et al., 2018a) which exclusively used an artificially generated virtual (simulated) world, Fang et al. (2018) used the Riegl scanner to generate point clouds based on real environments, thereby marking a transition from simulations to real-world data. This integration of real-world data offered a more accurate depiction of real-world scenarios. Similarly, in their work, Feng et al. emphasized the significance of naturalistic data for enhancing simulations for AV testing. Their method, showcased for driving intelligence testing in AVs, expedites testing procedures and generates vital adversarial examples crucial for AV development (Feng et al., 2021).

Acquiring data from multiple LiDAR placement scenarios in the real world requires significant time and effort in the form of model training, raw data collection, and deployment compared to utilizing artificially generated methods (Hu et al., 2022a). Therefore, it is paramount to find a way to evaluate the perception performance of LiDAR while minimizing cost and obtaining the required quantitative information. For this reason, researchers have occasionally used virtual environments such as CARLA (Berens et al., 2022; Hu et al., 2022; Kini, 2020). Using a virtual environment aids in evaluating the LiDAR placement in a more economical and less intensive process than physically installing LiDAR through collecting large volumes of data, training models, and evaluating alternative placements.

In AV research, 2D and 3D LiDAR sensors have been used. 2D LiDAR sensors produce distance information while 3D LiDAR sensors produce information on height and geometry (Catapang & Ramos, 2016). Most researchers have focused on 2D LiDAR. Zhao et al. (2017) collected information on vehicle trajectory using a vehicle equipped with 2D LiDAR sensors. In terms of placement, four LiDAR sensors were used: Two short-range models were placed in the front and right bumper of the vehicle, respectively, and two long-range sensors were placed in the front and rear of the vehicle. In contrast to Zhao et al. (2017), who used four 2D LiDAR sensors, He et al. (2014) placed five 2D LiDAR sensors on the vehicle: Three sensors were mounted at different positions and orientations along the vehicle's front bumper, and two were mounted on top of the vehicle at different locations.

The car used by Pereira et al. (2016) combined both 2D and 3D LiDAR sensors. In addition to the two 2D LiDAR placed on the sides of the bumper, another 3D LiDAR was installed on the AV. Meadows et al. (2019) used three LiDARs: two placed on different sides of the car bumper and the third placed on the vehicle's roof. The information obtained from all these LiDAR sensors is registered to provide the AV with rich 3D information and coverage of the surrounding area. Meadows et al. (2019) focused on determining the optimal position of the two sensors placed in front of the vehicle while keeping the position of the third one fixed.

Regarding AV design, Liu et al. (2019) stressed the importance of balancing computational burden with object detection performance; using fewer LiDARs could present issues related to object detection performance. Conversely, using more LiDARs, aside from the high cost, also results in a high computational burden and redundancy. Therefore, it is essential to create balance when determining the optimal number and LiDAR type for AV use. Liu et al.'s (2019) research used three types of LiDAR to evaluate performance from different perspectives. Their results can be used to guide AV designers in choosing LiDAR sensor types or in improving the design of existing LiDAR placements.

2.5 Multi-Criteria Decision Analysis

The exploration of LiDAR placement methodologies discussed in earlier sections has revealed a multifaceted landscape characterized by various approaches and strategies. Previous studies have delved into different facets of LiDAR deployment. This section introduces multi-criteria decision-making (MCDM), which is used for LiDAR placement optimization in this thesis by discussing concepts of scaling, weighting, and the amalgamation of criteria.

MCDA serves as a systematic approach for addressing complex decision-making that involves multiple criteria or factors of different units of measurement and different levels of importance. In MCDA, the decision-makers (DMs) assign weights to the criteria that reflect their respective levels of importance and establish scaling functions for each criterion. Then, they assess various alternatives based on the weighted and scaled criteria. This structured method provides a framework for comparing and ranking alternatives based on their combined outcomes across the multiple criteria (Bukhsh et al., 2017; Keeney & Raiffa, 1993; Sinha & Labi, 2007).

Through questionnaire surveys, the DMs allocate relative weights to these criteria to signify their importance and carry out scaling to standardize the measurement units of each criterion. The impacts of each alternative are then amalgamated using various tools and techniques, thus, assisting in the identification of the most suitable option. In instances where no single alternative outperforms the others across all criteria, formulations are introduced to accommodate constraints or tradeoffs. MCDA not only provides comprehensive structuring of the decision-making process but also enhances clarity, transparency, and defensibility, thereby facilitating informed choices in diverse decision contexts (Sinha & Labi, 2007).

2.5.1 Establishing the Alternatives

Establishing alternatives is a foundational step in systematic decision-making processes and cuts across various fields. It involves outlining objectives and constraints while identifying a range of potential options to address a particular problem or situation. Similar to everyday decision-making scenarios, the process entails cataloging the costs and benefits associated with each alternative and setting predefined thresholds or criteria for evaluation (Labi, 2014). Through systematic analysis, DMs assess the feasibility, cost-effectiveness, and alignment of alternatives with defined objectives. This iterative process aims to pinpoint the most suitable choice by scrutinizing and comparing alternatives against established criteria.

2.5.2 The Performance Criteria

Transportation decisions often aim to incorporate a broad spectrum of performance criteria that align with the interests of key stakeholders. These include considering agency goals, the perspectives of facility users, and the broader concerns of society at large (Sinha & Labi, 2007). Performance criteria vary across dimensions, spanning quantitative and qualitative aspects that define evaluation standards. For instance, when assessing a product, factors such as reliability, durability, cost-effectiveness, user-friendliness, and safety are critical considerations (Barclay & Osei-Bryson, 2010). Similarly, in project management contexts, meeting deadlines, remaining within budget, and achieving project objectives represent pivotal performance metrics (Institute, 2008).

These criteria serve as essential frameworks for evaluation and offer stakeholders a structured basis for comparison, informed decision-making, and the prioritization of actions based on their alignment with established criteria. In the realm of optimization, performance criteria also play a decisive role in shaping decisions. While some optimization processes may follow a single objective, many entail multiple criteria or constraints across various metrics, known as multi-attribute problems (Labi, 2014). Factors influencing the selection of criteria in these multi-attribute problems encompass agency policies, system or design nature, stakeholder concerns, and management levels. For instance, historic preservation might significantly influence highways in older communities, whereas isolated regions might prioritize uninterrupted accessibility (Labi, 2014).

2.5.3 Weighting Methods

The process of establishing relative weights for performance criteria in decision-making scenarios is fundamental to the effectiveness and credibility of the MCDM process. Various methods have been devised to address this challenge, each playing a pivotal role in shaping the hierarchy of criterion importance and streamlining the decision-making process (Ortiz-Barrios et al., 2021; Pamučar et al., 2018; Singh & Pant, 2021).

These methods typically involve the use of questionnaire surveys or interviews, which are administered to DMs, such as agency engineers and other stakeholders. The respondents' feedback, collected through diverse weighting techniques, shapes the outcome of the decision process. The choice of an appropriate weighting method significantly affects the final outcome of the MCDM analysis, hence, it is an important step (Bai et al., 2022; Keeney & Raiffa, 1993; Li & Sinha, 2000).

Some of the most commonly used weighting methods are explained in this section.

2.5.3 (a) Equal Weighting

The equal weighting approach is straightforward and involves assigning the same weight to all performance criteria. It is a common practice that is relatively simple to implement. An example of this approach in transportation studies is the use of equal weighting in the context of pavement investment decision-making through life-cycle cost analysis (Lamptey et al., 2005). In previous studies, both agency costs and user costs were often combined without explicitly assigning different weights to them. The direct addition of agency costs to user costs was a common practice, implying that one dollar of agency cost was considered equivalent to one dollar of user cost. This practice stemmed from the assumption that these two cost components held the same level of importance in the decision-making process (Peterson, 1985; Sinha et al., 2009; Sinha & Labi, 2007).

However, the equal weighting approach, while straightforward and commonly used, does not provide a representation of the DMs' preferences and priorities (Li, 2003). Incorporating relative preferences among criteria is essential to make well-informed decisions for transportation systems in MCDA.

2.5.3 (b) Direct Weighting

Direct weighting is a technique in MCDA that allows DMs to assign numerical weight values to performance criteria. This approach provides a quantitative representation of the relative importance of these criteria and offers some example methods, including point allocation, categorization, and ranking (Odu, 2019; Patidar et al., 2007).

Point allocation (PA) involves the allocation of a total of 100 points among decision criteria (Bottomley et al., 2000). Each criterion receives a weight that signifies its importance. The more points a criterion receives, the higher its weight in the decision-making process. Point allocation provides a cardinal scale, expressing weights as numerical values for ease of mathematical operations such as addition and multiplication. Categorization, in contrast, groups decision criteria into different categories representing their relative importance compared to other criteria. This method does not assign specific numerical values but rather measures the criteria's importance within predefined categories, such as "high," "medium," or "low." Categorization establishes an ordinal scale of importance, where criteria are assigned within each importance category but lack specific weight values. Ranking allows DMs to assign a rank to each decision criterion based on its importance. Typically, the criterion considered most important is assigned the highest weight (Keeney & Raiffa, 1993; Labi, 2014).

The choice of direct weighting method should be guided by the specific context of the decision-making process. Notably, ranking and categorization do not provide precise numerical weights and are categorized as ordinal scales. In contrast, point allocation offers numerical weights in a cardinal scale, making it the preferred choice when these weights need to be used in multivariate value or utility functions (Patidar et al., 2007).

2.5.3 (c) Observer-Derived Weighting

Observer-derived weights represent a methodology in which DMs unconsciously assign weights to various criteria without explicit awareness. This method estimates the relative importance of multiple objectives through an analysis of unaided subjective evaluations of alternatives (Hobbs & Meier, 2000). During this process, DMs provide scores for each objective for a set of alternatives and an overall score on a scale, which often ranges from 0 to 100. Subsequently, a statistical relationship is established by utilizing the overall score as the response variable and the scores assigned to individual objectives as explanatory variables through regression analysis. The coefficients resulting from this analysis represent the implicit or observer-derived weights associated with the various objectives as perceived by the DMs.

The methodology, as emphasized by notable researchers (Huber, 1974; Slovic & Lichtenstein, 1971), involves utilizing regression analysis to derive attribute weights aimed at minimizing deviations from actual rankings or ratings. The reliance on regression methodology is a distinctive advantage of this method, similar to the concept of "policy capturing," which is frequently used by psychologists and pollsters to predict opinions, reflecting an attempt to optimize the judgment process (Hobbs, 1980; Patidar et al., 2007).

However, MCDA aims to enhance, not merely replicate, holistic judgments. Research indicates that individuals often prioritize only a few attributes when making decisions involving numerous criteria (Edwards, 1977). This observation suggests that observer-derived weights may cluster on a subset of attributes. Moreover, since DMs may disregard less critical attributes when making holistic judgments, observer-derived weights may not be proportionate to the worth of each attribute. Therefore, the observer-derived weights method may not be the optimal choice, particularly when coping with a substantial number of criteria. In such scenarios, alternative weighting methods such as the analytic hierarchy process (Saaty, 1977), which involves examining one pair of criteria at a time, may offer a more effective approach to handling the complexity of the decision-making process (Patidar et al., 2007).

2.5.3 (d) Gamble Method

The gamble method, as outlined by Keeney and Raiffa (1993), offers a systematic approach to weight assignment within MCDA. It allows the DMs to assess and compare individual goals sequentially. The process begins by identifying the most critical goal, the one with the highest significance in transitioning from its least desirable state to its most desirable state. This goal takes precedence in the weight assignment process. Next, two scenarios are evaluated. In the "sure thing scenario," the chosen goal is set to its optimal level, representing the best possible outcome, while all other goals remain set at their least desirable states. Conversely, the "gamble scenario" introduces an element of uncertainty. Probabilities are assigned, with p representing the likelihood of achieving the most desirable levels for all goals and $(1 - p)$ signifying the probability of attaining their worst values. The objective is to find the specific *p* value at which the two scenarios, "sure thing" and "gamble," become equally appealing to the DM (Z. Li, 2003).

This process is repeated iteratively for the remaining goals, with each goal's relative importance decreasing in each subsequent step. Weights are assigned to each goal based on the previously established probabilities. It is important to note that the hypothetical probabilities for achieving the best or worst conditions of each goal may vary among different assessors, thus, reflecting the subjective nature of the evaluation process.

The gamble method is particularly valuable in scenarios involving outcome risk, where precise outcomes are unknown, but their probability distributions are known. This method helps in determining the relative importance of different performance criteria. However, it may present challenges in terms of comprehension and administration owing to the need to assess the relative desirability of uncertain outcomes (Sinha & Labi, 2007).

2.5.3 (e) Analytical Hierarchy Process (AHP)

The AHP, often referred to as the pairwise comparison method, is a systematic decision-making technique designed to assess and prioritize the relative importance of multiple decision criteria. AHP is grounded in the principles of decomposition, comparative judgments, and priority synthesis, offering a structured framework to assign weights to these criteria. It accommodates various factors, including qualitative and quantitative elements, and tangible and intangible aspects (Saaty, 1977).

In the AHP framework, decision criteria are organized hierarchically, with each level of the hierarchy representing a specific aspect of the decision process (Bukhsh et al., 2017). The AHP process commences with pairwise comparisons of decision criteria to determine their respective weights, which reflect their relative significance in the decision-making process. To facilitate these comparisons, a structured system is used, as shown in Table 2.4, where values are assigned to represent the degree of importance or preference between two criteria:

Table 2.4: Pairwise Comparison Ratio for Weighting

Importance Level	Description	Assigned Value
Equal Importance	When criteria X and Y hold the same level of importance	1
Slightly More Important	If criteria X is slightly more important than criteria Y	3
Moderately More Important	If criteria X is moderately more important than criteria Y	5
Strongly More Important	If criteria X is strongly more important than criteria Y	7
Extremely More Important	If criteria X is extremely more important than criteria Y	9
Slightly Less Important	If criteria X is slightly less important than criteria Y	1/3
Moderately Less Important	If criteria X is moderately less important than criteria Y	1/5
Strongly Less Important	If criteria X is strongly less important than criteria Y	1/7
Extremely Less Important	If criteria X is extremely less important than criteria Y	1/9

2.5.3 (f) Value swinging

The value swinging method (Goicoechea, 1982) offers a systematic approach to addressing MCDM. This method involves envisioning a scenario in which all performance criteria are at their lowest possible values. The goal is to identify the criterion for which it is the most advantageous to transition from its worst value to its best value while keeping all other criteria at their worst levels. This step is repeated for all criteria under consideration.

To assign weights to the criteria, the most critical criterion is given the highest weight within a specified range (e.g., a range of 1 to 100, with 100 being the highest weight). Subsequently, the remaining criteria are assigned weights in proportion to their rank in importance. This systematic approach ensures that the most crucial criteria receive the greatest emphasis in the decision-making process, which means it is a valuable tool for evaluating complex scenarios with multiple criteria (Bai et al., 2008; Sinha & Labi, 2007).

2.5.3 (g) Delphi Approach

The Delphi method is a valuable approach for determining the relative importance of criteria, particularly in situations in which existing knowledge is limited or unavailable (Nasa et al., 2021). This method engages a panel of experts in a collaborative process aimed at reaching a consensus regarding the significance of various criteria. The Delphi approach unfolds across a series of distinct phases that incorporate expert perspectives, thereby creating a structured feedback loop that facilitates the process of consensus-building.

To address the necessity for building consensus and achieving a comprehensive assessment, the Delphi technique (Dalkey & Helmer, 1963) has proven to be suitable for group decision-making and serves the purpose of aggregating the viewpoints of individual experts (Bendaña et al., 2008; Cavalli-Sforza & Ortolano, 1984; de la Cruz et al., 2008). Within the Delphi technique, the initial results obtained from questionnaire surveys undergo thorough analysis and summarization. The summary statistics obtained, which include parameters such as the average and standard deviation, are then conveyed to the survey participants. In response, the participants review their initial responses based on the summary statistics. This step provides the experts with the flexibility to adjust the weights they initially assigned based on the feedback received. This iterative process continues until no further alterations occur in the scores (Sinha & Labi, 2007)

One significant advantage of the Delphi method is its approach to interaction management (Martino, 1983; Mullen, 2003). Interaction within the Delphi process is entirely anonymous (Sourani & Sohail, 2015), allowing participants to successively change their opinions without publicly disclosing such changes. This anonymity allows participants to alter their opinions without the need for public disclosure, fosters an environment that encourages candid input by focusing solely on the value of ideas, and minimizes the potential negative impacts associated with committee dynamics, such as group pressure, status, and dominant personalities. However, anonymity also has its disadvantages, including the lack of accountability for expressed views and potential limitations on exploratory thinking and idea generation (Mullen, 2003).

2.5.4 Scaling Methods

In MCDA, scaling is the step that ensures that the criteria are transformed into a common scale or range that makes the different criteria directly comparable. Scaling serves to standardize data and harmonize the measurement levels of various criteria, thereby facilitating analysis, weighting, and amalgamation.

Scaling is indispensable when working with diverse criteria that may contain different units or measurement scales, as is frequently the case in decision-making scenarios. Two main categories of scaling methods include certainty and risk scenarios, each of which is suitable for specific contexts (Labi, 2014).

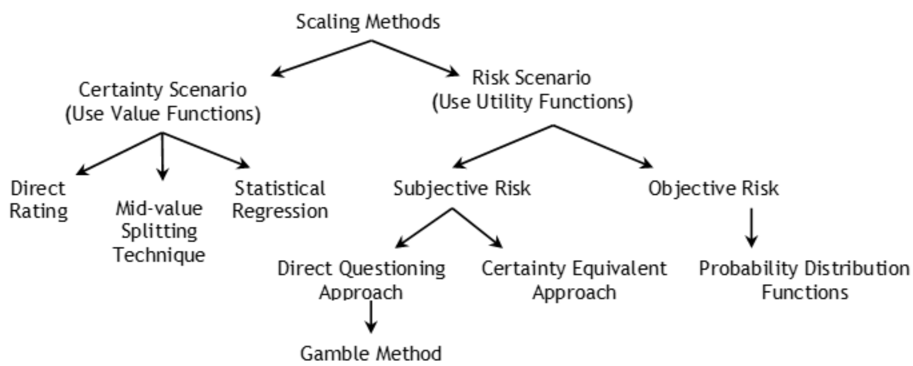

Figure 2.13: Scaling Categories with some existing methods (Sinha & Labi, 2007)

2.5.4 (a) Decision-Making Under Certainty Scenarios

Decision-making under certainty is characterized by having complete and precise knowledge of the consequences (in terms of the multiple criteria) associated with each alternative. In such a scenario, DMs can rely on methods that effectively capture, construct, or quantify their preferences regarding the levels of each performance criterion. These methods play a role in facilitating decision-making by providing a structured approach to comparing the alternatives.

As the outcomes of each alternative are known with absolute certainty, this scenario ensures that the decision-making process aligns closely with the DMs' preferences, allowing for a more straightforward and objective selection of the most favorable alternative based on the established criteria. In the certainty scenarios, value functions or deterministic scaling functions are used to quantify the desirability of the criteria (Bai et al., 2008).

The scaling methods that fall under certainty scenarios draw from value theory (Keeney & Raiffa, 1993) and rely on the concept of value functions, which are scalar indices representing DMs' preferences for various levels of a performance criterion under conditions of certainty. In practical terms, if a scale that ranges from 0 to 100 is considered, then the values 0 and 100 are associated with the worst and best levels of the criterion, respectively. The values assigned to intermediate levels are determined by the DMs themselves. These value functions serve as mathematical representations of the DMs' preference structure and can assume linear or nonlinear forms. This mathematical representation captures the DMs' preference structure, allowing for a systematic evaluation of alternatives.

The multivariate value function, denoted as v(z), is expressed as the following (Patidar et al., 2007):

$$v(\boldsymbol{z}) = v(z_1, z_2, ..., z_p)$$

where ***z*** symbolizes the consequence set of an alternative in terms of evaluating criterion *p*. The consequence set encompasses the anticipated outcomes across the evaluation criteria after the decision is executed. Notably, the value function possesses a property (Keeney & Raiffa, 1993), which makes it useful for addressing tradeoffs between pairs of evaluation criteria.

The techniques that are used to construct value functions under certainty scenarios are explained in this subsection. The methods include the mid-value splitting technique, direct rating, and statistical regression. The methods are flexible and can be adapted to different criteria and decision contexts (Sinha & Labi, 2007).

2.5.4 (a.1) Direct Rating

The direct rating method is a straightforward approach that often uses questionnaire surveys to generate value functions. In this method, respondents, who are typically the DMs, are asked to directly assign values to each level of a given performance criterion. This technique is useful when addressing criteria that have a relatively small number of discrete levels and when DMs can be questioned directly using some form of survey instrument. This method allows DMs to provide their direct input in the form of value assignments, facilitating the construction of value functions (Hobbs & Meier, 2000). Its simplicity and effectiveness make direct rating an excellent choice for evaluations.

2.5.4 (a.2) Mid-Value Splitting Technique

The mid-value splitting technique seeks information from survey respondents regarding their indifference towards changes in the levels of a performance criterion (Keeney & Raiffa, 1993). This method is well-suited for criteria with a broader domain of possible levels. It helps in capturing the perspectives of DMs concerning the points at which they are indifferent to changes in the performance criterion, thereby enabling the development of value functions that reflect these preferences.

The method, executed through a questionnaire survey involving the DM, unfolds as an interactive conversation between the survey administrator and the respondent, who is the DM.

During this process, DMs are prompted to express the degree of their indifference concerning various levels of the performance criterion. The extent of their indifference is captured by the concept of "equal delight" or "zero relative desirability" between the two specified levels.

To establish the value function of a performance criterion X, with a potential value range from X_L to X_U units, the steps are as follows:

Step 0: Set $v(X = X_L) = 0$ and $v(X = X_U) = 100$

Step 1: Establish X_{50} for which $v(X_{50}) = 50$

Establish X_{50} such that the survey respondent is equally delighted with (i) and (ii) as follows:

(i) is an improvement of X from 0 to X_{50} and (ii) is an improvement of X from X_{50} to X_U

Step2: Establish X_{25} for which $v(X_{25}) = 25$

Establish X_{25} such that the survey respondent is equally delighted with (i) and (ii) as follows:

(i) is an improvement of X from 0 to X_{25} and (ii) is an improvement of X from X_{25} to X_{50}

Step 3: Establish X_{75} for which $v(X_{75}) = 75$

Establish X_{75} such that the survey respondent is equally delighted with (i) and (ii) as follows:

(i) is an improvement of X from X_{50} to X_{75} and (ii) is an improvement of X from X_{75} to X_U

Step 4: Consistency check

Is the survey respondent equally delighted with (i) and (ii) as follows:

(i) is an improvement of X from X_{25} to X50 and (ii) is an improvement of X from X_{50} to X_{75}?

Step 5: Adjustments

If the consistency check is affirmative, the values are consistent and, if not, DMs are to revise their responses in steps 1–3.

Based on these established values, the value function for the performance criterion can be constructed. This simple and practical mid-value splitting technique proves helpful for assessing value functions, especially in scenarios in which resource constraints limit the adoption of more complex methods.

2.5.4 (a.3) <u>Statistical Regression</u>

Refer to Section 2.5.4 (b.3) for information regarding statistical regression.

2.5.4 (b) Decision Making Under Risk Scenario

Decision making under risk is when the decision problem contains significant uncertainty. Unlike certainty-based scenarios, in which precise outcomes are known, the risk-based approach introduces intricacies by associating specific probabilities with the consequences of each alternative regarding the decision criteria (Patidar et al., 2007). This scenario, involving uncertainty regarding the outcomes of decisions, is relevant in some fields such as transportation because organizations often face challenges in accurately predicting the specific results of their decisions, whether they involve a physical intervention or a policy change (Sinha & Labi, 2007).

As such, it is useful, possibly even necessary, for agencies to incorporate risk and uncertainty concepts in scaling their evaluation criteria. In the risk scenario, the range and distribution of possible outcomes for each performance criterion are known. Risk is either subjective or objective. Subjective risk is based on personal perceptions, and objective risk is based on theory, experiment, or observation. In the uncertainty scenario, the range and distribution of possible outcomes for each performance criterion are unknown.

Utility functions are used for scaling evaluation criteria when there is uncertainty or risk in the problem. The DM specifies a certain level of “desirability” (or “utility”) for each decision outcome in terms of each performance criterion, and the expected overall utility of each alternative decision is calculated. The best intervention is that which yields the maximum expected utility (Keeney & Raiffa, 1976). By providing a scale showing the DMs’ preferences for different levels of a performance criterion, a utility function implicitly captures the risk preferences of the DMs for levels of the criterion. The risk behavior of the DM can be ascertained from the utility function shape and parameter values (Figure 2.14). A DM inclined toward risk-taking exhibits a strictly convex utility function, a risk-averse DM demonstrates a strictly concave utility function, and a risk-neutral DM shows a linear utility function (Winston, 1999).

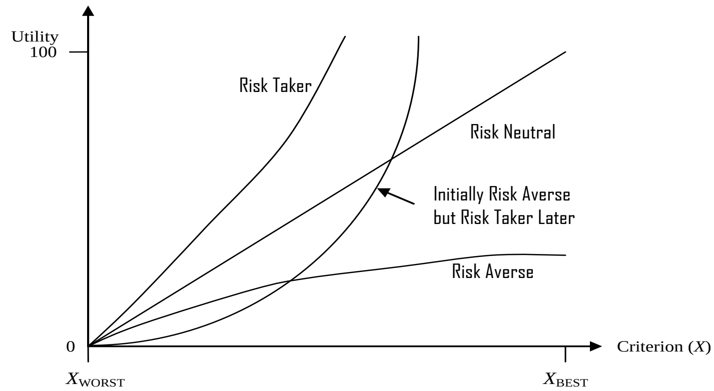

Figure 2.14: Different Risk Behaviors of Decision Makers (Sinha & Labi, 2007)

The concepts of utility and multi-attribute utility theory prove to be valuable for addressing decision-making problems marked by risk and uncertainty. Utility is treated as a random variable, and the “expected utility” represents the mean of the random variable. DMs specify the level of “desirability” or “utility” for each potential outcome of an action. By assigning suitable utility values to these outcomes and calculating the expected utility for each alternative, it becomes possible to identify the optimal course of action. The alternative with the highest expected utility is chosen as the most preferable option (Keeney and Raiffa, 1976).

The multi-attribute theory can be applied using the following steps (Goicoechea, 1982):

1. Formulate suitable assumptions regarding the preferences of the DM.
2. Determine an appropriate mathematical representation based on these assumptions.
3. Validate the assumptions by incorporating the DM's perceptions.
4. Develop preference rankings, also known as utility functions, for each performance criterion.
5. Integrate individual criterion utility functions using the established mathematical representation and considering the relative weights assigned to each criterion.
6. Establish a preference ranking for alternatives based on their expected utilities.

A utility function is a general form of a value function. This means that a value function is a specific form of a utility function in which the degree of uncertainty is 0%. A multi-attribute utility function captures DMs’ preferences regarding the levels of each decision criterion. It extends the concept of a value function but also captures the DMs’ risk preferences for various levels of each attribute. The expected values of the utility function serve as a basis for comparing alternatives. The alternative with the maximum expected utility is identified as the most preferable alternative. However, as noted by Patidar et al. (2007), constructing multi-attribute functions can be exceptionally challenging due to the multiplicity of dimensions.

To manage this complexity, an alternative approach is often used. Instead of attempting to reduce dimensionality through a multi-attribute function, several single-criterion (univariate) utility functions are developed individually (Goicoechea, 1982; Patidar et al., 2007).

In a risk scenario, risk can either be subjective or objective. Subjective risk is shaped by personal perceptions, reflecting an individual's subjective judgment of the likelihood and impact of various outcomes. In contrast, objective risk is grounded in more tangible sources such as established theories, empirical experiments, or observed data. Objective risk relies on more concrete and measurable foundations, which contrasts with the more personal and interpretive nature of subjective risk. The certainty equivalent approach and the direct questioning method fall within the subjective risk category and serve as indispensable tools for understanding DMs' risk-taking behaviors and preferences. Linear scaling, monetization, and probability distribution functions all fall within the objective risk category of the risk scenario. Objective risk methods are typically valuable in cases where the costs and benefits associated with criteria are inherently nonlinear and require a data-driven approach. The choice of scaling method depends on the nature of the criteria, the available data, and the context of the decision-making process.

2.5.4 (b.1) Certainty Equivalent Approach

The certainty equivalent approach is a method that enables a DM’s risk-taking behavior within a subjective risk situation to be identified. It establishes a connection between a DM’s single-criterion utility function and their risk attitude. This approach is valuable when confronting situations in which the exact consequences of actions are uncertain, and DMs must navigate a complex landscape of potential outcomes (Patidar et al., 2007). The approach provides insights into DMs’ attitudes toward risk and informs the decision-making process by shedding light on their risk preferences and willingness to embrace uncertainty.

2.5.4 (b.2) Direct Questioning Method

The direct questioning method is used within the risk-based scenario to directly collect information from DMs regarding their risk preferences and attitudes. DMs are surveyed or interviewed and asked to articulate their willingness to take risks, their risk tolerance, and their comfort levels with uncertainty. This method directly captures the subjective risk perceptions of DMs and plays a large role in developing a comprehensive understanding of their risk attitudes. The responses gathered through direct questioning are then used to develop utility functions and identify risk preferences, which are indispensable for making well-informed decisions under conditions of uncertainty.

The gamble method can be used in the direct questioning approach by developing a utility function for a performance criterion. The process begins by assigning utilities of $U(X_W) = 0$ for the worst level of the criterion and $U(X_B) = 100$ for the best level. The comparison involves two scenarios, a guaranteed prospect with an outcome of $X = 0.5 \times (X_B - X_W)$ and a risky prospect where an outcome of X_W occurs with probability p and an outcome of X_B with probability ($1 - p$; Bai et al., 2008; Labi, 2014; Sinha & Labi, 2007). The comparison is conducted by varying the probability parameter p until a threshold point is reached at which survey respondents' express indifference between the guaranteed and risky prospects. The process is iteratively applied for all other levels of the criterion.

2.5.2 (b.3) Probability Distribution Functions

This method of scaling falls under the objective risk category. The methods in this category do not involve subjective preferences and are data driven. These methods focus on objective and quantifiable data, enabling the transformation of criteria into a standardized format. The methods are often used when it is challenging to collect or incorporate subjective opinions or when a more objective approach is required.

Probability distribution functions do not consider the subjective opinions of the DMs and tend to be superior for making decisions in which the DMs input is of the utmost relevance (Bai et al., 2008; Patidar et al., 2007). The functions aim to transform the raw data associated with various criteria into a common and standardized scale, ensuring that all criteria are directly comparable.

Some common methods are min-max normalization, z-score normalization, decimal scaling, and absolute mean and zero-deviation.

One of the simplest and most widely used objective techniques is min-max normalization, which is effective when the upper and lower bounds (maximum and minimum values) of decision model scores are known. In such cases, it is relatively straightforward to adjust the minimum and maximum scores to a common range between 0 and 1. It is important to note that min-max normalization retains the original distribution of scores while rescaling them into a common range (Jain et al., 2005). Z-score normalization is an effective normalization method that transforms all input values into a common measure, ensuring a standardized data set with an average of zero and a standard deviation of one (Adeyemo et al., 2019). This procedure involves calculating the mean and standard deviation for each attribute, followed by individual normalization using these calculated statistics. The method's advantage lies in its ability to mitigate the impact of outliers, thereby rendering it suitable for datasets with varying levels of variability and unknown data distributions.

To address the limitations of traditional min-max normalization, the median absolute deviation normalization method is proposed. It is notable for its adaptability to data of varying sizes, robustness against outliers, and straightforward implementation. median absolute deviation normalization aligns data with a median of 0 and a median absolute deviation of 1, thus, effectively enhancing its suitability for analysis while minimizing issues such as multicollinearity (Kappal, 2019).

Decimal scaling, an alternative technique, serves as a data transformation method similar to conventional z-score normalization. This method adjusts the number of decimal points for each attribute value based on the highest number of placeholders among all columns (Sinsomboonthong, 2022). It is beneficial for logarithmic scale data by ensuring that scores are consistently scaled for comparative analysis. Decimal scaling assumes logarithmic scaling, which may not always hold true in diverse decision-making scenarios.

Similarly, the absolute mean and zero-deviation normalization method (Patro & Sahu, 2015) operates within the range of 0 to 1 and employs individual element scaling, processing each data point separately. Unlike some normalization techniques, absolute mean and zero-deviation is not dependent on data size or quantity and is exclusively applicable to integer numbers.

PDF-based methods provide a systematic way to make criteria directly comparable and are effective when coping with known and measurable criteria. However, they do have limitations. These limitations include their lack of adaptability to data with varying characteristics, sensitivity to outliers, assumptions of normality, limited customization options, challenges in handling missing data, and reduced flexibility in accommodating diverse decision-making scenarios. In situations in which decision criteria exhibit a high degree of variability or where specific requirements and preferences need to be considered, more flexible scaling methods may be preferred over these objective techniques to ensure a more accurate representation of the data.

2.5.5 Amalgamation Methods

Amalgamation, a crucial step in the MCDA process, serves as the point at which various decision alternatives undergo evaluation after individual performance criteria have been weighted and scaled (Bukhsh et al., 2017; Sinha & Labi, 2007). Its primary aim is to consolidate the numerous criteria into a unified criterion for each alternative, thereby facilitating the identification of the most favorable alternative or the ranking of the alternatives (Bell et al., 2003; Patidar et al., 2007).

Several methods are available for amalgamation in MCDA. These include the multiplicative utility function method, the weighted sum method (WSM), the weighted product model (WPM) method, the AHP method, the ELECTRE method, the goal programming method, the TOPSIS (Technique for Order Preference by Similarity to Ideal Solution) method, the global criterion or compromise programming method, the neutral compromise solution method, and the lexicographic order technique. These methods offer a wide spectrum of tools and techniques for DMs to choose from, each with its own advantages and limitations.

2.5.5 (a) Weighted Sum Method

This method is a widely adopted approach for amalgamating multiple criteria into a single unified criterion for each alternative (Li, 2003). In this method, the determination of relative weights for individual criteria is a critical consideration. It is important to note that the WSM, although user-friendly, offers only a linear approximation of the preference function. Consequently, the solution derived using this method may not faithfully preserve the DM's initial preferences, regardless of how the weights are configured (Marler & Arora, 2010). Additionally, an essential condition for the validity of the WSM must be considered, that is, that the values of the criteria remain linearly independent. This implies that the value assigned to each criterion should remain unaffected by or independent of the values assigned to other criteria. Failure to meet this condition could render the WSM incapable of producing a valid solution (Hazelrigg, 2019).

2.5.5 (b) Weighted Product Model

The WPM (Bridgman, 1922; Triantaphyllou & Mann, 1989) is a widely used technique in MCDA (Cristóbal, 2012; Mateo, 2012) that builds upon the WSM (Goswami et al., 2020). In the WPM, each alternative's assessment relative to the other alternatives is achieved by multiplying ratios, with each corresponding to a specific decision criterion.

This methodology first involves the distribution of weights to criteria, the normalization of performance values, and the subsequent calculation of preference scores by multiplying the normalized values with the assigned weights (AlAli et al., 2023). The effectiveness of WPM in addressing MCDM is well-established, with successful applications across a diverse range of scenarios involving various criteria (Supriyono & Sari, 2018; Triantaphyllou & Mann, 1989).

2.5.5 (c) Multiplicative Utility Function Method

In the foundational work on multi-criteria or multi-attribute utility theory (MAUT), Keeney and Raiffa (1976), presented a framework that leverages the concept of independence among attributes, leading to the development of the multiplicative multi-attribute utility function denoted as $u_M(z)$, which is given by the following:

$$u_M(\mathbf{z}) = \frac{1}{k}\left(\prod_{i=1}^{n}\left(1 + kk_i u_i(z_i)\right) - 1\right)$$

In this expression, $z = (z_1, ..., zn)$ represents evaluations, z_i signifies attribute evaluations, k_i represents the weight assigned to the ith criterion, and k is a scaling constant.

To effectively apply the multiplicative model, it is essential to ensure mutual utility independence. This means that subsets of criteria should be independent of their complements. (Dombi, 2009). The multiplicative MAUT model is a versatile tool, proficient in representing complex preference structures, embracing nonlinearities, and accounting for attribute interactions without reliance on unrealistic behavioral assumptions (Keeney & Raiffa, 1976). The optimal choice is determined by selecting the alternative with the highest overall utility, aligning with the utility-based approach, thereby yielding the best decision outcome (Labi, 2014).

2.5.5 (d) ELimination Et Choix Traduisant la REalité (ELECTRE) Method

The use of traditional aggregation methods in MCDA can yield results that are sensitive to score variations and the construction of individual indicators. In some cases, different composite indicators may favor one alternative over another (Josselin & Le Maux, 2017). To address this sensitivity and the need for a more rigorous approach, non-compensatory analysis has gained prominence. This methodology relies on pairwise comparisons of alternatives based on individual indicators, which has proved effective in sorting problems. While discussions have occurred that categorize ELECTRE as partially compensatory, it has been positioned within the non-compensatory subgroup, highlighting its distinctiveness within MCDA (Taherdoost & Madanchian, 2023). This distinctive feature makes ELECTRE a valuable alternative in MCDA, as it offers a departure from traditional compensatory methods.

Within the domain of non-compensatory models, the outranking methods category is designed to establish relationships of outranking among different alternatives based on a set of varying criteria. Among these methods, ELECTRE-based methods are known for their effectiveness. ELECTRE aims to determine the hierarchy among alternatives through a structured procedure, where one alternative is deemed superior to another only if it meets specific conditions (Li, 2003).

The primary condition relates to the concordance index, which is the sum of normalized weights favoring the first alternative. To meet this condition, the concordance index must surpass a predefined threshold value. The second condition pertains to the discordance index, signifying the number of attributes in which the second alternative outperforms the first by an amount exceeding a specified threshold value. To meet this condition, the discordance index should be zero (Josselin & Le Maux, 2017; Li, 2003).

ELECTRE excels in complex decision-making scenarios with a substantial number of criteria, often exceeding the typical threshold of five and extending to as many as 12 or 13 criteria. It effectively addresses the intricacies of these settings, managing challenges with which conventional compensatory methods may struggle. For example, ELECTRE is extremely effective when actions are evaluated using ordinal scales for at least one criterion. The use of ordinal scales poses challenges in establishing meaningful coding for preference differences. ELECTRE's non-compensatory nature makes it suitable for addressing these situations (Martel et al., 1988).

Furthermore, ELECTRE proves to be effective in situations that are characterized by significant heterogeneity among the scales associated with the criteria. These criteria often span a wide range of measurement scales, making it impractical to establish a uniform and common scale for comparison (Figueira et al., 2016; Taherdoost & Madanchian, 2023). For DMs averse to accepting tradeoffs between criteria, ELECTRE's non-compensatory aggregation procedures are indispensable (Taherdoost & Madanchian, 2023).

2.5.3 (e) Technique for Order Preference by Similarity to Ideal Solution (TOPSIS) Method

The TOPSIS method has garnered significant attention within the field of MCDM, thereby proving its versatility and effectiveness (Behzadian et al., 2012; S.-J. Chen & Hwang, 1992; Hwang & Yoon, 1981). This method aims to identify the most favorable alternative by assessing its proximity to the ideal solution and its divergence from the worst solution, ultimately leading to a comprehensive evaluation of each alternative (Papathanasiou & Ploskas, 2018).

TOPSIS operates under the assumption that each criterion's preference structure follows either a monotonically decreasing or increasing pattern, signifying "the more, the better" or "the fewer, the better," respectively. This fundamental characteristic equips TOPSIS to handle a wide range of decision-making scenarios in which criteria exhibit diverse and contrasting preferences, making it an invaluable tool in MCDA (Labi, 2014).

Over time, the TOPSIS methodology has undergone extensive experimentation and refinement, particularly in areas such as normalization procedures, the accurate determination of ideal and anti-ideal solutions, and the selection of appropriate metrics for calculating distances from these solutions (Papathanasiou & Ploskas, 2018). These refinements have further enhanced the applicability and robustness of the TOPSIS method in various practical settings.

2.5.3 (f) Global Criterion (Compromise Programming) Method

The global criterion or compromise programming method (Yu, 1973) offers a unique perspective on MCDM. It focuses on the identification of the optimal solution that minimizes its distance from the global reference point (GRP), which embodies the global optimal values of all decision criteria (Miettinen, 1998). The GRP serves as a comprehensive reference point for assessing the feasibility of alternative solutions.

This distinctive approach has gained significance in MCDM by enabling the prioritization and selection of alternatives based on their proximity to the GRP. As a result, it facilitates effective decision-making in complex scenarios (Cochrane & Zeleny, 1973; Miettinen, 1998; Yu, 1973). The method not only aids in selecting the most suitable alternative but also promotes a balanced consideration of all relevant criteria, thus, contributing to well-rounded and robust decision outcomes.

By following this unique approach, DMs can systematically assess a wide range of decision alternatives, considering the importance of each criterion and striving to strike a balance among these considerations. With decisions becoming increasingly complex and involving multiple, and often conflicting, objectives, the global criterion or compromise programming method offers an effective way to navigate the complexities of decision-making, making it a valuable tool in MCDM (Cochrane & Zeleny, 1973; Miettinen, 1998).

2.5.5 (g) Neutral Compromise Solution Method

The neutral compromise solution method (Gal et al., 2013) is similar to the global criterion method but differs in its underlying assumption regarding the ideal solution. In this approach, it is assumed that the optimal performance target or ideal solution is positioned at the midpoint within the range of possible values for each performance objective (Setämaa-Kärkkäinen et al., 2006). Consequently, the objective is to find the alternative that minimizes the maximum deviation from this midpoint for each performance objective, subject to the constraint that the alternative falls within the decision space.

The simplicity of this method is one of its key advantages, providing DMs with a straightforward approach to optimize decision alternatives. However, it is important to recognize that the assumption of the ideal performance level at the midpoint can be overly restrictive or impractical in real decision scenarios. Nonetheless, this method offers a structured approach that can prove valuable in decision-making, particularly when the midpoint ideal solution assumption holds (Branke, 2008).

2.5.5 (h) Lexicographic Order Technique

In the lexicographic order method (Fishburn, 1974), DMs exercise control over objective functions according to their absolute interests. This approach involves a systematic optimization process in which each objective is addressed in a predetermined order of importance. Initially, the highest-priority objective is optimized, and the method checks whether it yields a unique solution. If a unique solution emerges, it is considered optimal. However, if multiple solutions arise, the process proceeds to the second objective, along with new constraints derived from the outcome of the first objective. This sequential process continues until all objectives are considered, enabling DMs to make well-structured choices based on their hierarchical objective preferences (Gunantara, 2018).

The method offers a systematic approach for MCDM without using complex mathematical models. It begins by assigning weights to each decision criterion. The first step involves identifying the most significant criterion and determining the value for each alternative with respect to this primary criterion. The alternatives are compared with reference to the primary criterion to identify the optimal alternatives. If a single alternative obviously has the best value for the primary criterion, it is selected as the optimal solution. However, if multiple alternatives share the same optimal value for the primary criterion, their performance is further assessed based on the second most important criterion. This iterative process continues until only one solution remains or all the criteria have been considered (Fishburn, 1974).

Despite its simplicity and user-friendliness, the lexicographic order method presents two notable limitations (Branke et al., 2008). Firstly, assigning ranks and importance to decision criteria can prove to be a challenging task for DMs. Secondly, the method may prematurely conclude without a comprehensive evaluation of other criteria apart from the most important one. In situations where a single alternative excels in terms of the primary criterion, the evaluation of other alternatives may cease, even if the chosen solution performs poorly in most of the other decision criteria (Labi, 2014). To use the lexicographic method effectively, DMs must define preferences to establish the lexicographic order of the objectives. However, determining these preferences can be a challenging task (Castro-Gutierrez et al., 2010).

2.6 Summary of the Literature Review

Table 2.5 summarizes the literature closely related to this thesis's subject matter and study objective, and Table 2.6 summarizes the MCDM methods.

Table 2.5: Summary of LiDAR placement approaches

Reference	Subject Matter	Study Objective
(Mou et al., 2018b)	Optimal LiDAR Placement	The Sparsity and discreteness of LiDAR was considered in defining an ROI. The ROI was further subdivided into smaller conical subspaces and presented as a non-linear optimization issue.
(T.-H. Kim & Park, 2020)	Placement Optimization of Multiple LiDAR sensors or AV	In order to maximize the point cloud density and minimize the dead zone, a Probability Occupancy Grid was introduced. A genetic algorithm was developed to carry out experiments. The results show that placement improves perception performance in AV.
(Hu et al., 2022)	Investigating Multi-LiDAR Placement on Object detection performance in AV	The ROI of the LiDAR was modelled as a cuboid similar to (Mou et al., 2018b). The cuboid was further subdivided into voxels. The LiDAR placement was evaluated by using proposing a Probability Occupancy Grid. The experiments were conducted using CARLA.
(Kini, 2020)	Sensor Position Optimization for Multiple LiDARs in AVs	The point cloud density i.e., LiDAR Occupancy is maximized and used as an objective function to minimize the dead zone (blind spots). The environment used for the experiment is CARLA using some algorithms from Point Cloud Library (PCL) and the ROI is defined using LiDAR occupancy boards (LOB).
(Dybedal & Hovland, 2017)	Optimal Placement of 3D Sensors considering Range and Field of view	A mixed integer linear programming framework was used to address the challenge of determining the best placement for 3D sensors. The space covered by each sensor is represented as a cone, considering limitations in both field of view and range. This cone model is subsequently divided into smaller cubes, and constraints are established to resolve the optimization problem.
(Domínguez et al., 2011)	LiDAR Based Perception Solution for AVs	Different obstacles are perceived and tracked based on real world acquired photos and LiDAR point clouds. The task is classified into four phases. i.e., Segmentation, fragmentation detection, clustering, and tracking.
(Berens et al., 2022)	Genetic Algorithm for the Optimal LiDAR sensor configuration on a vehicle.	This paper considers redundancy and the shape of the car to propose a genetic algorithm that finds the optimal position of multiple sensors concurrently. The environment used for the experiment is CARLA by setting up the Region of Interest as a cylinder with the height and radius depending on what the car is applicable for.

Table 2.6: Summary of MCDA methods

Method	Summary
AHP (Analytic Hierarchy Process)	Hierarchical decision-making method using pairwise comparisons to derive priority scales, facilitating complex decisions by breaking them down into simpler pairwise comparisons.
ELECTRE (ELimination Et Choix Traduisant la REalité)	Outranking method that assesses alternatives based on criteria and assigns ranks using concordance and discordance indices, allowing for the identification of preference relations.
TOPSIS (Technique for Order Preference by Similarity to Ideal Solution)	Compares alternatives based on their distance to the ideal and anti-ideal solutions, ranking them by their proximity to the best solution and farthest from the worst solution.
MAUT (Multi-Attribute Utility Theory)	It assesses alternatives by analyzing their utility functions for each criterion. This allows for comparing alternatives using utility values obtained from individual preferences.
Weighted Sum Model	Aggregates scores by multiplying criterion scores by respective weights and summing them to rank alternatives based on their total weighted scores.
WPM (Weighted Product Model)	Ranks alternatives by multiplying the ratings of each alternative across criteria by their respective weights and aggregating these products to determine the best alternative.

CHAPTER 3. METHODS AND EXPERIMENTAL SET UP

3.1 Multi-Criteria Decision Framework

Figure 3.1 presents the steps of the multi-criteria decision framework. The first step is to establish the relevant alternatives for the LiDAR sensor placement. The next step is criteria identification. The criteria considered in this thesis consist of the point density, blind spot area, sensor cost, power consumption, ease of installation, sensor redundancy, and aesthetics. The next step is the weighting, whereby the relative levels of importance across the criteria are established. A direct weighting approach, executed through a questionnaire, is utilized to provide a clear understanding of the significance of each criterion in the decision-making process.

Subsequently, the different criteria are scaled using value functions. This process harmonizes diverse metrics and criteria, thus, transforming performance evaluations into a unified scale. This standardization facilitates meaningful comparisons among alternatives, particularly given the different measurement associated with each criterion. Following that, the amalgamation step integrates criteria weighting with the scaled performance evaluations. This process computes overall scores or rankings for each alternative, thereby delivering a clear assessment of their suitability. Finally, a decision is made based on the obtained results, which represent the top-performing LiDAR placement designs.

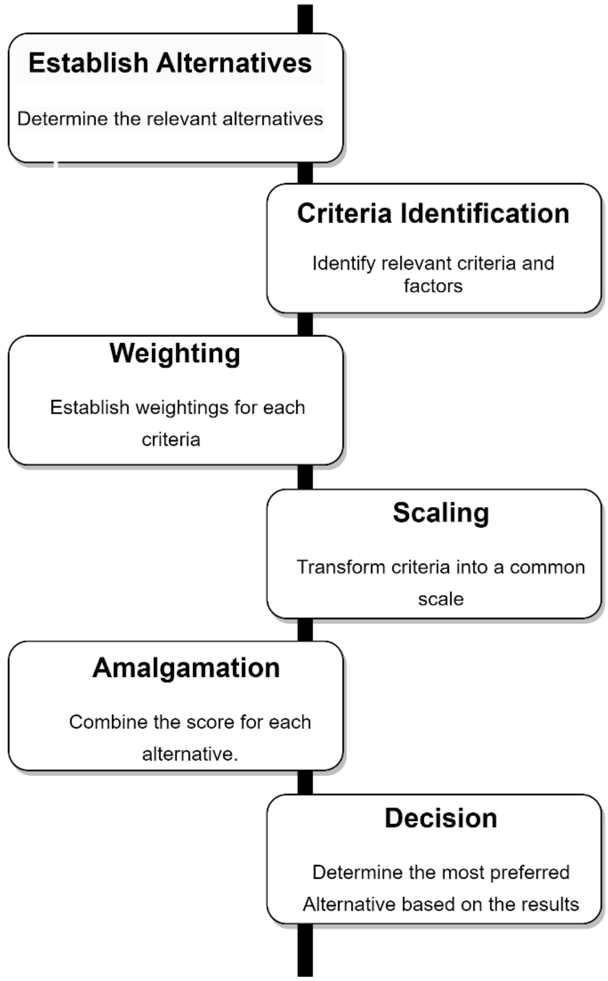

Figure 3.1: Multi-Criteria Decision Framework

3.1.1 Establishing Alternatives

This is the first phase of the methodology in which the alternatives are identified. A systematic approach was used to identify the different LiDAR placement alternatives to optimize the LiDAR placement for AVs. The initial step involved identifying key variables: LiDAR positions on the AV roof (Front left, front right, rear left, rear right, center, front, back, side left, side right), channel counts (16, 32, 64), sensor numbers (1, 2, 3, 4), and elevation (High – 20 inches, Low – 10 inches).

Figure 3.2 provides a visualization of the car's coordinate system, outlining the X, Y, and Z axes, which play an important role in understanding the LiDAR sensor placement on the roof of the AV. In this context, the four corners of the vehicle's roof are marked to designate the front left, front right, rear left and rear right positions on the vehicle. The center point is the center of the roof. Additionally, the top front location is situated between the front left and front right corners and the side left, and side right is between the front left and rear left and front right and rear right, respectively. These precise location references are used for the placement of the LiDAR sensors during each experiment within the experimental environment. Figure 3.2's delineation of the car's spatial dimensions and key reference points facilitated consistent and accurate sensor placement, ensuring that data collection and evaluation aligned with the naming convention for the alternatives.

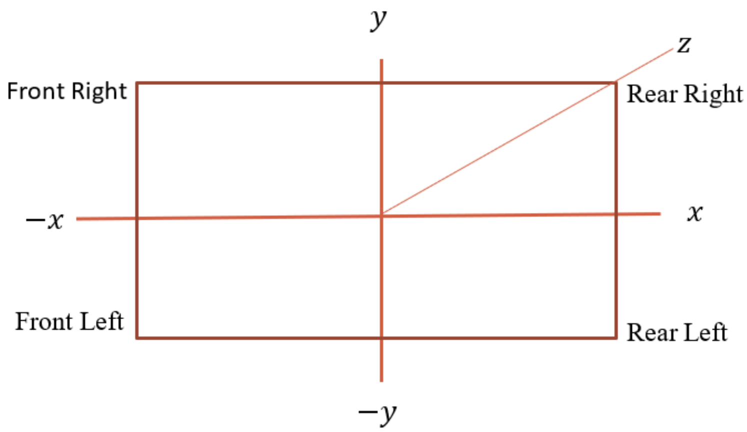

Figure 3.2: LiDAR placement Scenario for Roof of the Car

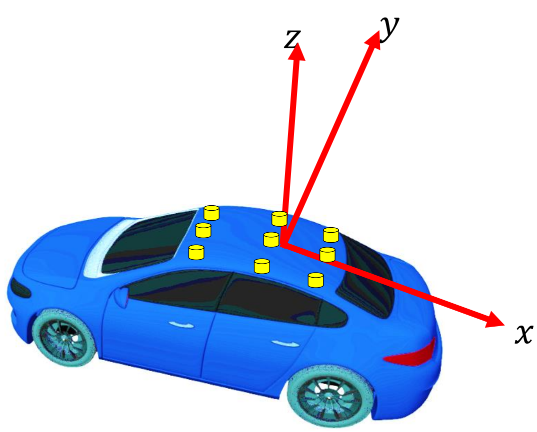

Figure 3.3: 3D representation of LiDAR placement Scenario for Roof of the Car

The LiDAR placement alternatives were developed through combining all the variables. This approach ensured the consideration of a broad range of placement scenarios. This was obtained by running a code that combines the different factors under consideration while retaining only unique placements. For example, for a single LiDAR sensor, reasonable placement positions included the front or center of the roof. With two sensors, suitable placements were at the front and back. Three LiDAR sensors could be positioned at the front, side left, and side right or front left, front right, and rear. For four sensors, options entailed front, rear, side left, and side right placements or front left, front right, rear left, and rear right (Figures 3.3 – 3.5).

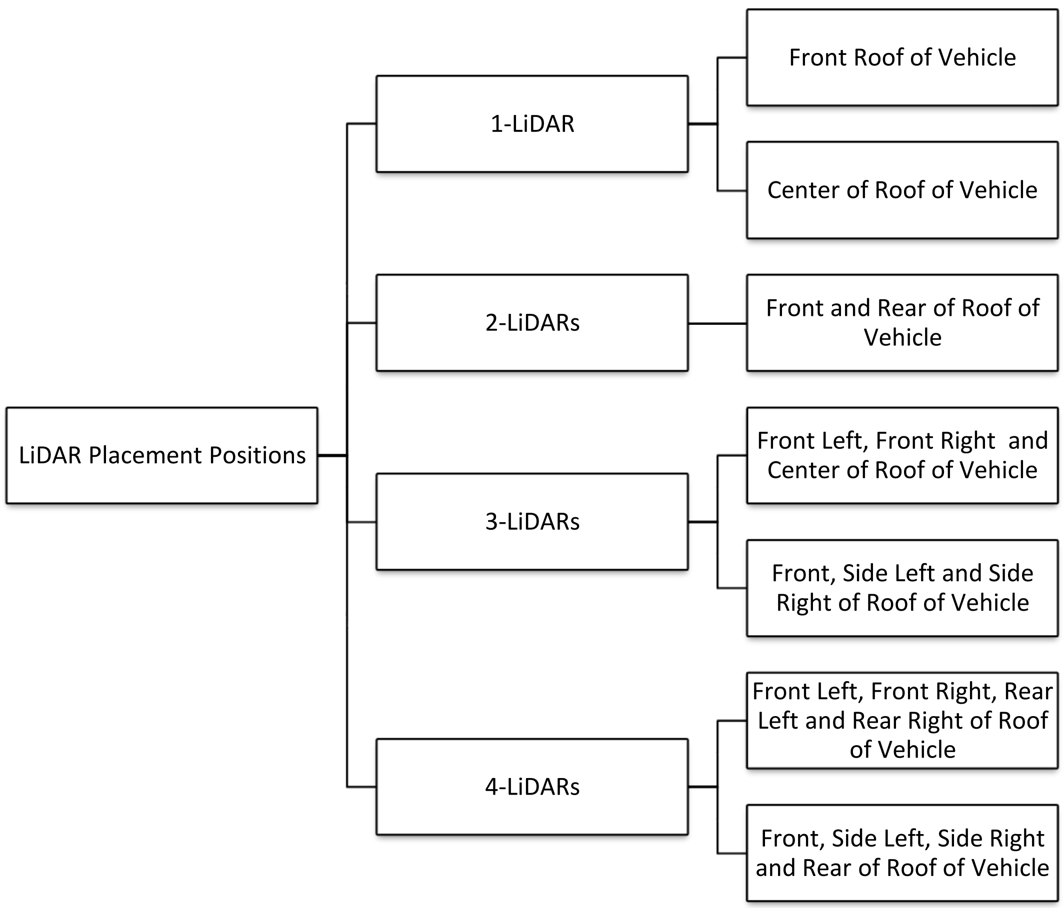

Figure 3.4: LiDAR Placement positions

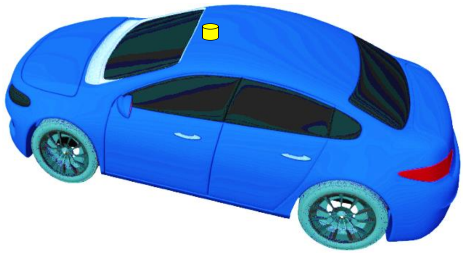

a. 1-LiDAR: Front Roof of vehicle

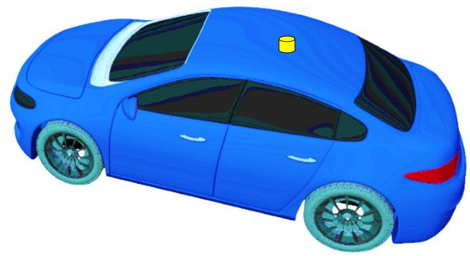

b. 1-LiDAR: Center of Roof of vehicle

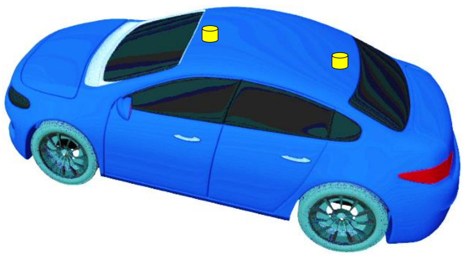

c. 2-LiDAR: Front and Rear of Roof of vehicle

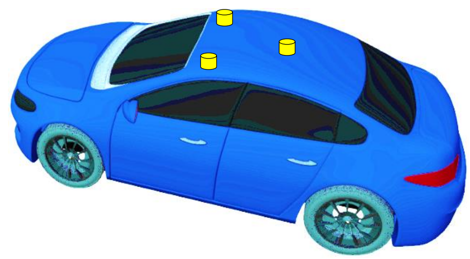

d. 3-LiDAR: Front Left, Front Right and Center of Roof of Vehicle

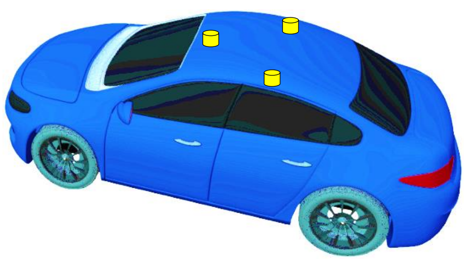

e. 3-LiDAR: Front, Side Left, and Side Right of Roof of Vehicle

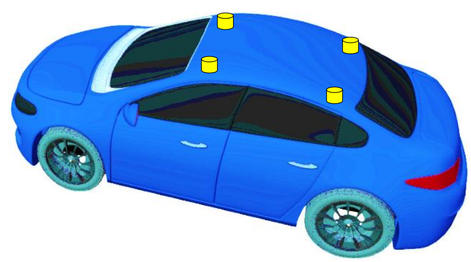

f. 4-LiDAR: Front Left, Front Right, Rear Left and Rear Right of Roof

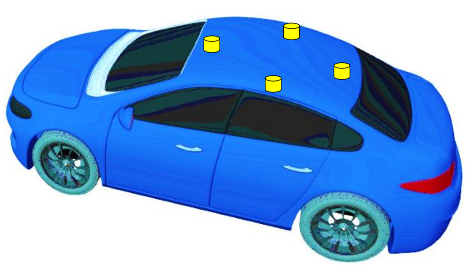

g. 4-LiDAR: Front, Side Left, Side Right and Rear of the Roof of Vehicle

Figure 3.5: 3D models of LiDAR (yellow color) placement options

Furthermore, channel counts were considered when additional sensors were positioned at the back. For example, in the three LiDAR sensor placement, all three sensors could have the same channel, (e.g., 32, 32, 32), or a scenario could exist in which the two sensors at the front had a higher channel, while the sensor at the back had a lower channel (e.g., 64, 64, 16). This consideration allowed for a reasonable approach to sensor configuration, ensuring compatibility and optimizing LiDAR placement. Placing a lower channel LiDAR at the front and a higher channel LiDAR at the back was deemed unreasonable, as objects ahead are of greater importance. These varying conditions played a role in refining the placements to include unique yet sensible alternatives. In total, the LiDAR placement alternatives were streamlined to 72 options, consisting of 12 one-LiDAR placements, 12 two-sensor placements, 24 three-sensor placements, and 24 four-sensor placements (Table 3.1).

Table 3.1: LiDAR Placement Alternatives

ID	LiDAR Number	Location on Roof of Vehicle	Elevation	Corresponding LiDAR Channels
1	1-LiDAR	Center	High	16
2	1-LiDAR	Center	High	32
3	1-LiDAR	Center	High	64
4	1-LiDAR	Center	Low	16
5	1-LiDAR	Center	Low	32
6	1-LiDAR	Center	Low	64
7	1-LiDAR	Front	High	16
8	1-LiDAR	Front	High	32
9	1-LiDAR	Front	High	64
10	1-LiDAR	Front	Low	16
11	1-LiDAR	Front	Low	32
12	1-LiDAR	Front	Low	64
13	2-LiDARs	Front, Rear	High	16-16
14	2-LiDARs	Front, Rear	High	32-32
15	2-LiDARs	Front, Rear	High	64-64
16	2-LiDARs	Front, Rear	Low	16-16
17	2-LiDARs	Front, Rear	Low	32-32
18	2-LiDARs	Front, Rear	Low	64-64
19	2-LiDARs	Front, Rear	High	32-16
20	2-LiDARs	Front, Rear	High	64-32
21	2-LiDARs	Front, Rear	Low	32-16
22	2-LiDARs	Front, Rear	Low	64-32
23	2-LiDARs	Front, Rear	High	64-16
24	2-LiDARs	Front, Rear	Low	64-16
25	3-LiDARs	Front Left, Front Right, Rear	High	16-16-16
26	3-LiDARs	Front Left, Front Right, Rear	High	32-32-16
27	3-LiDARs	Front Left, Front Right, Rear	High	32-32-32
28	3-LiDARs	Front Left, Front Right, Rear	High	64-64-16
29	3-LiDARs	Front Left, Front Right, Rear	High	64-64-32
30	3-LiDARs	Front Left, Front Right, Rear	High	64-64-64
31	3-LiDARs	Front Left, Front Right, Rear	Low	16-16-16
32	3-LiDARs	Front Left, Front Right, Rear	Low	32-32-16
33	3-LiDARs	Front Left, Front Right, Rear	Low	32-32-32
34	3-LiDARs	Front Left, Front Right, Rear	Low	64-64-16
35	3-LiDARs	Front Left, Front Right, Rear	Low	64-64-32
36	3-LiDARs	Front Left, Front Right, Rear	Low	64-64-64
37	3-LiDARs	Front, Side Left, Side Right	High	16-16-16
38	3-LiDARs	Front, Side Left, Side Right	High	32-16-16
39	3-LiDARs	Front, Side Left, Side Right	High	32-32-32
40	3-LiDARs	Front, Side Left, Side Right	High	64-16-16

Table 3.1 continued

41	3-LiDARs	Front, Side Left, Side Right	High	64-32-32
42	3-LiDARs	Front, Side Left, Side Right	High	64-64-64
43	3-LiDARs	Front, Side Left, Side Right	Low	16-16-16
44	3-LiDARs	Front, Side Left, Side Right	Low	32-16-16
45	3-LiDARs	Front, Side Left, Side Right	Low	32-32-32
46	3-LiDARs	Front, Side Left, Side Right	Low	64-16-16
47	3-LiDARs	Front, Side Left, Side Right	Low	64-32-32
48	3-LiDARs	Front, Side Left, Side Right	Low	64-64-64
49	4-LiDARs	Front Left, Front Right, Rear Left, Rear Right	High	16-16-16-16
50	4-LiDARs	Front Left, Front Right, Rear Left, Rear Right	High	32-32-16-16
51	4-LiDARs	Front Left, Front Right, Rear Left, Rear Right	High	32-32-32-32
52	4-LiDARs	Front Left, Front Right, Rear Left, Rear Right	High	64-64-16-16
53	4-LiDARs	Front Left, Front Right, Rear Left, Rear Right	High	64-64-32-32
54	4-LiDARs	Front Left, Front Right, Rear Left, Rear Right	High	64-64-64-64
55	4-LiDARs	Front Left, Front Right, Rear Left, Rear Right	Low	16-16-16-16
56	4-LiDARs	Front Left, Front Right, Rear Left, Rear Right	Low	32-32-16-16
57	4-LiDARs	Front Left, Front Right, Rear Left, Rear Right	Low	32-32-32-32
58	4-LiDARs	Front Left, Front Right, Rear Left, Rear Right	Low	64-64-16-16
59	4-LiDARs	Front Left, Front Right, Rear Left, Rear Right	Low	64-64-32-32
60	4-LiDARs	Front Left, Front Right, Rear Left, Rear Right	Low	64-64-64-64
61	4-LiDARs	Front, Side Left, Side Right, Rear	High	16-16-16-16
62	4-LiDARs	Front, Side Left, Side Right, Rear	High	32-16-16-16
63	4-LiDARs	Front, Side Left, Side Right, Rear	High	32-32-32-32
64	4-LiDARs	Front, Side Left, Side Right, Rear	High	64-16-16-16
65	4-LiDARs	Front, Side Left, Side Right, Rear	High	64-32-32-16
66	4-LiDARs	Front, Side Left, Side Right, Rear	High	64-64-64-64
67	4-LiDARs	Front, Side Left, Side Right, Rear	Low	16-16-16-16
68	4-LiDARs	Front, Side Left, Side Right, Rear	Low	32-16-16-16
69	4-LiDARs	Front, Side Left, Side Right, Rear	Low	32-32-32-32
70	4-LiDARs	Front, Side Left, Side Right, Rear	Low	64-16-16-16
71	4-LiDARs	Front, Side Left, Side Right, Rear	Low	64-32-32-16
72	4-LiDARs	Front, Side Left, Side Right, Rear	Low	64-64-64-64

To develop an effective naming convention, which is used in the remainder of the thesis, Table 3.1 was used to develop a name for each of the LiDAR placement alternatives. The position on the roof of the vehicle, the elevation, and the channel configuration of the LiDAR sensors were utilized.

Table 3.2 provides the breakdown of the naming convention, offering clear meanings for each nomenclature. These descriptions enable an understanding of the placement and configuration of LiDAR sensors on the vehicle for each of the placement alternatives. By deciphering the naming convention, the location, elevation, and channel configuration of the LiDAR sensors are identified.

Table 3.2: Naming Convention for the LiDAR Alternatives

Alternatives	**Location on AV**
CHigh16	Center of the car roof elevated high with a 16-channel LiDAR sensor
FLow64	Front of the car roof elevated low with a 64-channel LiDAR sensor
FBHigh16-16	Front and back of the car roof elevated high, each equipped with a 16-channel LiDAR sensor
FLFRBHigh16-16-16	Front left, front right, and back of the car roof elevated high, each using a 16-channel LiDAR sensor
FSLSRHigh32-16-16	Front, side left, and side right of the car roof elevated high, with sensors of 32, 16, and 16 channels, respectively
FLFRRLRRHigh16-16-16-16	Front left, front right, rear left, and rear right of the car roof elevated high, each with a 16-channel LiDAR sensor
FSLSRBLow64-32-32-16	Front, side left, side right, and back of the car roof elevated low, equipped with 64, 32, 32, and 16 channel LiDAR sensors, respectively

3.1.2 Identification of Evaluation Criteria

Table 3.3 presents the criteria used in this thesis and their descriptions. An in-depth explanation of each criterion is presented in this section.

Table 3.3: Identified Criteria, Definition, and Importance

Criterion	Explanation	Importance
Point Density	The number of LiDAR points collected per unit area or volume. Higher point density provides more detailed and accurate data for detecting small or distant objects.	Assesses the level of detail and accuracy required for object detection.
Cost of Sensor	This is the financial cost associated with acquiring the LiDAR sensor(s).	Considers the budget constraints and the cost-effectiveness of the sensor(s) in relation to the benefits they provide.
Power Consumption	This measures the amount of electrical power (in watts) that the LiDAR sensor(s) consume during operation.	Evaluates the importance of conserving power in autonomous vehicles where energy efficiency can affect range and operating costs.
Blind Spot Area	This criterion focuses on the area around the vehicle that is not covered or is poorly covered by the LiDAR sensor(s).	Evaluates the significance of minimizing blind spots to enhance safety.
Sensor Redundancy	The number of LiDAR sensors used on the autonomous vehicle. More sensors can provide redundancy, increase coverage, and enhance the robustness of the perception system.	Assesses the importance of including redundancy in the LiDAR setup and whether multiple sensors are needed for safety and reliability.
Aesthetics	Aesthetics considers the visual appearance of the LiDAR sensor(s) and how well they integrate with the vehicle's design.	Aesthetics may be relevant in consumer markets in which appearance matters.
Ease of Installation	Ease of installation assesses how straightforward and efficient it is to install and set up the LiDAR sensor(s) on the vehicle. Factors may include the time, complexity, and expertise required.	Ease of installation can impact the deployment timeline and cost, making it important for practical considerations.

3.1.2 (a) Point Density

This metric is assessed by quantifying the number of LiDAR points per unit volume of object. The data for the metric is collected using the CARLA simulator (previously explained in this chapter). The numbers of points of spawned objects at intervals to the ego vehicle (the AV equipped with sensors and systems for self-navigation) we recollected and used to calculate the point density per unit volume of the object. The average point density is used as a metric for decision-making. Segmentation techniques were used to isolate the objects of interest and to enclose them within bounding boxes. Subsequently, the point density per volume of each object was determined based on the LiDAR points captured within the corresponding bounding box. This metric was used to evaluate the level of detail for each object.

$$Point\ Density = \frac{Nr\ of\ points}{Bounding\ box\ Volume}$$

where *Nr of points* represents the total number of LiDAR points acquired for the specific object under consideration. The *Object Volume* is determined based on the object's dimensions, including its length, width, and height, obtained from the bounding box surrounding the object.

$$Bounding\ box\ volume\ =\ length\ \times\ width\ \times height\ of\ bounding\ box\ (points/m^3)$$

Figure 3.6 presents a high-density and low-density sample of acquired point clouds, and Figure 3.7 presents a pedestrian point cloud at varying distances from the ego vehicle in a bounding box.

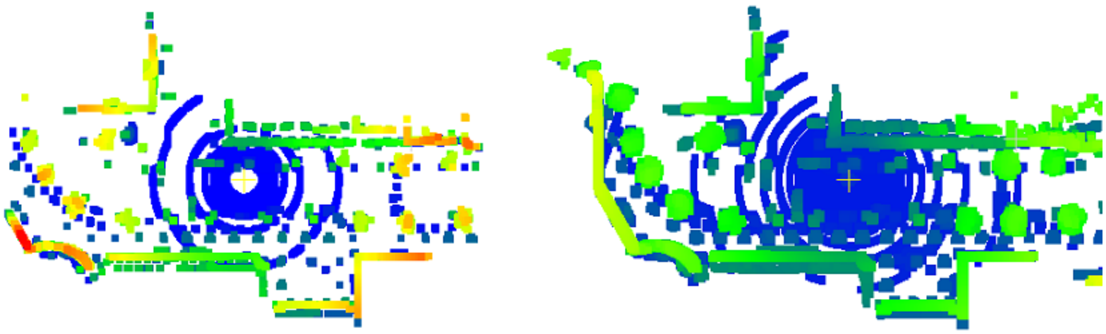

(a) Low Density Point Cloud (b) High Density Point Cloud

Figure 3.6: Point Clouds

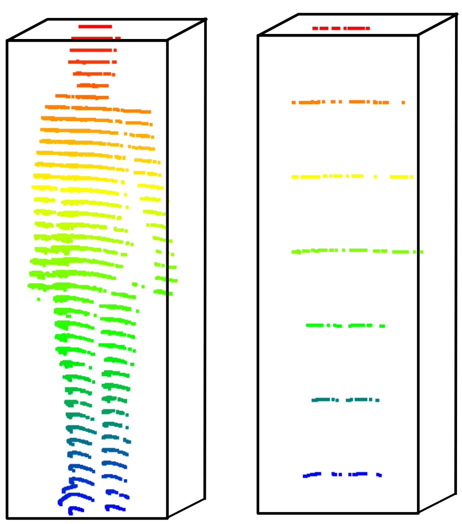

Figure 3.7: Pedestrian point cloud illustrated in a bounding box at 10m and 90m respectively, from the ego vehicle

3.1.2 (b) Cost of Sensor

Selecting the most suitable LiDAR sensor involves finding a balance between cost and performance. While high-cost sensors may necessitate a larger initial investment, they are often equipped with advanced features that significantly enhance operational efficiency or offer higher accuracy (Ortiz Arteaga et al., 2019). These advanced capabilities translate into the acquisition of more precise and reliable data, which is paramount for the safe and effective operation of AVs.

One of the factors driving the cost of LiDAR systems is the high precision their lasers require. These lasers must emit light at precise wavelengths, thus, demanding costly and intricate manufacturing processes. Moreover, the optics responsible for directing and focusing the laser beams contribute substantially to the overall cost, with their complexity further raising expenses (Hassan, 2023). Nonetheless, the past two decades have witnessed significant strides in industrial laser technology, which has led to cost reductions in LiDAR systems and their operational deployment (Wang & Menenti, 2021).

In evaluating the cost of LiDAR sensors for optimal placement, it is important to carefully assess specific requirements and strike the right balance with operational objectives. Achieving this equilibrium ensures that the chosen LiDAR sensor seamlessly aligns with the operational goals of the AVs. On average, LiDAR sensor costs vary based on their specifications. A 16-channel LiDAR sensor typically falls within the range of US$4,000 and $5,000, while a 32-channel LiDAR sensor is priced between US$9,000 and $14,000. In comparison, a 64-channel LiDAR sensor usually ranges from US$10,000 to $15,000. These cost considerations play a significant role in determining the most cost-effective and performance-driven LiDAR sensor placement for AVs.

3.1.2 (c) Power Consumption

Power consumption is considered a metric for optimizing the LiDAR sensor placement because efficiency and reliability are of paramount importance. As automakers and new mobility companies assess LiDAR technology, the power consumption implications are important. The difference in power consumption between LiDAR sensors can have a significant impact on the overall performance and efficiency of an AV system. Power consumption is not merely a technical detail but carries tangible consequences for various aspects of AV operations and sustainability (Maynard, 2021).

Consequently, the choice of LiDAR sensor technology can have far-reaching implications for energy efficiency, operational costs, and environmental impact, hence, power consumption is a pivotal consideration for automakers and companies involved in advancing AV technology. The decision to opt for LiDAR sensors that consume less power not only contributes to sustainability but also enhances the overall performance and economic feasibility of AV systems. A 16-channel LiDAR sensor consumes approximately 8 watts, a 32-channel LiDAR sensor requires around 10 watts, and a 64-channel LiDAR sensor typically consumes approximately 20 watts.

3.1.2 (d) Blind Spot Regions

The blind spot region is another metric that can be obtained from the LiDAR point clouds. Blind spot regions are areas around the vehicle that are not visible to the LiDAR sensor (see Figure 3.8 for typical LiDAR sensor coverage and blind spot regions). These areas can pose a significant risk for collisions with objects, pedestrians, or other vehicles. Therefore, evaluating these regions is necessary to ensure the safety of passengers, pedestrians, and other drivers on the road, and to make reliable decisions for vehicle navigation.

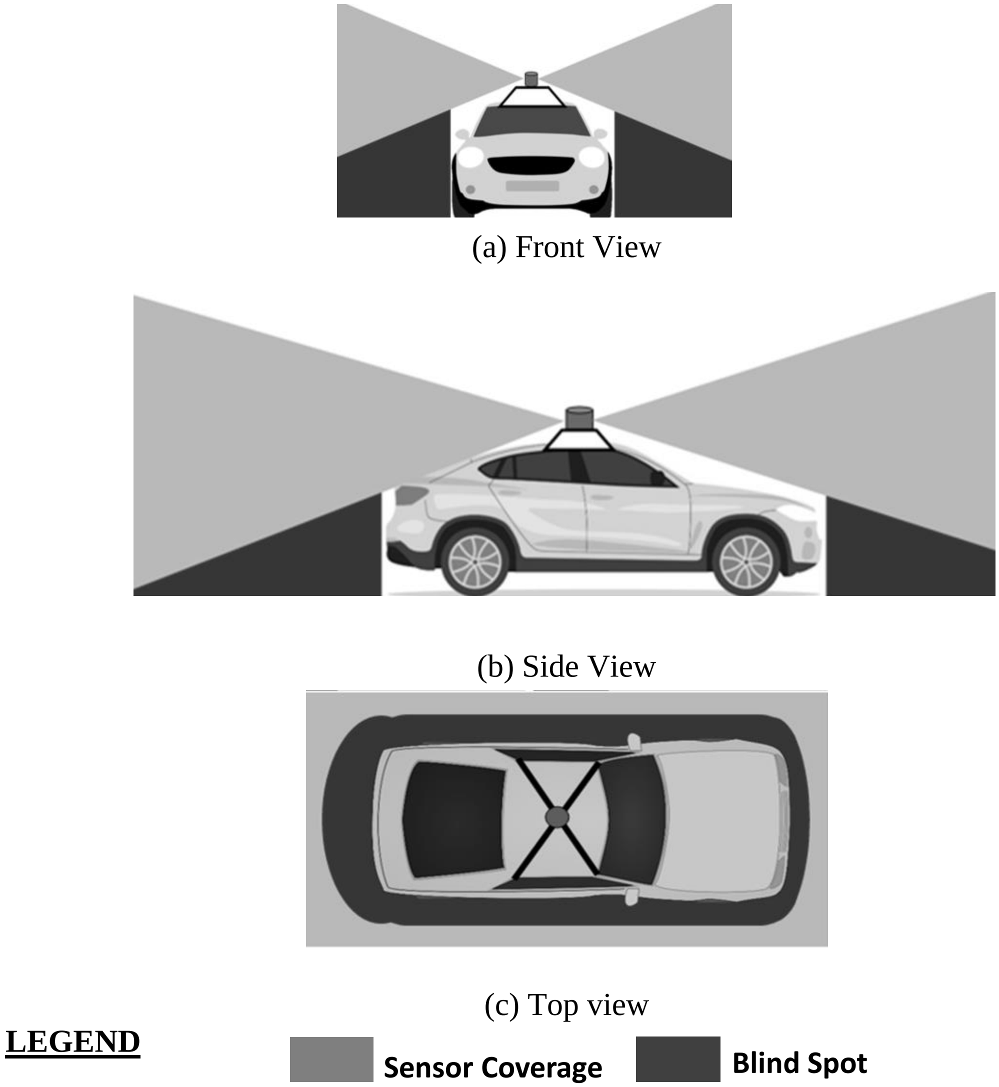

Figure 3.8: Sensor Coverage and Blind Spot Regions of LiDAR Sensor

Estimating the blind spot regions for the purpose of this research involved processing distinct point cloud data outputs from the simulator. In this way, variations in coverage in areas proximate to the vehicle across different placement alternatives were identified. This information served as the basis for rating the alternatives derived from the blind spot regions by assigning a higher value to the highest blind spot region and a lower value to smaller blind spot regions. The blind spot regions varied across placement alternatives (Figure 3.9). Figure 3.9 shows regions around the ego vehicle for two different LiDAR placement alternatives.

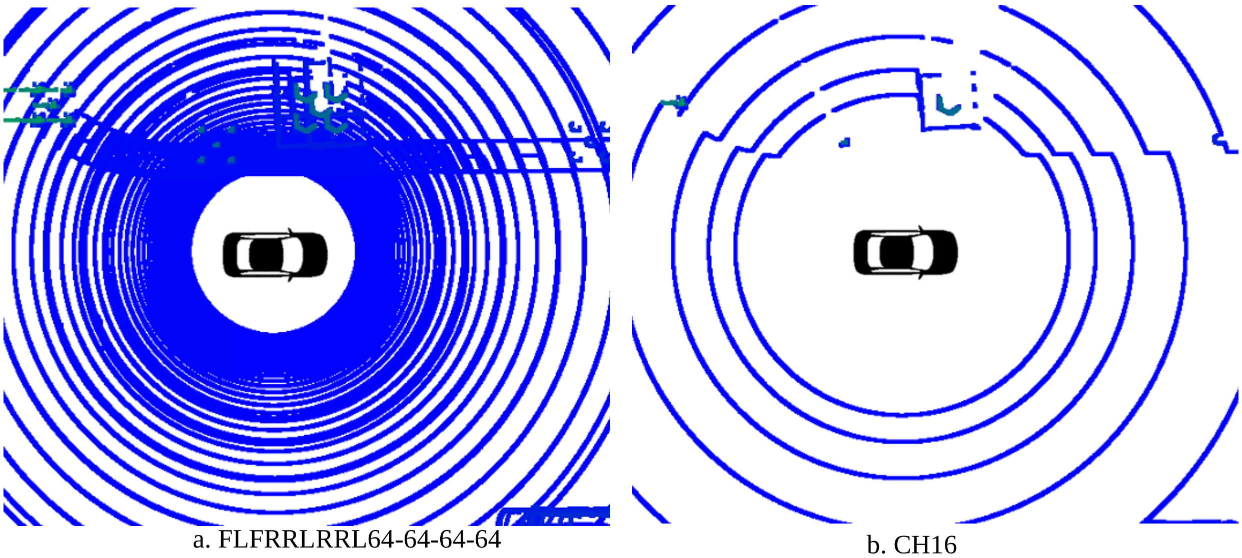

(a) Blindspot region sample1 (b) Blindspot region sample 2

Figure 3.9: Blindspot Region Coverage

3.1.2 (e) Sensor Redundancy

Sensor redundancy pertains to the utilization of multiple LiDAR sensors, either of the same type or different types, providing overlapping or complementary data. This redundancy serves as an additional layer of safety and reliability in the context of AVs. In the event of sensor failure, discrepancies, or adverse environmental conditions, these redundant LiDAR sensors can seamlessly assume control to ensure the continued accuracy and safety of the system. This not only ensures the protection of passengers and pedestrians but also reinforces the reliability of AV technology.

3.1.2 (f) Aesthetics

The visual appeal of AVs is relevant in shaping public perceptions. While the fundamental performance is essential and the most important factor of AVs, people also place significant emphasis on design and aesthetics. If the sensor on the AV is relatively large or too high, the form may not be accepted by the public (Chen et al., 2021).

In this thesis, the aesthetic consideration is associated with the number (count) and elevation of the LiDAR sensors in the AV. Aesthetic judgments in this context are entirely subjective and have the potential to exert some influence on design decisions in AV development based on the weight assigned to the aesthetics criteria. The number of sensors could significantly impact the aesthetic appeal of an AV's external design, which primarily relies on users' perceptual judgments. An excessive number of sensors could potentially create a less appealing appearance. Conversely, a better arrangement of sensors could contribute to a modern visual design. The strategic incorporation of multiple sensors could convey a distinct impression of cutting-edge technology.

The elevation of the sensors, particularly their integration within the vehicle's structure, is equally important for overall aesthetics. Sensors situated at specific elevations must be seamlessly integrated to ensure a visually pleasing vehicle exterior. While aesthetic considerations may not outweigh concerns about vehicle safety and robustness for participants, they remain an important factor. Striking the right balance is imperative to fostering confidence in AV technology and ensuring that AVs are both safe and appealing to passengers and the general public. Well-designed sensor placement not only enhances the vehicle's aesthetics but also displays a commitment to safety and innovation.

3.1.2 (g) Ease of Installation

The ease of installation describes how complex or demanding the installation process is. It directly affects the efficiency and cost-effectiveness of sensor installation and its integration with other sensors. In this research, the factor revolves around the assumption that as the number of sensors increases, the installation process becomes progressively more complex and demanding.

With a single sensor configuration, the installation process is characterized by relative simplicity. This configuration typically demands less physical and structural alterations to the vehicle, making it a convenient and cost-effective choice for manufacturers. The ease of installation can streamline the production process and reduce associated costs. As the number of sensors in a configuration increases, so does the complexity of the installation process. Multiple sensors necessitate a more extensive network of wiring, mounting points, and calibration procedures. Consequently, the installation process becomes more labor-intensive and time-consuming.

3.1.3 Weighting Method

The significance of each criterion in the LiDAR placement optimization framework was determined using three different sources: equal weighting, sensitivity analysis, and responses from questionnaire surveys. These sources were used to allocate weights to each criterion, ensuring that the sum of all allocated weights equaled 100. A higher weight indicates a greater degree of importance in the decision-making process. Table 3.4 presents the weights allocation table used for all instances. The results for the weights in each category are presented in Chapter 4.

Table 3.4: Direct weighting table

Criteria	**Weight**
Point Density	
Cost of Sensor	
Power Consumption	
Blindspot Area	
Sensor Redundancy	
Aesthetics	
Ease of Installation	
Total	100

3.1.4 Scaling Method

The primary objective of scaling is to establish a consistent scale across the criteria to allow comparative analysis. Given that the performance criteria have diverse measurement units, for example, cost in dollars and power consumption in watts, this process involves the use of a value function to standardize the various performance criterion levels to a unified scale ranging from 0 to 100. In this scale, a rating of 100 denotes the most favorable level of performance, while lower values signify progressively less desirable outcomes.

Value functions and utility functions serve as indispensable tools in different decision-making scenarios. The value function approach is used when decisions unfold in a scenario of certainty, allowing DMs to confidently assess and compare attribute levels. Conversely, the utility function approach applies when decision-making occurs in conditions of risk and uncertainty (Bai et al., 2008; Sinha & Labi, 2007). In scenarios in which outcomes are subject to probabilistic elements and not guaranteed, utility functions are invaluable.

Value scaling offers a systematic framework for transforming attributes into quantifiable indicators of worth and desirability. The value function embodies the DM's preferences concerning diverse attribute levels when certainty prevails. Within this framework, the most favored outcome is assigned a value of 1 or 100%, symbolizing the most desirable level of attainment, while the least favorable outcome receives a value of zero, denoting the least desirable. Utility functions represent a more specialized form of value function because they represent not only the intrinsic value associated with various attribute levels but also the DM's stance on risk. In other words, they account for the DM’s attitude toward risk – from risk-prone to risk-neutral and risk-averse (Li & Sinha, 2004).

To derive the value scaling functions in this thesis, a questionnaire using the mid-value splitting technique was dispensed to respondents. In this technique, the respondent (DM) assigns specific values to each level of the criterion (Figure 3.8) to assign values to various criteria.

The value function establishes a connection between different levels of the performance criterion X and values ranging from 0 to 100, where 100 signifies the most favorable level. The development of a value function involves determining the values for specific points within the function. These points play a critical role in assessing the desirability of different levels of a performance criterion (X). The objective is to establish the value associated with three intermediate points (X_{25}, X_{50}, and X_{75}) with appropriate values that are within the range of 0 to 100.

The process begins by defining reference values for the worst (most unfavorable) and best (most favorable) levels. The worst level is assigned a value of 0, indicating the lowest desirability. In contrast, the best level is assigned a value of 100, representing the highest desirability. The following steps then ensue:

- Identify X_{50}: X_{50} is the point within the value function where equal satisfaction is derived from these two conditions: (a) performance improvement from the worst level to X_{50} and (b) performance improvement from X_{50} to the best level.
- Determine X_{25}: X_{25} is identified as the point at which an equal level of satisfaction is achieved regarding performance improvement from the worst level to X_{25} and performance improvement from X_{25} to X_{50}.
- Determine X_{75}: X_{75} is the point where an equal level of satisfaction is derived from performance improvement from X_{50} to X_{75} and performance improvement from X_{75} to the best level.
- Finally, a consistency check is carried out to validate the values assigned to X_{25}, X_{50}, and X_{75}. This check involves ensuring that the perceived improvements from X_{25} to X_{50} and

from X_{50} to X_{75} display an equal level of satisfaction. If the response to this consistency check is affirmative, indicating consistent values, the evaluation proceeds. If not, reevaluation and adjustment is performed.

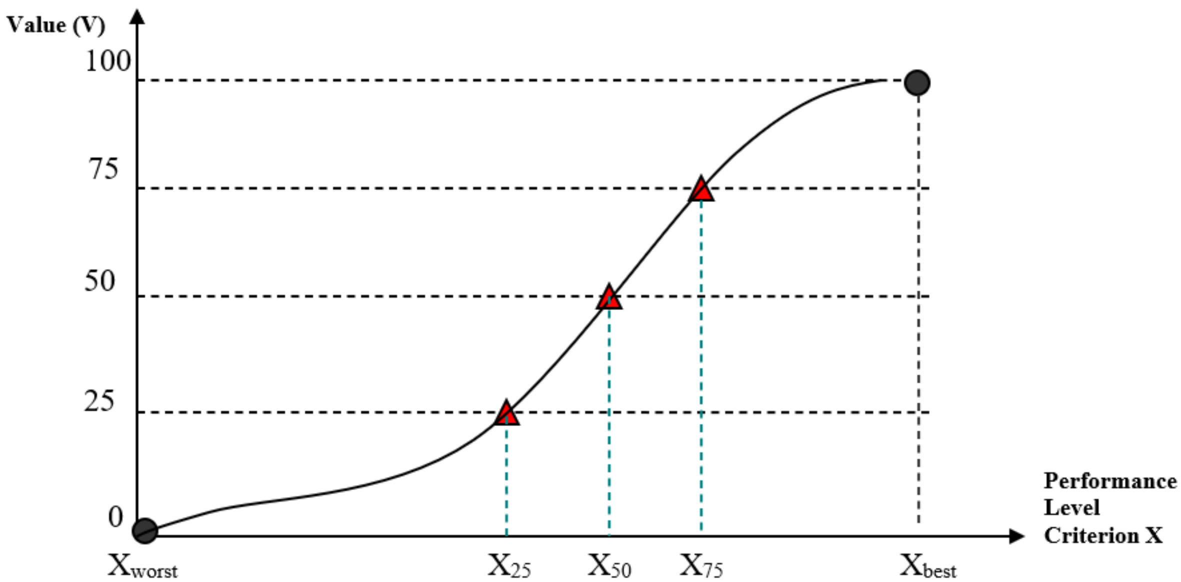

Figure 3.10: A conceptual Value Function

The value function establishes a connection between different levels of the performance criterion X and values ranging from 0 to 100, where 100 signifies the most favorable level. The development of a value function involves determining the values for specific points within the function. These points play an important role in assessing the desirability of distinct levels of a performance criterion (X). The objective is to establish the value associated with three intermediate points (X_{25}, X_{50}, and X_{75}) to appropriate values that are within the range from 0 to 100.

The process begins by defining reference values for the worst (most unfavorable) and best (most favorable) levels. The worst level is assigned a value of 0, indicating the lowest desirability. In contrast, the best level is assigned a value of 100, representing the highest desirability. The following steps are then followed:

- Identify X_{50}: X_{50} is the point within the value function where equal satisfaction is derived from these two conditions: (a) performance improvement from the worst level to X_{50} and (b) performance improvement from X_{50} to the best level.

- Determine X_{25}: X_{25} is identified as the point at which an equal level of satisfaction is achieved regarding performance improvement from the worst level to X_{25} and performance improvement from X_{25} to X_{50}.
- Determine X_{75}: X_{75} is the point where an equal level of satisfaction is derived from performance improvement from X_{50} to X_{75} and performance improvement from X_{75} to the best level.
- Finally, a consistency check is carried out to validate the values assigned to X_{25}, X_{50}, and X_{75}. This check involves ensuring that the perceived improvements from X_{25} to X_{50} and from X_{50} to X_{75} display an equal level of satisfaction. If the response to this consistency check is affirmative, indicating consistent values, the evaluation proceeds. If not, reevaluation and adjustment is done.

An example of the implementation of the value function used to collect data is shown in Figure 3.11.

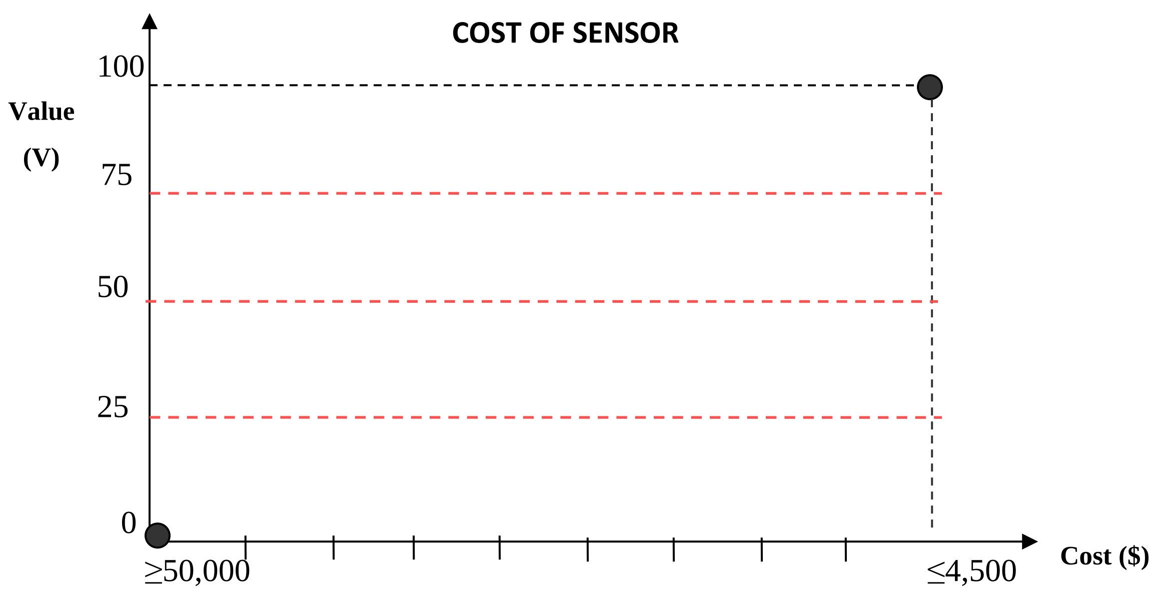

Figure 3.11: Value Function example for Sensor Cost

3.1.5 Amalgamation

This is the step that combines the weighted and scaled levels of all the performance criteria for each LiDAR placement alternative. In this thesis, the amalgamation technique used is the weighted sum method. This is presented below. For j alternatives and I criteria, the weighted sum of all the criteria for each alternative j, is:

$$WS_j = \sum_{i=1}^{m} w_i \times S_{ij}$$

where:

- $i = criterion, i = 1,2, \ldots \ldots I$
- $j\ is\ the\ alternative, j = 1,2, \ldots .J$
- WS_j is the weighted sum for alternative *j*.
- W_i denotes the weight allocated to criterion *i*.
- S_{ij} is the performance of alternative j on criterion *i*.
- I is the total number of criteria.
- J is the total number of alternative LiDAR placement designs

The result of the amalgamation stage is a score, or value assigned to each LiDAR placement design alternative. These scores facilitate a straightforward ranking of the alternatives, with higher scores generally signifying superior overall.

3.1.6 Decision

This is the final stage of the MCDA process. During this phase, the most preferred alternative is chosen based on the results of the amalgamation step. Typically, the alternative that ranks highest or scores the best across the established criteria is selected after conducting a sensitivity analysis. Before arriving at the final decision, a sensitivity analysis is conducted to evaluate how adjustments in the criteria weights could influence the ultimate choice. If the DM deems it necessary, the weight and value functions may be fine-tuned using a Delphi process, and the alternatives re-evaluated. Doing so could provide a deeper understanding of the robustness of the chosen alternative. In this thesis, the sensitivity analysis was carried out using only the weights.

3.2 Questionnaire Survey Method

To conduct the questionnaire, the initial step involved designing a questionnaire following the guidelines outlined by the Institutional Review Board protocols at Purdue University, West

Lafayette, Indiana. The survey questionnaire was granted an exemption category under #IRB-2023-1570 and refrained from collecting any personally identifiable information.

The questionnaire was administered to capture participants' preferences regarding the relative importance of various criteria. To ensure that the respondents could offer valuable insights into the research, individuals with expertise in the subject matter were selectively recruited. All recruitment and associated procedures strictly adhered to the protocols set forth by the Institutional Review Board at Purdue University.

3.1 Experimental Setup

For the subsequent data collection (Chapter 4) to assess the various LiDAR placement alternatives, an experimental setup involving CARLA was used. CARLA is an open-source driving simulator that supports the training and validation of different aspects of AV driving, such as perception and control. In this thesis, the CARLA platform provided the tools and resources needed for the LiDAR data collection and experimentation within a controlled virtual environment. The simulation environment is built on the Unreal Engine, a high-performance game engine that provides realistic graphics and physics simulation (Dosovitskiy et al., 2017). In CARLA, the sensors include LiDAR, camera, radar, and GPS. CARLA also includes a vehicle dynamics model that allows researchers to simulate different types of vehicles with realistic driving behavior, as well as digital information such as urban layouts, automobiles, buildings, pedestrians, traffic lights, and street signs.

One significant advantage of CARLA is its flexibility (Gómez-Huélamo et al., 2021), which allows for the modification of the simulation environment to create custom scenarios for testing and evaluation. Labi (2014) underscores how simulation tools offer unparalleled flexibility by seamlessly allowing specific input parameters to be adjusted. This flexibility fosters an adaptable experimental environment, crucial for testing diverse scenarios, including those pertinent to this thesis. Specifically, in this study, the flexibility of CARLA facilitated the simulation of scenarios essential to the research objectives. To interact with the simulator, a set of Python APIs was used that enable users to develop custom codes for their experiments (Malik et al., 2022). Figure 3.12 presents the simulation environment.

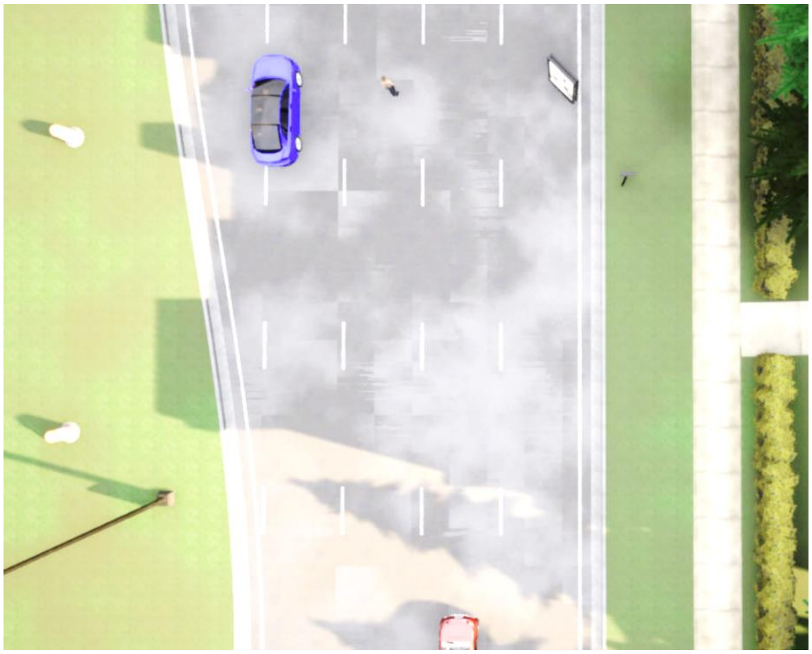

Figure 3.12: Experimental Setup

The Python API in CARLA enables users to interact with the CARLA simulator using the Python programming language through a set of tools and libraries. With the use of the API, users can create and control vehicles, access different sensors, and test their algorithms. This helps reduce the complexity and cost of physical experiments. The Python API also provides code examples demonstrating how to interact with the simulator, which serves as a starting point for users to develop custom scripts depending on their demands. Additionally, the CARLA documentation provides extensive information on the API functions and parameters. Figure 3.13 presents the CARLA software architecture (obtained from open-source CARLA documentation).

Some terminologies used in connecting to the simulator are explained below:

- A ***Client*** object is created to establish a connection with the CARLA simulator running on the local machine at the default port 2000.
- The ***get_world()*** method is used to obtain a reference to the current simulation world object, which represents the virtual environment of the simulator.
- The ***set_timeout()*** method is used to set the timeout for network requests between the client and the simulator to 2000 milliseconds.

- The ***get_blueprint_library()*** method is used to retrieve the blueprint library, which contains all the possible actors that can be spawned in the simulation, such as vehicles, props, and pedestrians.
- The ***get_map()*** method is used to obtain the current map, which in this case, is Town 03 where the experiments are conducted.
- The ***get_spawn_points()*** method is used to obtain a list of available spawn points on the map. These spawn points represent different locations where actors can be placed in the simulation. For this thesis, the experiments were conducted using the same spawn point.
- The filter () method is used to filter the actor list to only include vehicles in specific cases.

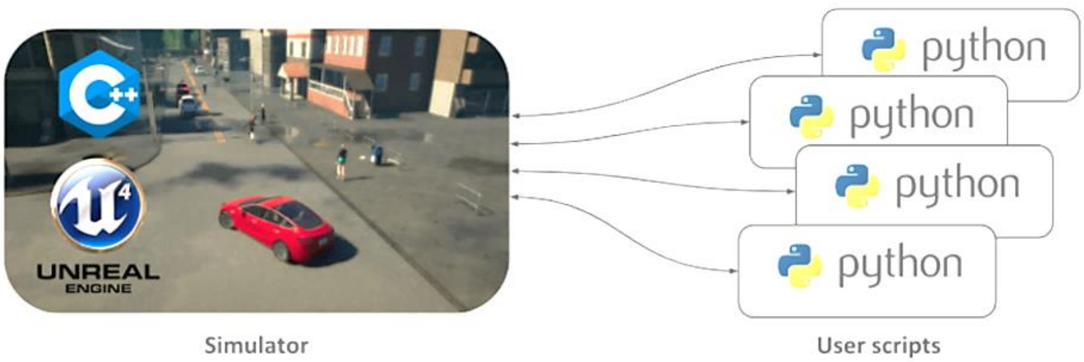

Figure 3.13: CARLA software architecture (obtained from open-source CARLA documentation)

The vehicles available in CARLA’s menu are based on real-world vehicles and include models such as Audi, Citroen, Chevrolet Impala, Tesla, and Lincoln MKZ. However, there could be some minor differences in the vehicle dimensions due to the limitations of the simulation environment (as shown in Table 3.5 and 3.6). The Audi A2 was used in this thesis. The Audi A2 was selected due to its unique physical design and engineering features. This vehicle strikes a balance between advanced technology and practical urban mobility, making it a good choice for LiDAR placement testing within the simulation. The dimensions of the car (Tables 3.5 and 3.6) were important to determining the different positions and elevation in which to place the LiDAR. Tables 3.5 and 3.6 are important because the dimensions are taken into consideration to specify the exact placement points of the LiDAR sensors.

Table 3.5: Real-World Dimensions of Audi a2 Vehicle

	Dimensions (inches)	Dimensions (meters)
Height	61.1	1.553
Width (without mirrors)	65.9	1.673
Length	150.6	3.826

Table 3.6: CARLA Dimensions of Audi a2 Vehicle

	Dimensions (inches)	Dimensions (meters)
Height	61.0	1.549
Width (without mirrors)	67.1	1.790
Length	145.9	3.705

3.2 Summary of Chapter 3

Chapter 3 discusses the study methods and experimental setup, establishing the foundation for the MCDM framework applied in the thesis. The chapter commences by outlining the steps involved in establishing LiDAR placement design alternatives, which serves as a fundamental phase in the decision-making process. This involves meticulous identification and enumeration of various evaluation criteria, providing a comprehensive spectrum for assessment. These criteria encompass diverse aspects such as point density, sensor cost, power consumption, blind spot regions, sensor redundancy, aesthetics, and ease of installation.

The chapter further explores the methodologies used in the decision framework. It explains the approach used to assign weights to these criteria, thereby recognizing their relative significance in the decision-making process. Additionally, the chapter addresses the scaling method used to standardize the diverse metrics into a unified measurement system. The process of amalgamation, in which the disparate measurements are combined into an overall assessment, is also detailed, leading up to the decision-making phase.

The significance of the questionnaire survey is also highlighted, underscoring the value of garnering empirical insights from DMs. This particular methodology aids in validating and refining the evaluation criteria and methodologies inherent in the decision framework. Finally, the chapter concludes by explaining the experimental setup and presenting the simulation environment used in conducting the experiments.

CHAPTER 4. DATA COLLECTION

4.1 Introduction

The data collection methodology in this thesis encompasses a multifaceted approach involving diverse sources to ensure the comprehensive acquisition of information. First, simulator data was gathered using CARLA, an open-source driving simulator. This simulator provided data in the form of LiDAR point clouds, which were subsequently processed to derive insights from the data. Then, data was compiled from the datasheets of LiDAR sensor manufacturers. This inclusion was pivotal because it supplies technical details directly from manufacturers, providing information on sensor specifications, capabilities, and performance benchmarks. Finally, the data collection process involved questionnaire surveys, adding a human element by gathering perspectives and feedback from respondents.

Regarding the weighting data categories, the thesis employs three distinct approaches: equal weighting, respondent-assigned weighting, and randomly assigned weights. Equal weighting ensures the balanced importance of all data points by assigning equal significance to each criterion. In contrast, respondent-assigned weighting involves assigning weights based on the relevance of the criteria perceived by the respondents, thereby integrating a subjective yet informed perspective into the dataset. Randomly assigned weights introduce a stochastic element, allowing the impact of variability to be explored in the overall analysis.

4.1.1 Data Collected From CARLA

Experiments were conducted in CARLA using the Python API to interface with the simulator via custom-written code. From the simulator, data on the point density and blind spot regions was obtained. Table 4.1 presents the data extracted from the simulator. The average vehicle point density (PDV), average pedestrian point density (PDP), and blind spot region ratings (BR) were all obtained from the experiments. The values for PDV and PDP were all derived from the number of LiDAR points for each vehicle and pedestrian generated over a 100-meter distance. The blind spot region rankings were established by evaluating the extent of the blind spot regions surrounding the ego vehicle in each point cloud obtained for all alternatives. The ratings range from 10 (indicating the least blind spot regions) to 120 (representing the alternative with the highest degree of blind spot regions).

Table 4.1: Criteria data Collected from the simulation experiments

Alternatives	PDP (pts/m^3)	PDP (pts/m^3)	BR (Rating)
CHigh16	54	55	70
CHigh32	84	95	70
CHigh64	104	115	70
CLow16	96	100	60
CLow32	116	115	60
CLow64	145	193	60
FHigh16	94	89	50
FHigh32	153	196	50
FHigh64	145	79	50
FLow16	93	104	40
FLow32	128	164	40
FLow64	158	236	40
FBHigh16-16	189	174	120
FBHigh32-32	311	400	120
FBHigh64-64	311	394	120
FBLow16-16	197	210	30
FBLow32-32	317	239	30
FBLow64-64	302	438	30
FBHigh32-16	256	315	120
FBHigh64-32	310	390	120
FBLow32-16	256	332	30
FBLow64-32	325	423	30
FBHigh64-16	269	327	120
FBLow64-16	261	358	30
FLFRBHigh16-16-16	220	205	90
FLFRBHigh32-32-16	300	382	90
FLFRBHigh32-32-32	334	424	90
FLFRBHigh64-64-16	301	386	90
FLFRBHigh64-64-32	346	451	90
FLFRBHigh64-64-64	346	448	90
FLFRBLow16-16-16	217	235	20
FLFRBLow32-32-16	292	392	20
FLFRBLow32-32-32	340	470	20
FLFRBLow64-64-16	297	404	20
FLFRBLow64-64-32	333	449	20

Table 4.1 continued

FLFRBLow64-64-64	337	453	20
FSLSRHigh16-16-16	309	279	90
FSLSRHigh32-16-16	348	381	90
FSLSRHigh32-32-32	438	578	90
FSLSRHigh64-16-16	367	411	90
FSLSRHigh64-32-32	466	604	90
FSLSRHigh64-64-64	472	592	90
FSLSRLow16-16-16	294	317	80
FSLSRLow32-16-16	344	432	80
FSLSRLow32-32-32	450	628	80
FSLSRLow64-16-16	349	440	80
FSLSRLow64-32-32	461	659	80
FSLSRLow64-64-64	475	670	80
FLFRRLRRHigh16-16-16-16	404	372	110
FLFRRLRRHigh32-32-16-16	524	648	110
FLFRRLRRHigh32-32-32-32	617	799	110
FLFRRLRRHigh64-64-16-16	565	684	110
FLFRRLRRHigh64-64-32-32	606	779	110
FLFRRLRRHigh64-64-64-64	617	780	110
FLFRRLRRLow16-16-16-16	397	410	10
FLFRRLRRLow32-32-16-16	514	662	10
FLFRRLRRLow32-32-32-32	621	804	10
FLFRRLRRLow64-64-16-16	571	749	10
FLFRRLRRLow64-64-32-32	605	791	10
FLFRRLRRLow64-64-64-64	617	803	10
FSLSRBHigh16-16-16-16	387	355	110
FSLSRBHigh32-16-16-16	452	493	110
FSLSRBHigh32-32-32-32	571	730	110
FSLSRBHigh64-16-16-16	437	464	110
FSLSRBHigh64-32-32-16	606	745	110
FSLSRBHigh64-64-64-64	591	737	110
FSLSRBLow16-16-16-16	398	415	100
FSLSRBLow32-16-16-16	436	532	100
FSLSRBLow32-32-32-32	581	788	100
FSLSRBLow64-16-16-16	457	581	100
FSLSRBLow64-32-32-16	546	731	100
FSLSRBLow64-64-64-64	594	775	100
FSLSRBLow32-32-32-32	581	788	100
FSLSRBLow64-16-16-16	457	581	100
FSLSRBLow64-32-32-16	546	731	100
FSLSRBLow64-64-64-64	594	775	100

4.1.2 Data Collected From Other Sources

Of the seven criteria used in this study, some, including average sensor cost, power consumption, sensor redundancy, and ease of installation, were not obtained from the CARLA simulator.

The data for average sensor cost was collected from online datasheets provided by LiDAR sensor vendors and through direct communication with sellers. To calculate the average sensor cost, the average between the lower and upper cost range was determined. Power consumption information was extracted from the datasheets of the LiDAR sensors. Sensor redundancy within this thesis denotes the level of backup or failover capability inherent in the sensor setup. It quantifies the system's resilience to sensor malfunction or failure by considering the number of additional sensors beyond a singular unit. This approach aims to mitigate the risk of data loss or system impairment by providing backup sensors: A greater number of sensors used translates into higher redundancy percentage, thereby enhancing the system's reliability and operational robustness against potential sensor failures. The percentages were assigned based on the number of sensors used relative to the highest number considered in this study, which was four. One sensor was defined as having no redundancy, hence, it was assigned a value of 0%. Two sensors were considered to have 50% redundancy, three sensors had 66.67% redundancy, and the maximum of four sensors was considered to have 75% redundancy. This information was obtained in the following way:

$$\frac{Nr\ of\ Sensors - 1}{Nr\ of\ Sensors} \times 100$$

Ease of installation was assessed using an ordinal ranking from 1 to 4, where 1 indicates the easiest installation and 4 the most difficult. The ranking is based on the number of sensors to be installed, with one sensor receiving a raw value of 1, and four sensors assigned a value of 4. The assumption of assessing ease of installation based on an ordinal ranking is based on the assumption of a logical correlation between complexity and quantity.

Table 4.2 presents the relevant data.

Table 4.2: Criteria data collected from other sources

Alternatives	SC (Dollars)	PC (Watts)	SR (Rating)	AES (Rating)	EOI (Rating)
CHigh16	4,500	8	0.00	2	1
CHigh32	11,500	10	0.00	2	1
CHigh64	12,500	20	0.00	2	1
CLow16	4,500	8	0.00	4	1
CLow32	11,500	10	0.00	4	1
CLow64	12,500	20	0.00	4	1
FHigh16	4,500	8	0.00	4	1
FHigh32	11,500	10	0.00	2	1
FHigh64	12,500	20	0.00	2	1
FLow16	4,500	8	0.00	4	1
FLow32	11,500	10	0.00	4	1
FLow64	12,500	20	0.00	4	1
FBHigh16-16	9,000	16	50.00	2	2
FBHigh32-32	23,000	20	50.00	2	2
FBHigh64-64	25,000	40	50.00	2	2
FBLow16-16	9,000	16	50.00	4	2
FBLow32-32	23,000	20	50.00	4	2
FBLow64-64	25,000	40	50.00	4	2
FBHigh32-16	16,000	18	50.00	2	2
FBHigh64-32	24,000	30	50.00	2	2
FBLow32-16	16,000	18	50.00	4	2
FBLow64-32	24,000	30	50.00	4	2
FBHigh64-16	17,000	28	50.00	2	2
FBLow64-16	17,000	28	50.00	4	2
FLFRBHigh16-16-16	13,500	24	66.67	1	3
FLFRBHigh32-32-16	27,500	28	66.67	1	3
FLFRBHigh32-32-32	34,500	30	66.67	1	3
FLFRBHigh64-64-16	29,500	48	66.67	1	3
FLFRBHigh64-64-32	36,500	50	66.67	1	3
FLFRBHigh64-64-64	37,500	60	66.67	1	3
FLFRBLow16-16-16	13,500	24	66.67	3	3
FLFRBLow32-32-16	27,500	28	66.67	3	3
FLFRBLow32-32-32	34,500	30	66.67	3	3
FLFRBLow64-64-16	29,500	48	66.67	3	3
FLFRBLow64-64-32	36,500	50	66.67	3	3
FLFRBLow64-64-64	37,500	60	66.67	3	3
FSLSRHigh16-16-16	13,500	24	66.67	1	3
FSLSRHigh32-16-16	20,500	26	66.67	1	3
FSLSRHigh32-32-32	34,500	30	66.67	1	3
FSLSRHigh64-16-16	21,500	36	66.67	1	3

Table 4.2 continued

FSLSRHigh64-32-32	35,500	40	66.67	1	3
FSLSRHigh64-64-64	37,500	60	66.67	1	3
FSLSRLow16-16-16	13,500	24	66.67	3	3
FSLSRLow32-16-16	20,500	26	66.67	3	3
FSLSRLow32-32-32	34,500	30	66.67	3	3
FSLSRLow64-16-16	21,500	36	66.67	3	3
FSLSRLow64-32-32	35,500	40	66.67	3	3
FSLSRLow64-64-64	37,500	60	66.67	3	3
FLFRRLRRHigh16-16-16-16	18,000	32	75.00	1	4
FLFRRLRRHigh32-32-16-16	32,000	36	75.00	1	4
FLFRRLRRHigh32-32-32-32	46,000	40	75.00	1	4
FLFRRLRRHigh64-64-16-16	34,000	56	75.00	1	4
FLFRRLRRHigh64-64-32-32	48,000	60	75.00	1	4
FLFRRLRRHigh64-64-64-64	50,000	80	75.00	1	4
FLFRRLRRLow16-16-16-16	18,000	32	75.00	3	4
FLFRRLRRLow32-32-16-16	32,000	36	75.00	3	4
FLFRRLRRLow32-32-32-32	46,000	40	75.00	3	4
FLFRRLRRLow64-64-16-16	34,000	56	75.00	3	4
FLFRRLRRLow64-64-32-32	48,000	60	75.00	3	4
FLFRRLRRLow64-64-64-64	50,000	80	75.00	3	4
FSLSRBHigh16-16-16-16	18,000	32	75.00	1	4
FSLSRBHigh32-16-16-16	25,000	34	75.00	1	4
FSLSRBHigh32-32-32-32	46,000	40	75.00	1	4
FSLSRBHigh64-16-16-16	26,000	44	75.00	1	4
FSLSRBHigh64-32-32-16	40,000	48	75.00	1	4
FSLSRBHigh64-64-64-64	50,000	80	75.00	1	4
FSLSRBLow16-16-16-16	18,000	32	75.00	3	4
FSLSRBLow32-16-16-16	25,000	34	75.00	3	4
FSLSRBLow32-32-32-32	46,000	40	75.00	3	4
FSLSRBLow64-16-16-16	26,000	44	75.00	3	4
FSLSRBLow64-32-32-16	40,000	48	75.00	3	4
FSLSRBLow64-64-64-64	50,000	80	75.00	3	4

4.1.3 Weighting and Scaling Data Collected Using the Questionnaire

The data obtained through the questionnaire include the weighting data and the scaling data (used to derive the value functions).

4.1.3 (a) Weighting Data

A total of 20 responses were collected to assign weights to each criterion. Table 4.3 presents the weighting results. In Chapter 5, this data is used in the amalgamation phase of the analysis.

Table 4.3: Weighting data generated from the survey results

Respondents ID	PD	COS	PC	BR	SR	AES	EOI
1	38	8	8	8	15	8	15
2	27	11	13	17	16	7	9
3	25	6	13	25	19	3	10
4	0	45	0	27	27	0	0
5	33	13	7	20	20	3	4
6	20	20	13	7	20	7	13
7	30	19	3	20	6	10	13
8	26	18	11	14	13	8	11
9	33	17	11	11	11	7	11
10	25	15	6	18	13	15	9
11	20	13	20	13	13	7	13
12	29	7	14	21	14	7	7
13	29	14	14	14	7	7	14
14	25	19	19	19	13	0	6
15	29	18	6	24	18	0	6
16	50	13	13	17	3	3	2
17	13	25	13	25	13	0	13
18	20	20	20	18	7	4	12
19	27	27	7	20	13	0	7
20	31	31	8	15	8	0	8
Average:	26.46	17.88	10.84	17.63	13.36	4.68	9.14

4.1.3 (b) Scaling Data

Table 4.4 presents the data obtained from the mid-value splitting questionnaire results. In Table 4.4, the criteria values corresponding to values of 25, 50, and 75 were assigned by respondents and the criteria values corresponding to 0 and 100 were provided to them.

Table 4.4: Scaling data generated from the survey results (mid-value splitting)

Value	PD	COS	PC	BR	SR	AES	EOI
0	40	50,000	80	120	0	0	4.00
0	40	50,000	80	120	0	0	4.00
0	40	50,000	80	120	0	0	4.00
0	40	50,000	80	120	0	0	4.00
0	40	50,000	80	120	0	0	4.00
0	40	50,000	80	120	0	0	4.00
0	40	50,000	80	120	0	0	4.00
0	40	50,000	80	120	0	0	4.00
0	40	50,000	80	120	0	0	4.00
0	40	50,000	80	120	0	0	4.00
0	40	50,000	80	120	0	0	4.00
0	40	50,000	80	120	0	0	4.00
0	40	50,000	80	120	0	0	4.00
0	40	50,000	80	120	0	0	4.00
0	40	50,000	80	120	0	0	4.00
0	40	50,000	80	120	0	0	4.00
0	40	50,000	80	120	0	0	4.00
0	40	50,000	80	120	0	0	4.00
0	40	50,000	80	120	0	0	4.00
0	40	50,000	80	120	0	0	4.00
25	200	35,000	40	30	75	1	3.00
25	190	40,000	40	50	60	1	3.00
25	180	40,000	65	80	70	1	3.00
25	75	15,000	60	70	10	1	3.00
25	150	40,000	72	62	60	1	3.00
25	50	10,000	25	70	15	1	3.00
25	90	30,000	50	74	2	1	3.00
25	100	25,000	60	80	25	1	3.00
25	90	25,000	30	80	40	1	2.00
25	60	40,000	70	95	25	1	3.80
25	50	35,000	60	95	15	1	3.00
25	120	30,000	75	50	50	1	3.50
25	50	10,000	40	60	70	1	2.00
25	55	30,000	40	50	25	1	3.00
25	50	7,100	55	80	35	1	3.50
25	200	30,000	40	50	25	1	3.00
25	70	12,000	40	40	25	1	2.00
25	100	12,000	60	60	55	1	2.50
25	55	20,000	50	60	50	1	3.50
25	60	15,000	50	55	55	1	3.00

Table 4.4 continued

50	240	30,000	30	20	80	2	2.00
50	200	30,000	30	40	70	2	2.00
50	200	35,000	55	60	80	2	2.00
50	100	10,000	40	45	35	2	2.00
50	200	20,000	65	50	75	2	2.00
50	180	8,000	15	45	50	2	2.00
50	200	8,500	35	51	11	2	2.00
50	200	10,000	40	50	50	2	2.00
50	150	15,000	15	40	70	2	1.50
50	100	25,000	50	70	50	2	2.50
50	70	25,000	40	60	45	2	2.50
50	200	20,000	60	25	75	2	3.00
50	200	7,500	20	40	80	2	1.50
50	90	20,000	20	20	50	2	2.00
50	200	6,800	40	60	65	2	3.00
50	300	20,000	20	20	50	2	2.50
50	100	8,500	35	30	50	2	1.70
50	120	10,000	50	40	75	2	2.00
50	100	15,000	45	45	75	2	2.00
50	110	10,000	35	40	65	2	2.00
75	150	10,000	10	15	75	3	1.00
75	150	5,200	20	30	80	3	2.00
75	500	10,000	10	15	75	3	1.00
75	150	7,500	25	20	85	3	1.50
75	135	7,000	30	25	90	3	1.50
75	200	10,000	35	30	85	3	1.50
75	125	8,500	20	20	90	3	1.50
100	800	4,500	8	10	100	4	1.00
100	800	4,500	8	10	100	4	1.00
100	800	4,500	8	10	100	4	1.00
100	800	4,500	8	10	100	4	1.00
100	800	4,500	8	10	100	4	1.00
100	800	4,500	8	10	100	4	1.00
100	800	4,500	8	10	100	4	1.00
100	800	4,500	8	10	100	4	1.00
100	800	4,500	8	10	100	4	1.00
100	800	4,500	8	10	100	4	1.00
100	800	4,500	8	10	100	4	1.00
100	800	4,500	8	10	100	4	1.00
100	800	4,500	8	10	100	4	1.00
100	800	4,500	8	10	100	4	1.00

Table 4.4 continued

100	800	4,500	8	10	100	4	1.00
100	800	4,500	8	10	100	4	1.00
100	800	4,500	8	10	100	4	1.00
100	800	4,500	8	10	100	4	1.00
100	800	4,500	8	10	100	4	1.00
100	800	4,500	8	10	100	4	1.00

Table 4.5 presents the direct rating assigned to aesthetics by respondents. The LiDAR placement alternatives were categorized based on the number and elevation of the sensors. Respondents were asked to assign values of 0, 25, 50, 75, and 100 to the different categories with 0 being their least favorable and 100 being their most preferred option. The categories are no sensors, 1–2 sensors at high elevations, 1–2 sensors at low elevations, 3–4 sensors at high elevations, and 3–4 sensors at low elevations.

Table 4.5: Scaling data for the Aesthetics Criterion (Survey Results)

Respondents ID	No-sensors	1-2 Sensors-Low	1-2 Sensors-High	3-4 Sensors-Low	3-4 Sensors-High
1	0	25	50	75	100
2	100	75	25	50	0
3	100	75	50	25	0
4	100	75	50	25	0
5	100	75	50	25	0
6	100	75	50	25	0
7	0	100	75	50	25
8	100	75	50	25	0
9	0	50	75	25	25
10	0	50	25	100	75
11	0	75	50	100	25
12	0	25	50	75	100
13	0	75	25	100	50
14	0	50	25	100	75
15	0	25	50	50	100
16	100	75	25	50	0
17	100	75	25	50	0
18	100	75	25	50	0
19	100	75	25	50	0
20	100	75	25	50	0
Average:	**55**	**65**	**41.25**	**55**	**28.75**

4.1.4 Sensitivity Analysis of the Weighting Data

A sensitivity analysis was carried out using randomly generated data to introduce diverse weights for each criterion. This approach helped to assess the impact of varying criteria on the overall rankings of the alternatives. Ten scenarios of criteria weights were generated and subsequently used (Chapter 5) to obtain an overall ranking for the LiDAR placement alternatives. Table 4.6 presents the randomly generated weight data. It is important to note that these weights were generated in such a way that there was no bias against any criterion.

Table 4.6: Criterion Weights for the Sensitivity Analysis

	PD	SC	PC	BR	SR	AES	EOI	Total
Scenario 1	19	21	14	12	14	13	7	100
Scenario 2	27	14	22	6	25	3	2	100
Scenario 3	17	19	16	21	1	9	17	100
Scenario 4	6	15	22	14	18	6	19	100
Scenario 5	8	17	14	17	18	17	10	100
Scenario 6	19	20	6	3	11	22	19	100
Scenario 7	21	19	17	14	1	23	6	100
Scenario 8	1	9	21	23	7	9	30	100
Scenario 9	26	18	5	9	23	6	12	100
Scenario 10	12	21	5	21	24	10	7	100

4.2 Summary of Chapter 4

Chapter 4 examines the data collection methods used throughout the thesis, beginning with an overview of the diverse sources from which information was gathered. These sources encompass data obtained from CARLA, the primary simulation platform, alongside additional datasets procured from various external sources. This compilation of data includes crucial information pivotal to evaluating performance criteria within the decision-making process. The chapter further details the methodologies used to collect data from these sources, emphasizing their individual significance within the broader context of the thesis.

The chapter also explores the intricacies of the weighting and scaling processes applied to the collected data. The different categories of weights utilized in the thesis were discussed, including respondent-assigned weights, randomly generated weights, and equal weights, with each contributing distinctively to the decision-making model.

Overall, Chapter 4 presents the methodologies used for data collection, emphasizing the importance of diverse data sources, the processes of weighting and scaling, and the impact of sensitivity analysis. These elements collectively played a fundamental role in the subsequent phases of the decision-making process within the thesis.

CHAPTER 5. RESULTS AND DISCUSSION

This chapter presents the findings of the thesis concerning the LiDAR placement optimization using a multi-criteria decision framework. Initially, respondent-assigned weights were used to obtain an overall ranking for the alternatives. Subsequently, equal weights and randomly generated weights were used to get an overall ranking of the alternative LiDAR placement designs. The equal weighting involved assigning each criterion a weight of 14.29, thus, assuming an equal level of importance for all criteria in the decision-making process. However, this method does not accurately reflect the true significance of each criterion within the research context. To address this, a sensitivity analysis was conducted using randomly generated weights to observe how changes in criteria weights influenced the ranking of the alternatives. This analysis helped to assess the impact of varying criteria weights on the ranking of the alternatives.

5.1 Results Based on Respondent-Assigned Weights

5.1.1 Summary of Weighting Results

In the evaluation of the decision criteria, 20 responses were considered to determine the average values, collectively reflecting the overall decision-making regarding the assignment of weights.

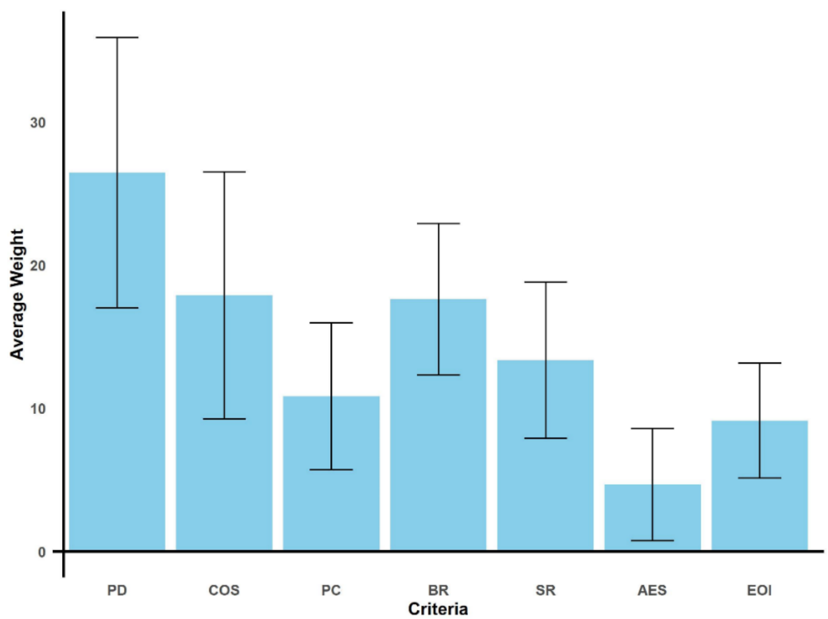

Figure 5.1: Weighting Results (Respondent-assigned)

The weighting results reveal the collective perspective of the respondents and their expertise in the subject matter. Notably, the criterion with the highest average weight is the point density (PD), which received an average value of 26.46. This high rating displays the overall importance attributed to the detection of objects, which is a safety component in the decision-making process. This result suggests a shared view that the precision and efficiency of detection capabilities significantly influence the performance of the AV.

Conversely, aesthetics (AES) and ease of installation (EOI) received lower average weights of 4.68 and 9.14, respectively. These comparatively lower weights indicate a consensus among the respondents that, while aesthetics and ease of installation are considerations, they are deemed less important than other criteria. This prioritization of technical and functional aspects over aesthetic appeal and ease of installation can be attributed to the main purpose of AVs; hence, performance and functionality are the primary concerns.

Furthermore, the variability within each criterion is highlighted by the standard deviations: PD (9.44), COS (8.62), PC (5.13), BR (5.29), SR (5.46), AES (3.92), and EOI (4.01). This variability showcases varying levels of consistency within the dataset. Higher standard deviations indicate greater diversity among data points, while lower deviations signify a more uniform trend across the criteria. This gradient in variability underscores the diverse ranges of values and dispersion around the mean, offering insights into the heterogeneity and consistency present within the evaluated criteria.

5.1.2 Summary of Scaling Results

To obtain the value functions used for the scaling process, a regression analysis was carried out to establish a function that represents the collective preferences of the data obtained from the respondents. To do so, a regression line was fitted to the data and the best-fit line was determined based on which option had the least deviation from the collected responses. This approach provided a holistic understanding of the respondents' preferences and aided in identifying the overall trend within the dataset.

Figure 5.2 illustrates the resulting value function charts. The regression line, representing the best fit for the data, was selected in the form of logarithmic, linear, or exponential functions, based on its alignment with the observed patterns in the dataset. The regression equations were then used to scale the data for amalgamation and to obtain results.

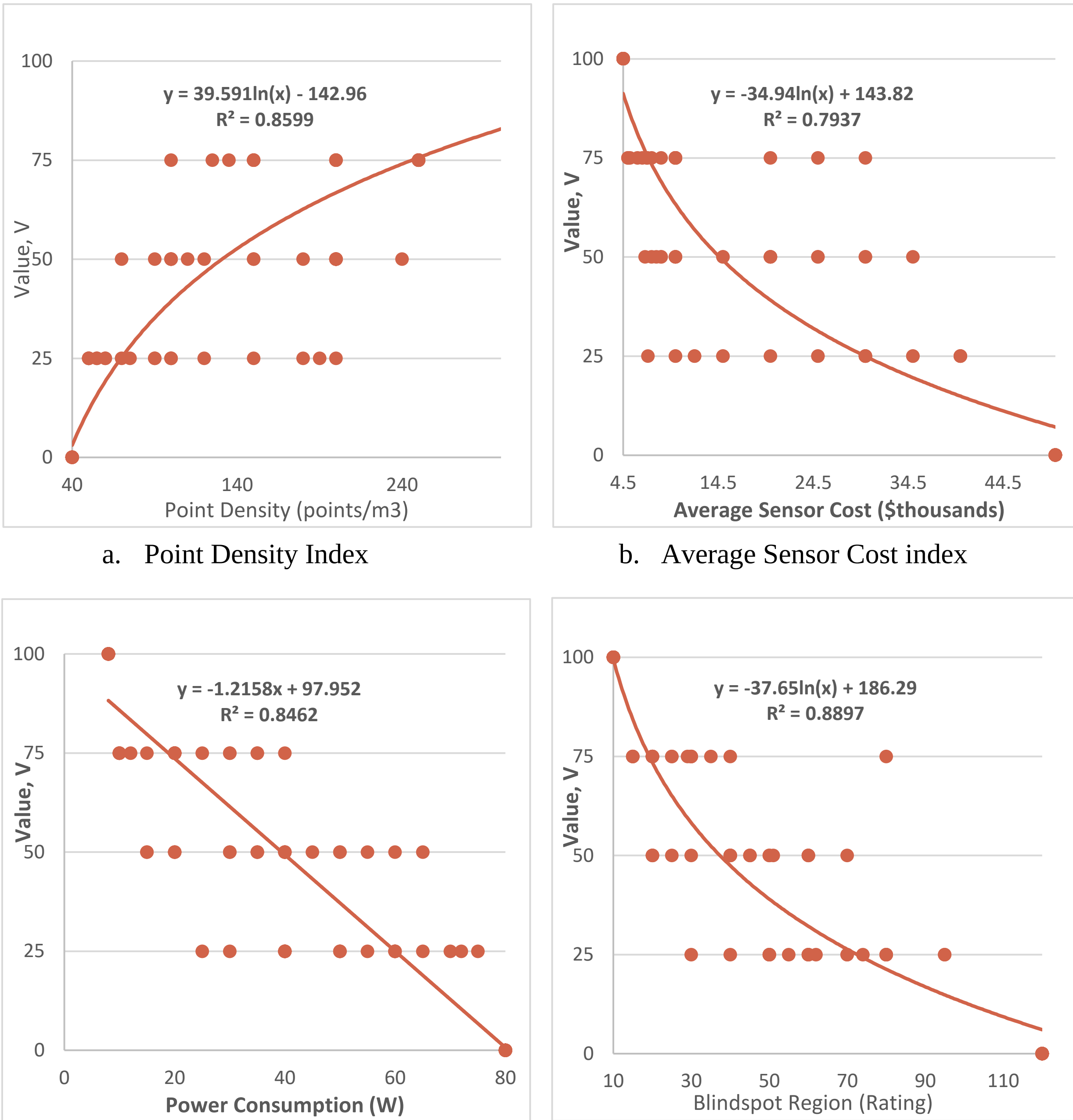

a. Point Density Index

b. Average Sensor Cost index

c. Power Consumption index

d. Blindspot Region index

Figure 5.2: Value Functions of the Decision Criteria

Figure 5.2 continued

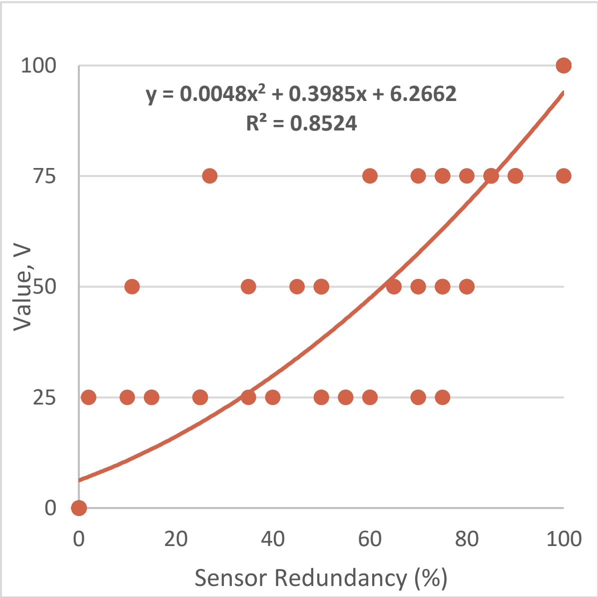

e. Sensor Redundancy index

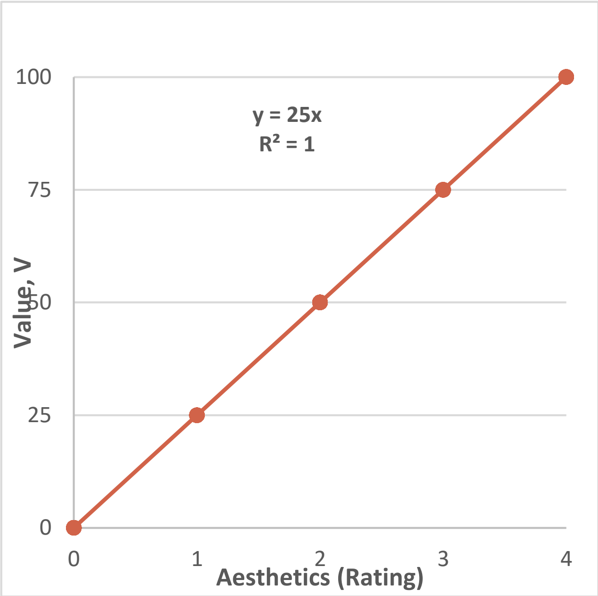

f. Aesthetics index

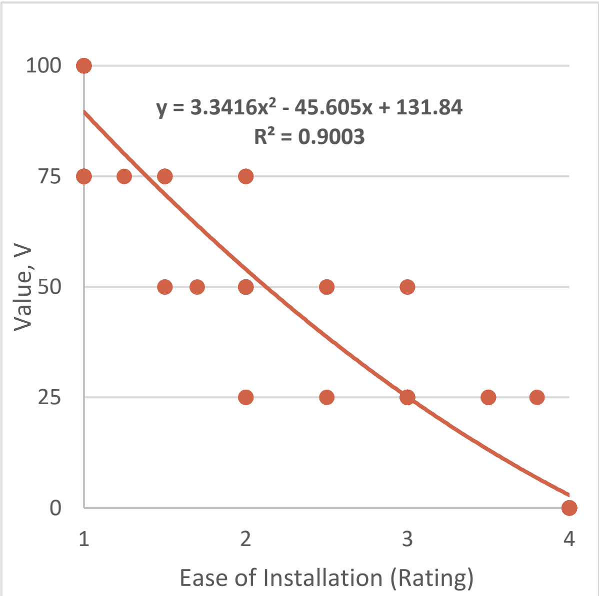

g. Ease of Installation index

The value functions were used to obtain the scaling results. Using the sensor redundancy index as an example, if the raw data (X) is 60, the value function (Y) = 0.0084X^2 - 0.0121X + 2.2483 is applied by replacing X in the equation Y = $0.0084(60)^2 - 0.0121(60) + 2.2483$ to get the Scaled Value $(Y) = 31.7633$. This process is repeated for all the criteria.

5.1.3 Amalgamation Results

This section presents the outcomes derived from the application of the WSM explained in Chapter 3. The utilization of this method in the amalgamation process involves the weighting and scaling of the raw values for each criterion. This culminates in the determination of the outcomes for each alternative. The methodology considers the “contributions” of each criterion, reflecting their respectively assigned weights. Based on the amalgamation results, the LiDAR placement alternatives were then ranked using their overall scores. This hierarchy streamlined the choice of the best design and also facilitates meaningful comparison.

5.2 Amalgamation Results Based on Respondent-Assigned Weights

In Tables 5.1 and 5.2, the results are presented by utilizing weights derived from the questionnaire. As detailed in previous chapters, the respondents provided their preferences, thereby contributing to the determination of criterion weights. Tables 5.1 and 5.2 offer insights into the outcomes achieved by incorporating these questionnaire-based weights into the evaluation process.

Table 5.1: Amalgamation Results: Sensing target–Vehicle, based on respondent-assigned weights of the criteria

Criteria / Weight / Alternatives	PDV	SC	PC	BR	SR	AES	EOI	Amalgamation Results	Rank
	26.46	17.88	10.84	17.63	13.36	4.68	9.14		
CHigh16	14.6	85.3	88.2	26.3	6.3	50	89.6	4469.8	67
CHigh32	32.2	57.3	85.8	26.3	6.3	50	89.6	4408.6	69
CHigh64	41.1	54.8	73.6	26.3	6.3	50	89.6	4466.6	68
CLow16	37.6	85.3	88.2	32.1	6.3	100	89.6	5414.7	25
CLow32	45.2	57.3	85.8	32.1	6.3	100	89.6	5086.9	37
CLow64	54.0	54.8	73.6	32.1	6.3	100	89.6	5143.9	36
FHigh16	36.9	85.3	88.2	39.0	6.3	100	89.6	5515.7	21
FHigh32	56.2	57.3	85.8	39.0	6.3	50	89.6	5266.1	31
FHigh64	54.0	54.8	73.6	39.0	6.3	50	89.6	5029.9	45
FLow16	36.6	85.3	88.2	47.4	6.3	100	89.6	5658.1	18
FLow32	49.1	57.3	85.8	47.4	6.3	100	89.6	5459.4	23
FLow64	57.4	54.8	73.6	47.4	6.3	100	89.6	5502.1	22
FBHigh16-16	64.5	64.6	78.5	6.0	38.2	50	54.0	5057.3	40
FBHigh32-32	84.3	36.5	73.6	6.0	38.2	50	54.0	5027.1	46
FBHigh64-64	84.3	34.1	49.3	6.0	38.2	50	54.0	4719.3	61
FBLow16-16	66.3	64.6	78.5	58.2	38.2	100	54.0	6259.5	6
FBLow32-32	85.1	36.5	73.6	58.2	38.2	100	54.0	6202.5	7
FBLow64-64	83.2	34.1	49.3	58.2	38.2	100	54.0	5843.7	15
FBHigh32-16	76.5	47.4	76.1	6.0	38.2	50	54.0	5041.4	43
FBHigh64-32	84.2	35.3	61.5	6.0	38.2	50	54.0	4869.8	54
FBLow32-16	76.5	47.4	76.1	58.2	38.2	100	54.0	6195.9	8
FBLow64-32	86.1	35.3	61.5	58.2	38.2	100	54.0	6073.8	11
FBHigh64-16	78.5	45.6	63.9	6.0	38.2	50	54.0	4930.8	51
FBLow64-16	77.3	45.6	63.9	58.2	38.2	100	54.0	6052.9	12
FLFRBHigh16-16-16	70.5	52.5	68.8	16.9	54.2	25	25.1	4917.9	52
FLFRBHigh32-32-16	82.9	31.2	63.9	16.9	54.2	25	25.1	4812.4	57
FLFRBHigh32-32-32	87.1	24.4	61.5	16.9	54.2	25	25.1	4776.8	59
FLFRBHigh64-64-16	83.0	29.1	39.6	16.9	54.2	25	25.1	4515.0	66
FLFRBHigh64-64-32	88.5	22.7	37.2	16.9	54.2	25	25.1	4519.5	65
FLFRBHigh64-64-64	88.6	21.9	25.0	16.9	54.2	25	25.1	4374.4	70
FLFRBLow16-16-16	70.1	52.5	68.8	73.5	54.2	75	25.1	6139.7	10
FLFRBLow32-32-16	81.7	31.2	63.9	73.5	54.2	75	25.1	6014.0	14
FLFRBLow32-32-32	87.8	24.4	61.5	73.5	54.2	75	25.1	6027.9	13
FLFRBLow64-64-16	82.4	29.1	39.6	73.5	54.2	75	25.1	5731.6	16
FLFRBLow64-64-32	87.0	22.7	37.2	73.5	54.2	75	25.1	5711.8	17
FLFRBLow64-64-64	87.4	21.9	25.0	73.5	54.2	75	25.1	5577.1	19
FSLSRHigh16-16-16	84.0	52.5	68.8	16.9	54.2	25	25.1	5273.6	30
FSLSRHigh32-16-16	88.7	40.0	66.3	16.9	54.2	25	25.1	5149.1	35

Table 5.1 continued

FSLSRHigh32-32-32	97.9	24.4	61.5	16.9	54.2	25	25.1	5060.4	39
FSLSRHigh64-16-16	90.8	38.6	54.2	16.9	54.2	25	25.1	5047.7	42
FSLSRHigh64-32-32	100.3	23.6	49.3	16.9	54.2	25	25.1	4978.4	50
FSLSRHigh64-64-64	100.8	21.9	25.0	16.9	54.2	25	25.1	4697.7	62
FSLSRLow16-16-16	82.1	52.5	68.8	21.3	54.2	75	25.1	5535.3	20
FSLSRLow32-16-16	88.3	40.0	66.3	21.3	54.2	75	25.1	5450.1	24
FSLSRLow32-32-32	98.9	24.4	61.5	21.3	54.2	75	25.1	5399.9	26
FSLSRLow64-16-16	88.9	38.6	54.2	21.3	54.2	75	25.1	5308.8	28
FSLSRLow64-32-32	99.8	23.6	49.3	21.3	54.2	75	25.1	5277.8	29
FSLSRLow64-64-64	101.0	21.9	25.0	21.3	54.2	75	25.1	5016.9	47
FLFRRLRRHigh16-16-16-16	94.6	43.9	59.0	9.3	63.2	25	2.9	5079.9	38
FLFRRLRRHigh32-32-16-16	105.0	26.7	54.2	9.3	63.2	25	2.9	4993.2	49
FLFRRLRRHigh32-32-32-32	111.4	15.8	49.3	9.3	63.2	25	2.9	4916.8	53
FLFRRLRRHigh64-64-16-16	107.9	24.9	29.9	9.3	63.2	25	2.9	4775.7	60
FLFRRLRRHigh64-64-32-32	110.7	14.6	25.0	9.3	63.2	25	2.9	4611.7	63
FLFRRLRRHigh64-64-64-64	111.4	13.3	0.7	9.3	63.2	25	2.9	4345.9	71
FLFRRLRRLow16-16-16-16	93.9	43.9	59.0	99.6	63.2	75	2.9	6887.6	1
FLFRRLRRLow32-32-16-16	104.2	26.7	54.2	99.6	63.2	75	2.9	6799.1	2
FLFRRLRRLow32-32-32-32	111.7	15.8	49.3	99.6	63.2	75	2.9	6749.7	3
FLFRRLRRLow64-64-16-16	108.3	24.9	29.9	99.6	63.2	75	2.9	6611.9	4
FLFRRLRRLow64-64-32-32	110.6	14.6	25.0	99.6	63.2	75	2.9	6436.8	5
FLFRRLRRLow64-64-64-64	111.4	13.3	0.7	99.6	63.2	75	2.9	6172.1	9
FSLSRBHigh16-16-16-16	93.0	43.9	59.0	9.3	63.2	25	2.9	5036.1	44
FSLSRBHigh32-16-16-16	99.0	34.1	56.6	9.3	63.2	25	2.9	4995.0	48
FSLSRBHigh32-32-32-32	108.4	15.8	49.3	9.3	63.2	25	2.9	4836.8	56
FSLSRBHigh64-16-16-16	97.8	32.9	44.5	9.3	63.2	25	2.9	4808.7	58
FSLSRBHigh64-32-32-16	110.7	20.0	39.6	9.3	63.2	25	2.9	4868.0	55
FSLSRBHigh64-64-64-64	109.7	13.3	0.7	9.3	63.2	25	2.9	4299.7	72
FSLSRBLow16-16-16-16	94.1	43.9	59.0	12.9	63.2	75	2.9	5362.5	27
FSLSRBLow32-16-16-16	97.7	34.1	56.6	12.9	63.2	75	2.9	5256.4	32
FSLSRBLow32-32-32-32	109.0	15.8	49.3	12.9	63.2	75	2.9	5150.8	34
FSLSRBLow64-16-16-16	99.5	32.9	44.5	12.9	63.2	75	2.9	5151.7	33
FSLSRBLow64-32-32-16	106.6	20.0	39.6	12.9	63.2	75	2.9	5056.4	41
FSLSRBLow64-64-64-64	109.9	13.3	0.7	12.9	63.2	75	2.9	4602.0	64

Table 5.2: Amalgamation Results: Sensing target–Pedestrian, based on respondent-assigned weights of the criteria

Alternatives \ Criteria / Weight	PDV	SC	PC	BR	SR	AES	EOI	Amalgamation Results	Rank
	26.46	17.88	10.84	17.63	13.36	4.68	9.14		
CHigh16	15.5	85.3	88.2	26.3	6.3	50	89.6	4493.4	71
CHigh32	37.4	57.3	85.8	26.3	6.3	50	89.6	4545.6	69
CHigh64	45.0	54.8	73.6	26.3	6.3	50	89.6	4570.4	68
CLow16	39.4	85.3	88.2	32.1	6.3	100	89.6	5462.2	30
CLow32	44.8	57.3	85.8	32.1	6.3	100	89.6	5077.7	51
CLow64	65.3	54.8	73.6	32.1	6.3	100	89.6	5444.5	32
FHigh16	34.6	85.3	88.2	39.0	6.3	100	89.6	5455.3	31
FHigh32	65.9	57.3	85.8	39.0	6.3	50	89.6	5522.8	27
FHigh64	29.8	54.8	73.6	39.0	6.3	50	89.6	4391.5	72
FLow16	40.7	85.3	88.2	47.4	6.3	100	89.6	5766.7	20
FLow32	58.9	57.3	85.8	47.4	6.3	100	89.6	5719.0	22
FLow64	73.3	54.8	73.6	47.4	6.3	100	89.6	5923.8	17
FBHigh16-16	61.3	64.6	78.5	6.0	38.2	50	54.0	4972.4	56
FBHigh32-32	94.3	36.5	73.6	6.0	38.2	50	54.0	5290.7	38
FBHigh64-64	93.7	34.1	49.3	6.0	38.2	50	54.0	4967.3	57
FBLow16-16	68.8	64.6	78.5	58.2	38.2	100	54.0	6326.1	11
FBLow32-32	73.8	36.5	73.6	58.2	38.2	100	54.0	5904.5	18
FBLow64-64	97.9	34.1	49.3	58.2	38.2	100	54.0	6232.1	13
FBHigh32-16	84.8	47.4	76.1	6.0	38.2	50	54.0	5259.6	39
FBHigh64-32	93.3	35.3	61.5	6.0	38.2	50	54.0	5109.7	47
FBLow32-16	86.9	47.4	76.1	58.2	38.2	100	54.0	6470.2	6
FBLow64-32	96.4	35.3	61.5	58.2	38.2	100	54.0	6348.4	10
FBHigh64-16	86.3	45.6	63.9	6.0	38.2	50	54.0	5135.6	46
FBLow64-16	89.9	45.6	63.9	58.2	38.2	100	54.0	6385.6	8
FLFRBHigh16-16-16	67.8	52.5	68.8	16.9	54.2	25	25.1	4844.5	63
FLFRBHigh32-32-16	92.4	31.2	63.9	16.9	54.2	25	25.1	5064.8	52
FLFRBHigh32-32-32	96.6	24.4	61.5	16.9	54.2	25	25.1	5026.2	53
FLFRBHigh64-64-16	92.9	29.1	39.6	16.9	54.2	25	25.1	4775.2	65
FLFRBHigh64-64-32	99.0	22.7	37.2	16.9	54.2	25	25.1	4798.0	64
FLFRBHigh64-64-64	98.7	21.9	25.0	16.9	54.2	25	25.1	4642.6	66
FLFRBLow16-16-16	73.2	52.5	68.8	73.5	54.2	75	25.1	6220.8	14
FLFRBLow32-32-16	93.4	31.2	63.9	73.5	54.2	75	25.1	6323.0	12
FLFRBLow32-32-32	100.6	24.4	61.5	73.5	54.2	75	25.1	6365.6	9
FLFRBLow64-64-16	94.6	29.1	39.6	73.5	54.2	75	25.1	6053.3	15
FLFRBLow64-64-32	98.8	22.7	37.2	73.5	54.2	75	25.1	6024.5	16
FLFRBLow64-64-64	99.2	21.9	25.0	73.5	54.2	75	25.1	5887.5	19
FSLSRHigh16-16-16	79.9	52.5	68.8	16.9	54.2	25	25.1	5166.5	45
FSLSRHigh32-16-16	92.3	40.0	66.3	16.9	54.2	25	25.1	5245.7	41

Table 5.2 continued

FSLSRHigh32-32-32	108.8	24.4	61.5	16.9	54.2	25	25.1	5351.3	37
FSLSRHigh64-16-16	95.3	38.6	54.2	16.9	54.2	25	25.1	5166.8	44
FSLSRHigh64-32-32	110.6	23.6	49.3	16.9	54.2	25	25.1	5250.3	40
FSLSRHigh64-64-64	109.8	21.9	25.0	16.9	54.2	25	25.1	4935.5	59
FSLSRLow16-16-16	85.0	52.5	68.8	21.3	54.2	75	25.1	5612.7	25
FSLSRLow32-16-16	97.3	40.0	66.3	21.3	54.2	75	25.1	5689.6	23
FSLSRLow32-32-32	112.1	24.4	61.5	21.3	54.2	75	25.1	5749.7	21
FSLSRLow64-16-16	98.0	38.6	54.2	21.3	54.2	75	25.1	5549.7	26
FSLSRLow64-32-32	114.0	23.6	49.3	21.3	54.2	75	25.1	5652.6	24
FSLSRLow64-64-64	114.7	21.9	25.0	21.3	54.2	75	25.1	5378.2	35
FLFRRLRRHigh16-16-16-16	91.4	43.9	59.0	9.3	63.2	25	2.9	4994.0	54
FLFRRLRRHigh32-32-16-16	113.4	26.7	54.2	9.3	63.2	25	2.9	5215.8	42
FLFRRLRRHigh32-32-32-32	121.7	15.8	49.3	9.3	63.2	25	2.9	5188.4	43
FLFRRLRRHigh64-64-16-16	115.5	24.9	29.9	9.3	63.2	25	2.9	4975.7	55
FLFRRLRRHigh64-64-32-32	120.7	14.6	25.0	9.3	63.2	25	2.9	4875.8	61
FLFRRLRRHigh64-64-64-64	120.7	13.3	0.7	9.3	63.2	25	2.9	4591.3	67
FLFRRLRRLow16-16-16-16	95.2	43.9	59.0	99.6	63.2	75	2.9	6921.7	3
FLFRRLRRLow32-32-16-16	114.2	26.7	54.2	99.6	63.2	75	2.9	7063.0	1
FLFRRLRRLow32-32-32-32	121.9	15.8	49.3	99.6	63.2	75	2.9	7021.2	2
FLFRRLRRLow64-64-16-16	119.1	24.9	29.9	99.6	63.2	75	2.9	6896.4	4
FLFRRLRRLow64-64-32-32	121.2	14.6	25.0	99.6	63.2	75	2.9	6717.1	5
FLFRRLRRLow64-64-64-64	121.9	13.3	0.7	99.6	63.2	75	2.9	6447.7	7
FSLSRBHigh16-16-16-16	89.5	43.9	59.0	9.3	63.2	25	2.9	4944.2	58
FSLSRBHigh32-16-16-16	102.5	34.1	56.6	9.3	63.2	25	2.9	5086.4	49
FSLSRBHigh32-32-32-32	118.1	15.8	49.3	9.3	63.2	25	2.9	5093.7	48
FSLSRBHigh64-16-16-16	100.1	32.9	44.5	9.3	63.2	25	2.9	4871.2	62
FSLSRBHigh64-32-32-16	118.8	20.0	39.6	9.3	63.2	25	2.9	5083.3	50
FSLSRBHigh64-64-64-64	118.4	13.3	0.7	9.3	63.2	25	2.9	4531.2	70
FSLSRBLow16-16-16-16	95.7	43.9	59.0	12.9	63.2	75	2.9	5405.8	33
FSLSRBLow32-16-16-16	105.5	34.1	56.6	12.9	63.2	75	2.9	5464.3	29
FSLSRBLow32-32-32-32	121.1	15.8	49.3	12.9	63.2	75	2.9	5471.0	28
FSLSRBLow64-16-16-16	109.1	32.9	44.5	12.9	63.2	75	2.9	5404.5	34
FSLSRBLow64-32-32-16	118.1	20.0	39.6	12.9	63.2	75	2.9	5362.0	36
FSLSRBLow64-64-64-64	120.4	13.3	0.7	12.9	63.2	75	2.9	4881.9	60

The respondent-assigned weights closely reflect the most effective LiDAR placements, aligning closely with highly weighted criteria such as point density, cost of sensor, and blind spot regions. Across both the vehicle and pedestrian scenarios, the top four placements demonstrate a consistent pattern with minor distinctions. For vehicle detection, the top four placements—beginning with the top performing—are FLFRRLRRLow16-16-16-16, FLFRRLRRLow32-32-16-16, FLFRRLRRLow32-32-32-32, and FLFRRLRRLow64-64-16-16. In contrast, for pedestrian detection, the results are FLFRRLRRLow32-32-16-16, FLFRRLRRLow32-32-32-32, FLFRRLRRLow16-16-16-16, and FLFRRLRRLow64-64-16-16. Across both vehicle and pedestrian scenarios, these placements consistently involve four LiDAR sensors positioned at the front left, front right, rear left, and rear right locations at low elevations.

Figure 5.3 presents a 3D model illustrating the LiDAR placement design representing the top four performing results. The differences among the four designs lie in the channels of the LiDAR sensors, as depicted in the results.

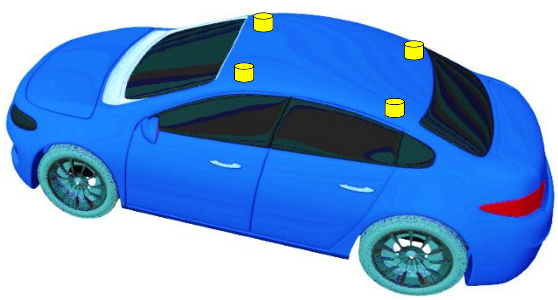

Figure 5.3: Model representing the top 4 LiDAR placement design

Figure 5.4 presents the heat map showing the ranking of all the LiDAR placement designs across both pedestrian and vehicle scenarios, with blue signifying lower scores and red signifying top-performing LiDAR placements.

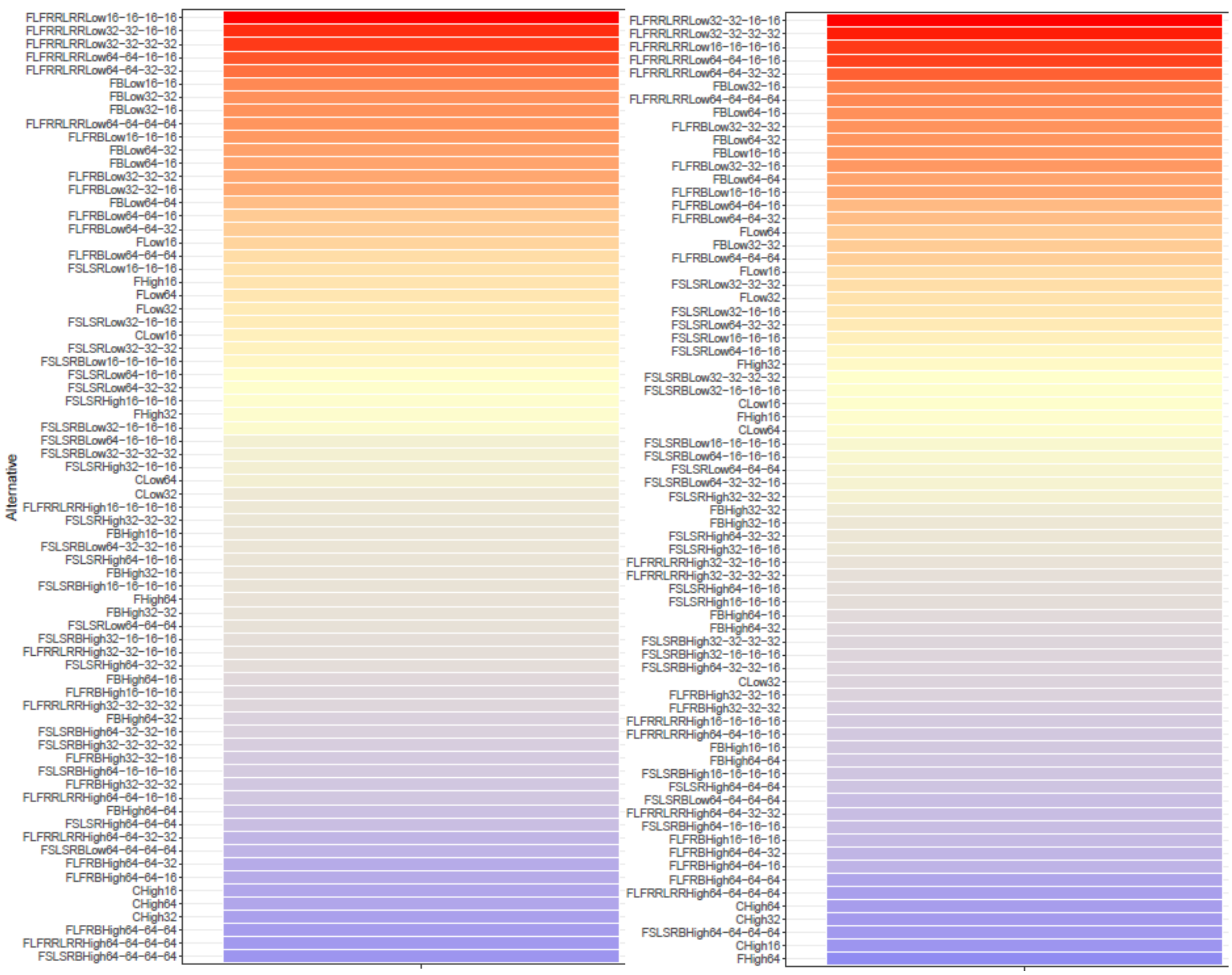

(a) Sensing target - Vehicle (respondent-assigned weights) **(b) Sensing target - Pedestrian (respondent-assigned weights)**

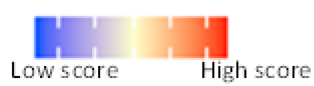

Figure 5.4: Heat Maps of Sensing targets (respondent-assigned weights)

5.3 Amalgamation Results Using Equal Weights

A uniform weighting approach was used, assigning equal weights of 14.286 to each of the eight criteria. This balanced distribution ensured that each criterion contributed equally to the overall assessment, preventing any single criterion from disproportionately influencing the results. Additionally, the scaling functions, previously outlined in this section (Chapter 5.1.2), were applied to obtain the scaled values. These scaling functions played a crucial role in standardizing and transforming the raw data, facilitating a coherent comparison and integration of diverse criterion values within the assessment framework. Tables 5.3 and 5.4 present the amalgamation results for both pedestrian and vehicle detections. The results are ranked based on the overall amalgamation score.

Table 5.3: Amalgamation Results: Sensing target–Vehicle, based on equal weights of the criteria

Criteria / Weight / Alternatives	PDV	SC	PC	BR	SR	AES	EOI	Amalgamation Results	Rank
Weight	14.29	14.29	14.29	14.29	14.29	14.29	14.29		
CHigh16	14.6	85.3	88.2	26.3	6.3	50	89.6	5148	31
CHigh32	32.2	57.3	85.8	26.3	6.3	50	89.6	4964	37
CHigh64	41.1	54.8	73.6	26.3	6.3	50	89.6	4881	40
CLow16	37.6	85.3	88.2	32.1	6.3	100	89.6	6273	6
CLow32	45.2	57.3	85.8	32.1	6.3	100	89.6	5946	16
CLow64	54.0	54.8	73.6	32.1	6.3	100	89.6	5863	17
FHigh16	36.9	85.3	88.2	39.0	6.3	100	89.6	6360	5
FHigh32	56.2	57.3	85.8	39.0	6.3	50	89.6	5487	22
FHigh64	54.0	54.8	73.6	39.0	6.3	50	89.6	5246	27
FLow16	36.6	85.3	88.2	47.4	6.3	100	89.6	6477	2
FLow32	49.1	57.3	85.8	47.4	6.3	100	89.6	6220	9
FLow64	57.4	54.8	73.6	47.4	6.3	100	89.6	6129	11
FBHigh16-16	64.5	64.6	78.5	6.0	38.2	50	54.0	5083	33
FBHigh32-32	84.3	36.5	73.6	6.0	38.2	50	54.0	4896	38
FBHigh64-64	84.3	34.1	49.3	6.0	38.2	50	54.0	4513	49
FBLow16-16	66.3	64.6	78.5	58.2	38.2	100	54.0	6569	1
FBLow32-32	85.1	36.5	73.6	58.2	38.2	100	54.0	6367	4
FBLow64-64	83.2	34.1	49.3	58.2	38.2	100	54.0	5957	15
FBHigh32-16	76.5	47.4	76.1	6.0	38.2	50	54.0	4974	36
FBHigh64-32	84.2	35.3	61.5	6.0	38.2	50	54.0	4703	43
FBLow32-16	76.5	47.4	76.1	58.2	38.2	100	54.0	6434	3
FBLow64-32	86.1	35.3	61.5	58.2	38.2	100	54.0	6189	10
FBHigh64-16	78.5	45.6	63.9	6.0	38.2	50	54.0	4804	41
FBLow64-16	77.3	45.6	63.9	58.2	38.2	100	54.0	6246	8
FLFRBHigh16-16-16	70.5	52.5	68.8	16.9	54.2	25	25.1	4470	50
FLFRBHigh32-32-16	82.9	31.2	63.9	16.9	54.2	25	25.1	4274	53
FLFRBHigh32-32-32	87.1	24.4	61.5	16.9	54.2	25	25.1	4203	57
FLFRBHigh64-64-16	83.0	29.1	39.6	16.9	54.2	25	25.1	3898	64
FLFRBHigh64-64-32	88.5	22.7	37.2	16.9	54.2	25	25.1	3851	66
FLFRBHigh64-64-64	88.6	21.9	25.0	16.9	54.2	25	25.1	3666	69
FLFRBLow16-16-16	70.1	52.5	68.8	73.5	54.2	75	25.1	5988	13
FLFRBLow32-32-16	81.7	31.2	63.9	73.5	54.2	75	25.1	5780	18
FLFRBLow32-32-32	87.8	24.4	61.5	73.5	54.2	75	25.1	5736	20
FLFRBLow64-64-16	82.4	29.1	39.6	73.5	54.2	75	25.1	5413	23
FLFRBLow64-64-32	87.0	22.7	37.2	73.5	54.2	75	25.1	5352	25
FLFRBLow64-64-64	87.4	21.9	25.0	73.5	54.2	75	25.1	5173	29
FSLSRHigh16-16-16	84.0	52.5	68.8	16.9	54.2	25	25.1	4662	45
FSLSRHigh32-16-16	88.7	40.0	66.3	16.9	54.2	25	25.1	4517	48
FSLSRHigh32-32-32	97.9	24.4	61.5	16.9	54.2	25	25.1	4356	51

Table 5.3 continued

FSLSRHigh64-16-16	90.8	38.6	54.2	16.9	54.2	25	25.1	4353	52
FSLSRHigh64-32-32	100.3	23.6	49.3	16.9	54.2	25	25.1	4205	56
FSLSRHigh64-64-64	100.8	21.9	25.0	16.9	54.2	25	25.1	3841	67
FSLSRLow16-16-16	82.1	52.5	68.8	21.3	54.2	75	25.1	5413	24
FSLSRLow32-16-16	88.3	40.0	66.3	21.3	54.2	75	25.1	5288	26
FSLSRLow32-32-32	98.9	24.4	61.5	21.3	54.2	75	25.1	5148	30
FSLSRLow64-16-16	88.9	38.6	54.2	21.3	54.2	75	25.1	5103	32
FSLSRLow64-32-32	99.8	23.6	49.3	21.3	54.2	75	25.1	4976	35
FSLSRLow64-64-64	101.0	21.9	25.0	21.3	54.2	75	25.1	4622	46
FLFRRLRRHigh16-16-16-16	94.6	43.9	59.0	9.3	63.2	25	2.9	4256	54
FLFRRLRRHigh32-32-16-16	105.0	26.7	54.2	9.3	63.2	25	2.9	4088	59
FLFRRLRRHigh32-32-32-32	111.4	15.8	49.3	9.3	63.2	25	2.9	3956	61
FLFRRLRRHigh64-64-16-16	107.9	24.9	29.9	9.3	63.2	25	2.9	3757	68
FLFRRLRRHigh64-64-32-32	110.7	14.6	25.0	9.3	63.2	25	2.9	3580	70
FLFRRLRRHigh64-64-64-64	111.4	13.3	0.7	9.3	63.2	25	2.9	3226	71
FLFRRLRRLow16-16-16-16	93.9	43.9	59.0	99.6	63.2	75	2.9	6250	7
FLFRRLRRLow32-32-16-16	104.2	26.7	54.2	99.6	63.2	75	2.9	6081	12
FLFRRLRRLow32-32-32-32	111.7	15.8	49.3	99.6	63.2	75	2.9	5963	14
FLFRRLRRLow64-64-16-16	108.3	24.9	29.9	99.6	63.2	75	2.9	5767	19
FLFRRLRRLow64-64-32-32	110.6	14.6	25.0	99.6	63.2	75	2.9	5584	21
FLFRRLRRLow64-64-64-64	111.4	13.3	0.7	99.6	63.2	75	2.9	5230	28
FSLSRBHigh16-16-16-16	93.0	43.9	59.0	9.3	63.2	25	2.9	4232	55
FSLSRBHigh32-16-16-16	99.0	34.1	56.6	9.3	63.2	25	2.9	4144	58
FSLSRBHigh32-32-32-32	108.4	15.8	49.3	9.3	63.2	25	2.9	3912	63
FSLSRBHigh64-16-16-16	97.8	32.9	44.5	9.3	63.2	25	2.9	3935	62
FSLSRBHigh64-32-32-16	110.7	20.0	39.6	9.3	63.2	25	2.9	3867	65
FSLSRBHigh64-64-64-64	109.7	13.3	0.7	9.3	63.2	25	2.9	3201	72
FSLSRBLow16-16-16-16	94.1	43.9	59.0	12.9	63.2	75	2.9	5013	34
FSLSRBLow32-16-16-16	97.7	34.1	56.6	12.9	63.2	75	2.9	4890	39
FSLSRBLow32-32-32-32	109.0	15.8	49.3	12.9	63.2	75	2.9	4687	44
FSLSRBLow64-16-16-16	99.5	32.9	44.5	12.9	63.2	75	2.9	4726	42
FSLSRBLow64-32-32-16	106.6	20.0	39.6	12.9	63.2	75	2.9	4573	47
FSLSBL64-64-64-64	109.9	13.3	0.7	12.9	63.2	75	2.9	3969	60

Table 5.4 Amalgamation Results: Sensing target–Pedestrian, based on equal weights of the criteria

Alternatives \ Criteria / Weight	PDV	SC	PC	BR	SR	AES	EOI	Amalgamation Results	Rank
	14.29	14.29	14.29	14.29	14.29	14.29	14.29		
CHigh16	15.5	85.3	88.2	26.3	6.3	50	89.6	5160	32
CHigh32	37.4	57.3	85.8	26.3	6.3	50	89.6	5038	35
CHigh64	45.0	54.8	73.6	26.3	6.3	50	89.6	4937	39
CLow16	39.4	85.3	88.2	32.1	6.3	100	89.6	6299	9
CLow32	44.8	57.3	85.8	32.1	6.3	100	89.6	5941	18
CLow64	65.3	54.8	73.6	32.1	6.3	100	89.6	6025	16
FHigh16	34.6	85.3	88.2	39.0	6.3	100	89.6	6328	8
FHigh32	65.9	57.3	85.8	39.0	6.3	50	89.6	5626	22
FHigh64	29.8	54.8	73.6	39.0	6.3	50	89.6	4901	41
FLow16	40.7	85.3	88.2	47.4	6.3	100	89.6	6536	3
FLow32	58.9	57.3	85.8	47.4	6.3	100	89.6	6360	5
FLow64	73.3	54.8	73.6	47.4	6.3	100	89.6	6356	6
FBHigh16-16	61.3	64.6	78.5	6.0	38.2	50	54.0	5037	36
FBHigh32-32	94.3	36.5	73.6	6.0	38.2	50	54.0	5038	34
FBHigh64-64	93.7	34.1	49.3	6.0	38.2	50	54.0	4647	47
FBLow16-16	68.8	64.6	78.5	58.2	38.2	100	54.0	6605	1
FBLow32-32	73.8	36.5	73.6	58.2	38.2	100	54.0	6206	12
FBLow64-64	97.9	34.1	49.3	58.2	38.2	100	54.0	6167	13
FBHigh32-16	84.8	47.4	76.1	6.0	38.2	50	54.0	5092	33
FBHigh64-32	93.3	35.3	61.5	6.0	38.2	50	54.0	4832	44
FBLow32-16	86.9	47.4	76.1	58.2	38.2	100	54.0	6582	2
FBLow64-32	96.4	35.3	61.5	58.2	38.2	100	54.0	6338	7
FBHigh64-16	86.3	45.6	63.9	6.0	38.2	50	54.0	4914	40
FBLow64-16	89.9	45.6	63.9	58.2	38.2	100	54.0	6426	4
FLFRBHigh16-16-16	67.8	52.5	68.8	16.9	54.2	25	25.1	4431	51
FLFRBHigh32-32-16	92.4	31.2	63.9	16.9	54.2	25	25.1	4410	53
FLFRBHigh32-32-32	96.6	24.4	61.5	16.9	54.2	25	25.1	4337	55
FLFRBHigh64-64-16	92.9	29.1	39.6	16.9	54.2	25	25.1	4039	63
FLFRBHigh64-64-32	99.0	22.7	37.2	16.9	54.2	25	25.1	4001	64
FLFRBHigh64-64-64	98.7	21.9	25.0	16.9	54.2	25	25.1	3811	69
FLFRBLow16-16-16	73.2	52.5	68.8	73.5	54.2	75	25.1	6031	15
FLFRBLow32-32-16	93.4	31.2	63.9	73.5	54.2	75	25.1	5947	17
FLFRBLow32-32-32	100.6	24.4	61.5	73.5	54.2	75	25.1	5918	20
FLFRBLow64-64-16	94.6	29.1	39.6	73.5	54.2	75	25.1	5587	23
FLFRBLow64-64-32	98.8	22.7	37.2	73.5	54.2	75	25.1	5521	24
FLFRBLow64-64-64	99.2	21.9	25.0	73.5	54.2	75	25.1	5341	28
FSLSRHigh16-16-16	79.9	52.5	68.8	16.9	54.2	25	25.1	4604	48
FSLSRHigh32-16-16	92.3	40.0	66.3	16.9	54.2	25	25.1	4569	49
FSLSRHigh32-32-32	108.8	24.4	61.5	16.9	54.2	25	25.1	4513	50

Table 5.4 continued

FSLSRHigh64-16-16	95.3	38.6	54.2	16.9	54.2	25	25.1	4417	52
FSLSRHigh64-32-32	110.6	23.6	49.3	16.9	54.2	25	25.1	4352	54
FSLSRHigh64-64-64	109.8	21.9	25.0	16.9	54.2	25	25.1	3969	66
FSLSRLow16-16-16	85.0	52.5	68.8	21.3	54.2	75	25.1	5454	25
FSLSRLow32-16-16	97.3	40.0	66.3	21.3	54.2	75	25.1	5418	26
FSLSRLow32-32-32	112.1	24.4	61.5	21.3	54.2	75	25.1	5337	29
FSLSRLow64-16-16	98.0	38.6	54.2	21.3	54.2	75	25.1	5233	30
FSLSRLow64-32-32	114.0	23.6	49.3	21.3	54.2	75	25.1	5178	31
FSLSRLow64-64-64	114.7	21.9	25.0	21.3	54.2	75	25.1	4817	45
FLFRRLRRHigh16-16-16-16	91.4	43.9	59.0	9.3	63.2	25	2.9	4209	56
FLFRRLRRHigh32-32-16-16	113.4	26.7	54.2	9.3	63.2	25	2.9	4208	57
FLFRRLRRHigh32-32-32-32	121.7	15.8	49.3	9.3	63.2	25	2.9	4102	61
FLFRRLRRHigh64-64-16-16	115.5	24.9	29.9	9.3	63.2	25	2.9	3865	68
FLFRRLRRHigh64-64-32-32	120.7	14.6	25.0	9.3	63.2	25	2.9	3723	70
FLFRRLRRHigh64-64-64-64	120.7	13.3	0.7	9.3	63.2	25	2.9	3358	71
FLFRRLRRLow16-16-16-16	95.2	43.9	59.0	99.6	63.2	75	2.9	6268	10
FLFRRLRRLow32-32-16-16	114.2	26.7	54.2	99.6	63.2	75	2.9	6224	11
FLFRRLRRLow32-32-32-32	121.9	15.8	49.3	99.6	63.2	75	2.9	6110	14
FLFRRLRRLow64-64-16-16	119.1	24.9	29.9	99.6	63.2	75	2.9	5920	19
FLFRRLRRLow64-64-32-32	121.2	14.6	25.0	99.6	63.2	75	2.9	5735	21
FLFRRLRRLow64-64-64-64	121.9	13.3	0.7	99.6	63.2	75	2.9	5379	27
FSLSRBHigh16-16-16-16	89.5	43.9	59.0	9.3	63.2	25	2.9	4182	59
FSLSRBHigh32-16-16-16	102.5	34.1	56.6	9.3	63.2	25	2.9	4193	58
FSLSRBHigh32-32-32-32	118.1	15.8	49.3	9.3	63.2	25	2.9	4051	62
FSLSRBHigh64-16-16-16	100.1	32.9	44.5	9.3	63.2	25	2.9	3969	67
FSLSRBHigh64-32-32-16	118.8	20.0	39.6	9.3	63.2	25	2.9	3983	65
FSLSRBHigh64-64-64-64	118.4	13.3	0.7	9.3	63.2	25	2.9	3326	72
FSLSRBLow16-16-16-16	95.7	43.9	59.0	12.9	63.2	75	2.9	5037	37
FSLSRBLow32-16-16-16	105.5	34.1	56.6	12.9	63.2	75	2.9	5002	38
FSLSRBLow32-32-32-32	121.1	15.8	49.3	12.9	63.2	75	2.9	4860	43
FSLSRBLow64-16-16-16	109.1	32.9	44.5	12.9	63.2	75	2.9	4862	42
FSLSRBLow64-32-32-16	118.1	20.0	39.6	12.9	63.2	75	2.9	4738	46
FSLSRBLow64-64-64-64	120.4	13.3	0.7	12.9	63.2	75	2.9	4120	60

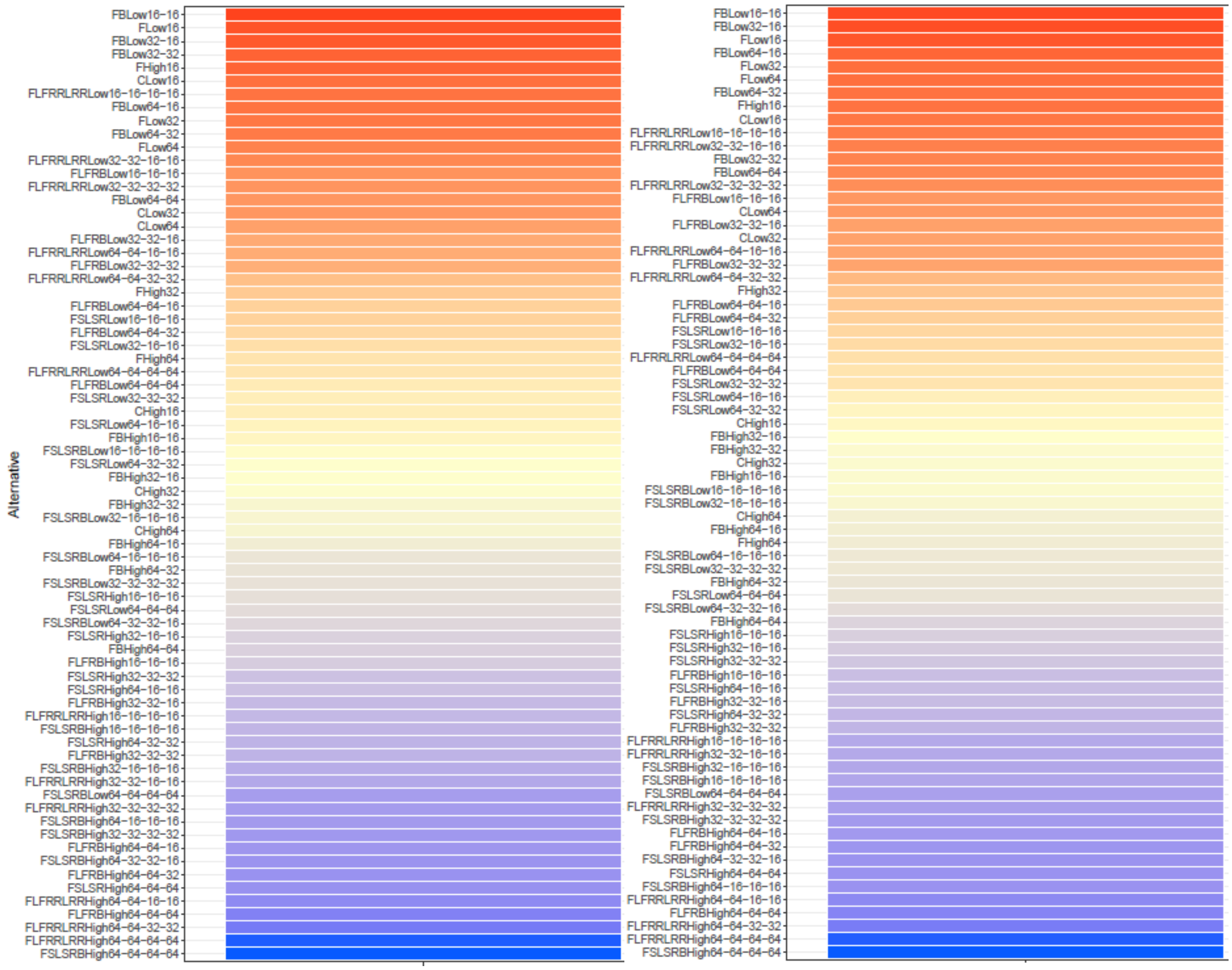

a. Sensing target - Vehicle (equal weights)

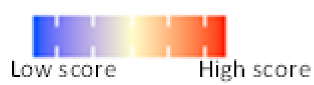

Figure 5.5: Heat Maps of Sensing targets (equal weights)

5.4 Results Based on Randomly Assigned Weights (Sensitivity Analysis)

In the analysis based on randomly assigned weights, the applied weights were generated without bias, ensuring an unbiased distribution across all criteria in the overall weight allocation. Unlike the approach with equal weighting, in which each criterion received a fixed weight of 14.29, in this method, random weights were generated independently for 10 scenarios across each criterion. Furthermore, the scaling functions, previously detailed in Chapter 5.1.2, remained consistent and were applied to derive scaled values.

Tables 5.5 and 5.6 present the sensitivity of the amalgamated results for the vehicle and pedestrian target scenarios, respectively. The random weights, generated as discussed in Chapter 4, were used as input. Each table presents the rankings obtained for each of the 10 weight scenarios. The table columns represent the outcomes from Rank 1 to Rank 72, thus, providing a detailed view of the performance associated with different weight configurations.

Table 5.5: Amalgamation Results: Sensing target–Vehicle, based on randomized weights of the criteria

Sensitivity Analysis Rank	Scenario 1	Scenario 2	Scenario 3	Scenario 4	Scenario 5	Scenario 6	Scenario 7	Scenario 8	Scenario 9	Scenario 10
CHigh16	43	71	20	9	29	25	36	9	71	46
CHigh32	54	70	24	18	37	40	41	13	72	66
CHigh64	56	72	25	22	40	36	43	16	70	67
CLow16	12	60	3	3	6	3	6	4	49	21
CLow32	21	67	9	7	18	10	13	6	65	31
CLow64	24	68	11	13	20	8	15	8	59	32
FHigh16	10	59	2	2	5	2	3	2	43	20
FHigh32	32	63	13	11	28	16	23	7	64	39
FHigh64	41	69	17	17	33	19	31	12	69	44
FLow16	6	58	1	1	2	1	2	1	34	18
FLow32	15	61	4	5	11	6	7	3	54	23
FLow64	19	65	6	8	14	5	10	5	48	24
FBHigh16-16	31	44	29	23	34	21	35	25	42	35
FBHigh32-32	40	40	35	28	41	33	40	30	46	52
FBHigh64-64	55	56	43	45	50	44	48	38	58	62
FBLow16-16	2	13	5	4	1	4	1	10	6	6
FBLow32-32	5	14	8	10	7	9	5	14	8	12
FBLow64-64	16	47	18	21	15	13	16	18	13	16
FBHigh32-16	36	41	33	27	38	31	39	27	45	47
FBHigh64-32	49	50	39	36	48	42	46	35	53	57
FBLow32-16	3	18	7	6	4	7	4	11	9	9
FBLow64-32	11	30	14	16	12	12	11	17	10	14
FBHigh64-16	42	49	36	32	43	32	44	32	50	49
FBLow64-16	8	32	10	12	8	11	8	15	11	11
FLFRBHigh16-16-16	48	36	45	35	47	52	50	42	57	40
FLFRBHigh32-32-16	57	38	50	44	54	57	57	45	60	55
FLFRBHigh32-32-32	61	43	54	49	57	59	60	47	61	58
FLFRBHigh64-64-16	66	55	60	59	62	63	66	53	67	63
FLFRBHigh64-64-32	68	54	61	61	65	67	68	54	66	68
FLFRBHigh64-64-64	70	66	67	67	69	69	70	62	68	70
FLFRBLow16-16-16	9	7	16	14	9	15	17	19	12	7

Table 5.5 continued

FLFRBLow32-32-16	14	16	21	19	17	24	19	21	15	10
FLFRBLow32-32-32	18	12	23	24	19	26	20	22	14	13
FLFRBLow64-64-16	25	45	27	30	22	34	25	26	20	15
FLFRBLow64-64-32	27	46	28	34	24	38	26	28	21	17
FLFRBLow64-64-64	33	52	32	41	27	43	33	31	26	19
FSLSRHigh16-16-16	37	22	40	33	44	49	47	40	30	34
FSLSRHigh32-16-16	44	25	44	40	49	50	49	44	33	42
FSLSRHigh32-32-32	52	28	48	47	55	53	52	46	41	51
FSLSRHigh64-16-16	50	35	47	46	51	51	54	48	37	45
FSLSRHigh64-32-32	58	37	53	53	58	55	59	51	44	56
FSLSRHigh64-64-64	67	53	62	65	67	61	67	60	55	64
FSLSRLow16-16-16	20	8	30	26	23	14	22	33	16	22
FSLSRLow32-16-16	22	11	34	29	26	18	24	36	18	25
FSLSRLow32-32-32	28	19	37	37	32	23	27	37	19	29
FSLSRLow64-16-16	29	29	38	38	30	20	30	39	23	27
FSLSRLow64-32-32	34	31	41	43	36	28	34	43	24	33
FSLSRLow64-64-64	46	51	49	58	46	37	45	50	29	36
FLFRRLRRHigh16-16-16-16	45	9	55	50	52	54	51	57	31	41
FLFRRLRRHigh32-32-16-16	53	21	59	57	59	60	58	63	35	53
FLFRRLRRHigh32-32-32-32	60	23	64	63	63	65	61	65	40	61
FLFRRLRRHigh64-64-16-16	65	42	68	68	68	66	65	68	47	59
FLFRRLRRHigh64-64-32-32	69	48	70	69	70	70	69	69	56	69
FLFRRLRRHigh64-64-64-64	71	62	71	71	71	71	71	71	62	71
FLFRRLRRLow16-16-16-16	1	1	12	15	3	17	9	20	1	1
FLFRRLRRLow32-32-16-16	4	2	15	20	10	22	12	23	2	2
FLFRRLRRLow32-32-32-32	7	3	19	25	13	29	14	24	3	4
FLFRRLRRLow64-64-16-16	13	4	22	31	16	30	18	29	4	3
FLFRRLRRLow64-64-32-32	17	10	26	39	21	39	21	34	5	5
FLFRRLRRLow64-64-64-64	26	39	31	52	25	46	28	41	7	8
FSLSRBHigh16-16-16-16	47	15	57	51	53	56	53	58	32	43
FSLSRBHigh32-16-16-16	51	20	58	55	56	58	56	61	36	48
FSLSRBHigh32-32-32-32	62	26	65	64	64	68	63	66	52	65
FSLSRBHigh64-16-16-16	59	34	63	62	61	62	62	64	51	54
FSLSRBHigh64-32-32-16	63	33	66	66	66	64	64	67	39	60
FSLSRBHigh64-64-64-64	72	64	72	72	72	72	72	72	63	72
FSLSRBLow16-16-16-16	23	5	42	42	31	27	29	49	17	26
FSLSRBLow32-16-16-16	30	6	46	48	35	35	32	52	22	28
FSLSRBLow32-32-32-32	38	17	52	56	42	45	38	56	27	38
FSLSRBLow64-16-16-16	35	24	51	54	39	41	37	55	25	30
FSLSRBLow64-32-32-16	39	27	56	60	45	47	42	59	28	37
FSLSRBLow64-64-64-64	64	57	69	70	60	48	55	70	38	50

Table 5.6:Amalgamation Results: Sensing target–Pedestrian, based on randomized weights of the criteria

Sensitivity Analysis Rank	Scenario 1	Scenario 2	Scenario 3	Scenario 4	Scenario 5	Scenario 6	Scenario 7	Scenario 8	Scenario 9	Scenario 10
CHigh16	45	71	22	10	29	32	37	9	71	46
CHigh32	56	69	23	17	36	42	42	13	70	67
CHigh64	59	70	26	23	40	41	44	16	69	68
CLow16	12	65	5	3	7	2	7	4	54	22
CLow32	28	68	12	8	19	12	16	6	68	33
CLow64	22	66	9	13	20	8	14	8	52	32
FHigh16	15	67	4	2	5	4	8	2	60	20
FHigh32	33	60	10	9	28	14	22	7	61	37
FHigh64	64	72	25	19	37	47	46	12	72	65
FLow16	7	62	1	1	2	1	3	1	41	19
FLow32	18	59	3	5	10	5	6	3	47	24
FLow64	14	58	2	7	13	3	4	5	30	21
FBHigh16-16	38	52	34	24	33	34	40	25	62	39
FBHigh32-32	39	38	35	28	41	30	38	30	36	51
FBHigh64-64	53	57	41	45	50	44	47	38	51	61
FBLow16-16	1	21	6	4	1	6	2	10	12	7
FBLow32-32	16	44	14	12	11	13	13	14	29	17
FBLow64-64	11	36	15	20	15	11	12	18	10	15
FBHigh32-16	36	42	32	26	38	27	36	28	38	42
FBHigh64-32	43	51	40	36	47	40	45	35	46	56
FBLow32-16	3	12	7	6	3	7	1	11	7	9
FBLow64-32	8	26	11	15	12	10	9	17	9	13
FBHigh64-16	41	50	37	32	43	33	43	32	44	48
FBLow64-16	5	25	8	11	6	9	5	15	8	10
FLFRBHigh16-16-16	50	48	48	37	48	55	54	42	67	41
FLFRBHigh32-32-16	54	37	50	44	52	54	53	45	55	53
FLFRBHigh32-32-32	58	41	54	49	56	56	57	47	58	57
FLFRBHigh64-64-16	66	55	58	59	61	61	65	53	65	62
FLFRBHigh64-64-32	68	54	61	61	65	64	67	54	64	66
FLFRBHigh64-64-64	70	64	67	67	69	69	70	62	66	70
FLFRBLow16-16-16	10	15	18	14	9	17	18	19	15	6
FLFRBLow32-32-16	13	10	19	18	16	22	19	21	13	11
FLFRBLow32-32-32	17	5	20	22	18	23	20	22	11	12
FLFRBLow64-64-16	23	35	27	30	22	28	24	26	17	14
FLFRBLow64-64-32	26	39	28	33	23	31	26	27	18	16
FLFRBLow64-64-64	32	49	30	41	26	39	31	31	20	18
FSLSRHigh16-16-16	42	32	42	34	46	49	48	41	50	38
FSLSRHigh32-16-16	44	29	44	40	49	50	49	44	42	40
FSLSRHigh32-32-32	46	24	47	46	53	51	50	46	32	49

Table 5.6 continued

FSLSRHigh64-16-16	47	40	49	47	51	52	52	48	43	43
FSLSRHigh64-32-32	55	33	53	53	58	53	55	51	35	54
FSLSRHigh64-64-64	67	53	62	65	67	57	68	60	49	64
FSLSRLow16-16-16	20	16	31	27	24	15	23	33	25	23
FSLSRLow32-16-16	21	11	33	29	27	16	25	36	19	25
FSLSRLow32-32-32	24	6	36	35	31	18	27	37	14	28
FSLSRLow64-16-16	29	27	38	38	30	20	29	39	22	26
FSLSRLow64-32-32	31	19	39	43	35	24	30	43	16	30
FSLSRLow64-64-64	40	47	46	57	44	29	41	50	26	34
FLFRRLRRHigh16-16-16-16	48	28	56	50	54	59	59	57	53	44
FLFRRLRRHigh32-32-16-16	49	14	57	58	60	58	56	63	33	52
FLFRRLRRHigh32-32-32-32	57	17	63	63	63	63	61	65	34	60
FLFRRLRRHigh64-64-16-16	65	45	68	68	68	66	66	68	40	58
FLFRRLRRHigh64-64-32-32	69	46	70	69	70	70	69	69	48	69
FLFRRLRRHigh64-64-64-64	71	61	71	71	71	71	71	71	59	71
FLFRRLRRLow16-16-16-16	2	3	13	16	4	19	10	20	4	1
FLFRRLRRLow32-32-16-16	4	1	16	21	8	21	11	23	1	2
FLFRRLRRLow32-32-32-32	6	2	17	25	14	26	15	24	2	4
FLFRRLRRLow64-64-16-16	9	4	21	31	17	25	17	29	3	3
FLFRRLRRLow64-64-32-32	19	9	24	39	21	37	21	34	5	5
FLFRRLRRLow64-64-64-64	25	34	29	52	25	46	28	40	6	8
FSLSRBHigh16-16-16-16	52	31	60	51	55	62	60	58	57	45
FSLSRBHigh32-16-16-16	51	22	59	56	57	60	58	61	45	50
FSLSRBHigh32-32-32-32	60	23	64	64	64	67	62	66	39	63
FSLSRBHigh64-16-16-16	63	43	66	62	62	68	64	64	56	55
FSLSRBHigh64-32-32-16	62	30	65	66	66	65	63	67	37	59
FSLSRBHigh64-64-64-64	72	63	72	72	72	72	72	72	63	72
FSLSRBLow16-16-16-16	27	13	43	42	32	35	32	49	28	27
FSLSRBLow32-16-16-16	30	7	45	48	34	36	33	52	24	29
FSLSRBLow32-32-32-32	35	8	52	55	42	43	34	56	21	35
FSLSRBLow64-16-16-16	34	18	51	54	39	38	35	55	23	31
FSLSRBLow64-32-32-16	37	20	55	60	45	45	39	59	27	36
FSLSRBLow64-64-64-64	61	56	69	70	59	48	51	70	31	47

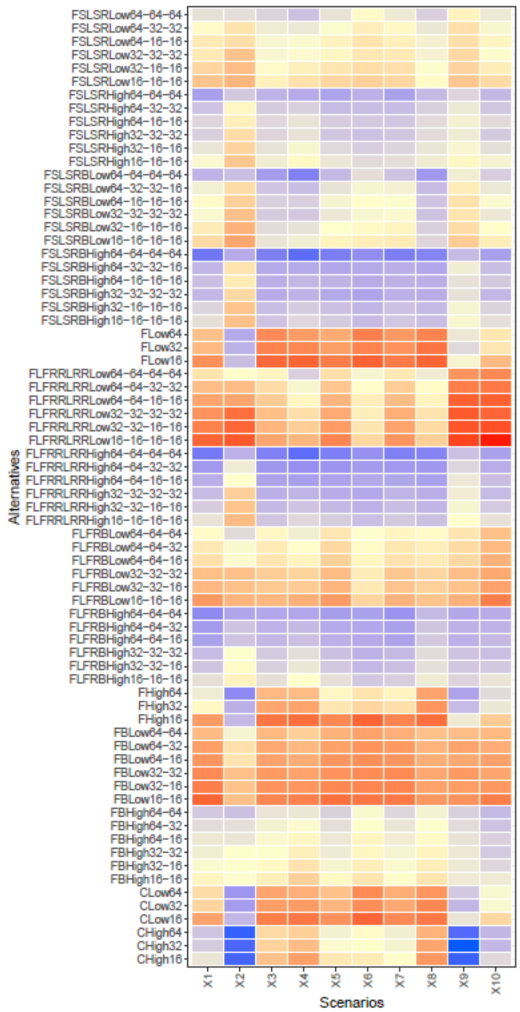

Sensing target - Vehicle (randomly-derived weights)

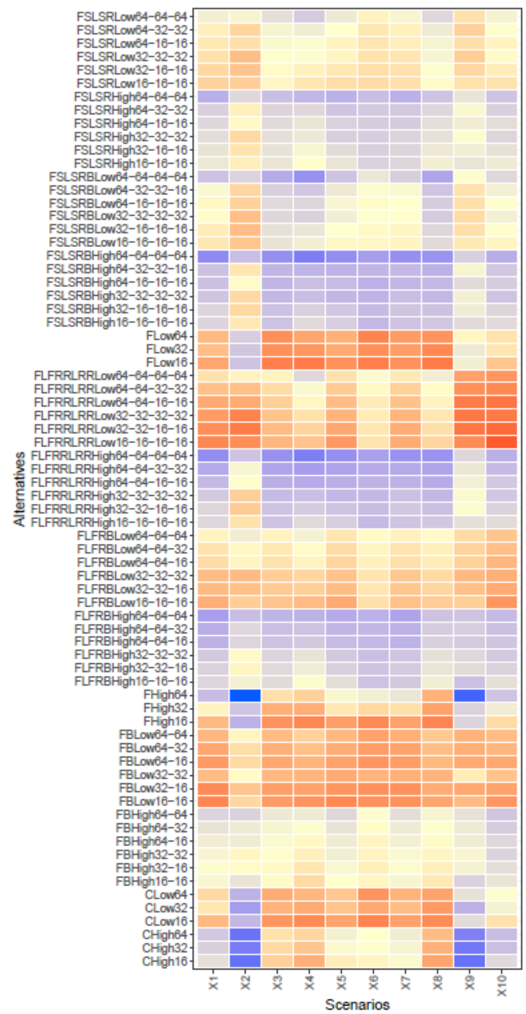

b. Sensing target - Pedestrian (randomly-derived weights)

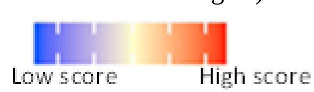

Figure 5.6: Heat Maps showing variations in outcome of random-derived weights

5.5 Discussion of the MCDA Results

This study applied a robust decision-making process to evaluate and rank various alternatives based on predefined criteria, including point density, blind spot regions, sensor cost, power consumption, ease of installation, sensor redundancy, and aesthetics. The results provide valuable insights into optimizing LiDAR placement for the detection of both vehicles and pedestrians.

The approach facilitated a comprehensive assessment, ensuring transparency in the decision-making process. Diverse metrics and criteria were used, and decision criteria were scaled using value functions derived through regression via the mid-value splitting technique. This transformation allowed meaningful comparisons despite variations in units associated with each criterion by bringing all criteria to a uniform scale.

Through a questionnaire, weights were established to reflect the preferences of individuals familiar with the field. These weights capture the true importance of each criterion. Based on the collective judgment of the criteria by knowledgeable individuals, point density was deemed the most important criterion and aesthetics the least important. Following this, using equally weighted criteria, analysis was carried out. Then, using the equal weighting results as a baseline, the weights were changed randomly, and a sensitivity analysis was carried out.

The MCDA results illustrate how different weighting combinations for these criteria influence LiDAR placement rankings. The integration of criteria weighting and scaled performance evaluations determined the ranking of the LiDAR placement alternatives. The sensitivity analysis, reflecting unbiased weight distributions across criteria, provided insights into the robustness of the findings.

5.5.1 Discussion of MCDA Results Based on the Weighting Approach

This section examines the MCDA results, with a specific focus on the weighting methodology used: the equal weighting approach and questionnaire-derived weighting. This discussion evaluates the strengths and limitations of these approaches. Through a detailed examination of the intricacies of the decision-making process, the goal is to offer insights into the robustness and practicality of the MCDA methodologies applied. The discussion covers key aspects of the methodologies, highlighting transparency, subjectivity, and the overall effectiveness of the approaches in generating outcomes that are contextually relevant for LiDAR placement alternatives.

5.5.1 (a) Respondent-Assigned Weights

This method involves gathering responses from stakeholders through a structured questionnaire to derive weights for various decision criteria, representing the collective decisions of the respondents. A significant advantage of involving DMs lies in their ability to incorporate diverse perspectives, thus, ensuring a decision-making process that more accurately reflects real-world considerations. By directly engaging DMs in the weight assignment process, this method effectively addresses the limitation encountered in approaches that fail to capture the preferences of DMs. The same holds true when using a questionnaire to derive scaling functions. Additionally, the transparency of the process provided clarity regarding how weights were assigned, thereby fostering a sense of trust among DMs. The structured nature of the questionnaire ensured a systematic approach to collecting information, reducing the likelihood of ambiguity or misinterpretation of DM preferences.

However, certain challenges may arise despite these advantages. The effectiveness of the respondent-assigned method depends heavily on the quality and representativeness of the responses obtained. Incomplete or biased responses could introduce inaccuracies into the weight assignment process, potentially impacting the reliability of the results. Moreover, the time and effort required to administer and collect responses from DMs could impact the duration of the study. Depending on the complexity of the decision context and the number of stakeholders involved, the questionnaire process may demand a substantial investment of time and human resources.

5.5.1 (b) Equal Weighting

The equal weighting approach offers a combination of advantages and disadvantages. On the positive side, this method serves as a convenient and straightforward way to directly assign weights to criteria. The uniform distribution of weights across all criteria simplifies the decision-making process and can be particularly appealing in situations in which a quick assessment is required. However, despite the convenience and timesaving benefits, the approach overlooks the unique perspectives and preferences of DMs. This aspect has particular significance across diverse fields that encompass a wide array of stakeholders, ranging from engineers to consumers, who are the users of the AVs in this case. This limitation undermines the comprehensiveness required for decision-making in a field as multifaceted as transportation, in which the input of various stakeholders is pivotal for successful and sustainable outcomes. Moreover, the equal weighting method tends to oversimplify the decision-making process by treating all criteria as equally important. This tendency may not align with the intricacies of real-world scenarios in which certain criteria carry greater weight due to their impact on the overall success or failure of the alternatives. The approach's inclination towards uniformity may lead to below-par decision outcomes, as it neglects the differing significance of the individual criteria.

Nonetheless, the equal weighting method can be an effective starting point, providing a baseline for comparisons and highlighting areas in which further analysis or customization of weights may be necessary. It can be a practical approach in situations in which there are time constraints, and a rapid, basic assessment is sufficient.

5.5.1 (c) Randomly Assigned Weights

The sensitivity analysis, conducted through 10 iterations with randomly-generated weights representing scenarios 1 to 10, introduced a dynamic dimension to the decision-making process. This method not only provided flexibility in exploring different weight assignments but also offered a wide range of weight distributions. This variability allowed for the accommodation of the potential preferences of the DMs, even if those preferences were not obtained directly. The different weight combinations could inadvertently align with the diverse perspectives and priorities of stakeholders, contributing to a more inclusive decision analysis.

Additionally, the approach aided in identifying the sensitivity of decision outcomes to changes in criteria weights. The wide range of weight distribution enhanced the adaptability of the sensitivity analysis, making it suitable for scenarios in which the precise determination of weights might be challenging. The exploration of a broad spectrum of weight possibilities ensured that the sensitivity analysis did not exclusively rely on a single set of predefined weights. Instead, it systematically considered various weight combinations, thereby accommodating uncertainties and variations in DM preferences. This approach provides the DMs with more insights into how changes in weightings can impact the overall results, thus, facilitating a more robust examination of the decision space.

Additionally, the approach tends to be timesaving as the weights can be easily generated, without the complexities of obtaining them directly from DMs, making the decision-making process efficient. In scenarios in which time is an important factor, this streamlined approach allows DMs to quickly assess a variety of weight combinations, expediting the exploration of different scenarios without the need for extensive data collection from stakeholders.

Despite the advantages of this approach, it is also accompanied by limitations. Interpreting results from multiple iterations with random weights poses a challenge, given the lack of clear patterns or trends. This ambiguity may hinder the ability to draw meaningful conclusions, causing potential confusion among DMs. The absence of direct stakeholder involvement is also a notable drawback, potentially resulting in the omission of important perspectives important for AV sensor deployment and development. This deficiency in real-world expertise may limit the accuracy and applicability of sensitivity analysis results generating unrealistic scenarios that may not represent the importance of each criterion.

For example, scenarios with randomly assigned higher weights for criteria such as ease of installation or aesthetics could significantly impact the decision results and deviating from the optimal outcome. This is noteworthy in the context of AVs, where safety is of the utmost importance. The misalignment with the actual preferences and priorities of DMs may lead to an analysis that inaccurately reflects the decision landscape.

5.5.2 Discussion of MCDA Results Based on the Best Alternatives

This section engages in a comprehensive analysis of the MCDA results that centers on the selected LiDAR placement alternatives across the approaches. The evaluation considers the three distinct perspectives: results from equal weighting, from randomized weights, and from respondent-assigned weights.

5.5.2 (a) MCDA Results Based on Respondent-Assigned Weights of the Criteria

The weights provided by the respondents were utilized to ascertain the top-performing LiDAR placement. According to the weighting results from respondents, the criteria that earned high weights were point density, cost of sensor, blind spot regions, and sensor redundancy, thus, signifying the heightened importance of these specifications to the respondents.

For the vehicle detection scenario, the recommended top-performing LiDAR placement was FLFRRLRRLow16-16-16-16. This configuration signifies the positioning of LiDAR sensors at the front left, front right, rear left, and rear right positions, with 16 channels for each sensor and installation at a lower elevation. This configuration aligns with the respondents' weightings by placing a significant emphasis on point density, blind spot regions, cost of sensor, and sensor redundancy. The results of the configuration emphasizes a strategic focus on optimizing detection capabilities by maximizing point density, minimizing blind spots, managing the cost of sensors, and including redundant sensors.

Regarding the pedestrian detection, the proposed LiDAR placement with the top overall score was the FLFRRLRRLow32-32-16-16. Notably, the front positions feature 32 channels each while the rear positions have 16 channels each, all positioned low. The slight disparity in the LiDAR placement alternatives suggests that a placement suitable for one scenario may not necessarily be optimal for another. This aligns with the findings of Hu et al. (2022a), indicating that different sensor placements are appropriate for distinct targets, such as vans, cars, box trucks, and cyclists.

The recommended LiDAR configurations for both scenarios align with the criteria weights assigned by the survey respondents. The results indicate careful consideration of various criteria is required in determining the most effective LiDAR placement alternatives for both vehicle and pedestrian targets.

5.5.2 (b) MCDA Results Based on Equal Weighting of the Criteria

The equal weighting approach assumes the equal importance of all criteria, thus, providing a baseline for evaluating the LiDAR placement alternatives. In this scenario, the alternative labeled FBLow1616 emerged as the top-ranking choice, indicating that two sensors positioned both at the front and back of the roof, each with 16 channels at low elevation, achieve the highest overall score. This outcome was consistent for both vehicle and pedestrian detection scenarios.

The assumption of equal importance across all criteria in the equal weighting approach can lead to unexpected results. While FBLow1616 excels in this scenario, the methodology overlooks variations in the significance of individual criteria. It is important to note that the weighting assignment in this case may not align with real-world priorities. For example, criteria such as blind spot areas, sensor cost, and power consumption may be of greater importance, especially in safety critical contexts, but are treated equivalently in the equal weighting approach.

5.5.2 (c) MCDA Results Based on Randomized Weights of the Criteria

The sensitivity analysis conducted across multiple iterations reveals distinct weight distributions, making each scenario unique. In the initial iteration, criteria such as point density, cost of sensor, power consumption, sensor redundancy, and aesthetics held relatively higher and similar weights compared to the other criteria. In this context, FLFRRLRRLow16-16-16-16 emerged as the top-performing LiDAR placement alternative for vehicle detection, while FBLow16-16 emerged as the top choice for pedestrian scenarios.

Subsequent iterations also produced results influenced by the assigned weights. The second iteration mirrored the first regarding different outcomes for pedestrian and vehicle scenarios. The top-ranking placements for the two scenarios were FLFRRLRRLow32-32-16-16 for pedestrians and FLFRRLRRLow16-16-16-16 for vehicles.

In the third iteration, higher weights were assigned to point density, cost of sensor, power consumption, blind spot regions, and ease of installation. The top-performing alternative for both vehicles and pedestrians, FLow16, highlighted the importance placed on the criteria, particularly power consumption, cost of sensor, blind spot region, and ease of installation, favoring the outcome of a single LiDAR sensor configuration. This setup, featuring LiDAR sensors at the front, excelled due to the importance of the criteria.

The fourth iteration assigned significant weights to cost of sensor, power consumption, sensor redundancy, and ease of installation, which resulted in FHigh64 and FLow16 being selected as the top-performing alternatives for vehicles and pedestrians, respectively. The results for the fifth iteration favored FBLow16-16 for both vehicles and pedestrians. In the eighth scenario, the outcome favored a single LiDAR placement, as aesthetics were assigned a relatively high weight. The criteria weights played a substantial role, with respondents favoring sensors with 1–2 sensors. Finally, in scenarios in which cost of sensor, blind spot regions, and sensor redundancy had relatively higher weights, FLFRRLRRLow16-16-16-16 was selected for both vehicle and pedestrian scenarios. The absence of criteria such as aesthetics, ease of installation, or power consumption were weighted highly, thus, significantly influencing the decision.

Throughout the different scenarios, varying weights influenced the decisions. Scenarios with higher weights for sensor redundancy resulted in configurations with more than one sensor. Aesthetic considerations favored single sensors, while cost-conscious scenarios leaned towards 16-channel sensors. Those prioritizing blind spots opted for low-positioned sensors. All these factors confirm the importance of using MCDA for LiDAR placement optimization, thereby allowing decisions to be made based on the most important criteria.

5.6 Summary of Chapter 5

Chapter 5 extensively discusses the results obtained through the MCDA framework. The chapter commences with an examination of the results derived from respondent-assigned weights, encompassing a summary of the weighting outcomes, scaling results, and the subsequent amalgamation of these findings. It explores how the varying weighting approaches – respondent-assigned, equal weights, and randomly assigned weights – influence the MCDA results, thus, providing an understanding of their impact on decision outcomes.

Additionally, the best alternatives occurred across different weighting approaches. Overall, Chapter 5 serves as a comprehensive exploration and analysis of the MCDA results, and the influence of different weighting strategies on decision-making within the study's framework.

CHAPTER 6. CONCLUDING REMARKS

6.1 Summary

The exploration of LiDAR sensor placement optimization presented in this thesis, provided insights into decision-making regarding LiDAR placement and its broader applications within autonomous vehicle (AV) technology. MCDA has been utilized in various aspects of AV technology adoption (Anastasiadou et al., 2021; Babaei et al., 2023; Dubljevic et al., 2021; A. Raj et al., 2020). However, this work is a unique study explicitly focused on LiDAR placement.

The thesis encompasses a combination of both single and multi-LiDAR configurations. Single LiDAR placements offer cost-effective means of environmental information collection and simplified integration, avoiding the complexities associated with multi-LiDAR configurations. However, their limitations, including potential blind spots and impact on object detection, necessitate the exploration of multiple LiDAR configurations to achieve comprehensive environment perception, albeit with challenges in integration, deployment costs, and data processing. The thesis investigates both single-LiDAR and multi-LiDAR setups.

In LiDAR placement within AVs, specific criteria are crucial for ensuring safety and operational efficiency. Foremost among these is the necessity for sensor redundancy, which is pivotal in mitigating the risks of sensor failure and enhancing the overall reliability of the AV's perception system. Redundancy ensures continuity in perceiving the environment accurately, even in the event of sensor malfunction. The aspect of point density is equally critical, which is instrumental in enabling the LiDAR system to capture and process detailed environmental data effectively. This density directly contributes to precise object recognition and tracking, which is indispensable for the safe navigation of AVs across diverse driving scenarios. While factors like minimizing blind spots enhance overall safety, they may be considered as "nice-to-haves" compared to sensor redundancy and point density, which are "must-haves," particularly considering the potential use of other sensors to address blind spot minimization. Criteria such as aesthetics, ease of installation, cost of sensors, and power consumption remain relevant, but their importance might vary. Aesthetics, for example, could influence public acceptance and adoption of AVs, yet safety and performance take precedence in AV design considerations. Similarly, while ease of installation and cost play essential roles in operational efficiency, their significance might be overshadowed by factors directly impacting safety and system reliability.

In essence, the critical criteria for LiDAR placement in AVs center around ensuring robust safety measures through redundancy and high point density, with secondary considerations encompassing factors like aesthetics, installation ease, cost, and power consumption, provided they do not compromise the primary objectives of safety and functionality.

6.2 Conclusions

In as much as the study primarily concentrates on LiDAR sensors, it is advisable to integrate these sensors with others to optimize the perception system. This integration can address LiDAR limitations by enhancing the overall capabilities of autonomous systems and ensuring robust performance. The sensor fusion of LiDAR with complementary sensors will foster a superior performance, leveraging the diverse strengths of each sensor to create a more comprehensive environmental perception for AVs and ADAS.

The findings in this thesis provide insights into optimal LiDAR sensor selection based on assigned criteria preferences and their importance. The study progresses from equal weighting of criteria to sensitivity analysis, ultimately employing weights from respondents, assigning ranks and scores to alternatives, and identifying the performance scores of the LiDAR placement alternatives. This thesis's methodology showcases a systematic approach to the complexities of LiDAR sensor placement, emphasizing criterion significance and enabling robust comparison among alternatives. The knowledge offered, and methodologies developed in the thesis can contribute significantly to the field, serving as a foundational resource for future studies in sensor placement within AVs and smart city infrastructure in general.

6.3 Study Limitations

The study limitations are as follows:

1) Choice of Sensor: The scope of the thesis does not include sensor fusion with other technologies, potentially overlooking the synergistic advantages of integrating LiDAR with complementary sensor systems.

2) Assumptions: Certain assumptions made regarding the ratings of decision criteria, like ease of installation, might affect the precision of results and their real-world relevance
3) External Factors and Real-world Constraints: The thesis did not comprehensively consider real-world constraints, such as regulatory limitations, technological constraints, or unforeseen environmental dynamics, potentially impacting the efficacy of the LiDAR placement strategy.
4) Decision Criteria: The selected evaluation metrics might only encompass part of the spectrum of relevant performance criteria, potentially deviating from real-world AV performance needs.
5) Sensitivity to Number of Respondents: A more extensive and diverse respondent pool might offer varied perspectives, affecting the generalizability of findings in LiDAR placement within Autonomous Vehicles (AVs), thereby impacting the evaluation and ranking of LiDAR configurations.
6) Adoption of other sensors: The cost factor associated with LiDAR may lead to alternative solutions, such as utilizing cheaper cameras that can be placed extensively throughout the vehicle. This cost consideration might prompt some decision makers to opt for camera-based systems over LiDAR due to affordability, potentially impacting the widespread adoption of LiDAR technology in AVs.
7) Human Factors and User Acceptance: Human-centric considerations regarding user acceptance of LiDAR placements within AV systems are not addressed extensively.
8) Temporal Considerations: Rapid advancements in AV technology, particularly in LiDAR sensors, might render specific findings outdated or less relevant over time as sensor technologies evolve.

6.4 Future Work

Future work in this area of research, may include:

1) Collaboration with Industry Stakeholders: Engage automotive manufacturers, LiDAR sensor suppliers, and AV developers to access real-world data and expertise, enhancing research outcomes.

2) Survey Respondents: Future surveys should prioritize individuals with extensive experience in LiDAR sensor technology. This targeted selection aims to better capture nuanced perspectives and expertise, potentially reducing response variation and enhancing consistency.
3) User-Centric Input: Incorporate user preferences and real-world scenarios to refine MCDA criteria and weights, ensuring alignment with human values.
4) Dynamic LiDAR Configurations: Explore adaptive MCDA models considering real-time data to accommodate changing driving scenarios effectively.
5) Machine Learning Integration: Investigate the integration of machine learning for accurate and adaptable LiDAR placement decisions, particularly in complex datasets.
6) Cost-Benefit Analysis and Scalability: Conduct a comprehensive cost-benefit analysis to evaluate the impact of optimized LiDAR placements on overall AV costs.
7) Scalability: Explore the scalability of the configurations across diverse vehicle types, from passenger cars to commercial trucks, to cater to a broad spectrum of transportation needs.
8) Regulatory and Safety Compliance: Address regulatory and safety considerations to ensure optimized LiDAR configurations meet the necessary standards for robust implementation in AVs.

Continuous research in LiDAR placement has immense potential to revolutionize transportation and mobility, contributing to the development of safer, more efficient, and user-centered AVs and ADAS systems. These efforts are expected to shape the future landscape of transportation technology. This research is a valuable reference point in exploring MCDA for LiDAR placement optimization in the context of AVs. The findings provide insights into the selection of LiDAR placement for AVs.

APPENDIX A. SURVEYS

Survey Questionnaire: LiDAR Placement using a Multi Criteria Analysis Approach

Researcher: Zainab Saka

Principal Investigator: Prof. Samuel Labi

Introduction

Multi-Criteria Analysis (MCA) is a framework that facilitates a systematic and structured approach for assessing the relative importance of different performance measures (PM) and for scaling them in order to reduce the PMs to commensurate units. It is needed to collect data on perceptions of LIDAR placement-related PMs including point density, sensor cost, aesthetics, and installation simplicity. The relative weights and scaled functions of these PMs will subsequently be collated and used in a multi-criteria analysis framework.

Section A: Direct Weighting Approach

Please allocate weight to each criterion based on **your level of preference** so that the total adds up to 100. A higher weight signifies greater importance.

Criteria	Weight
Point Density	
Cost of Sensor	
Power Consumption	
Blindspot Area	
Sensor Redundancy	
Aesthetics	
Ease of Installation	
Total	100

Section B: Scaling

The purpose of this section is to get your input regarding the performance of each criterion. The input you provide will be used to create a unified scale for comparison since the performance criteria are originally measured using different units.

Please mark three distinct points by drawing 3 lines to the corresponding X_{25}, X_{50} and X_{75} representing your **level of preference** or value associated to the criterion.

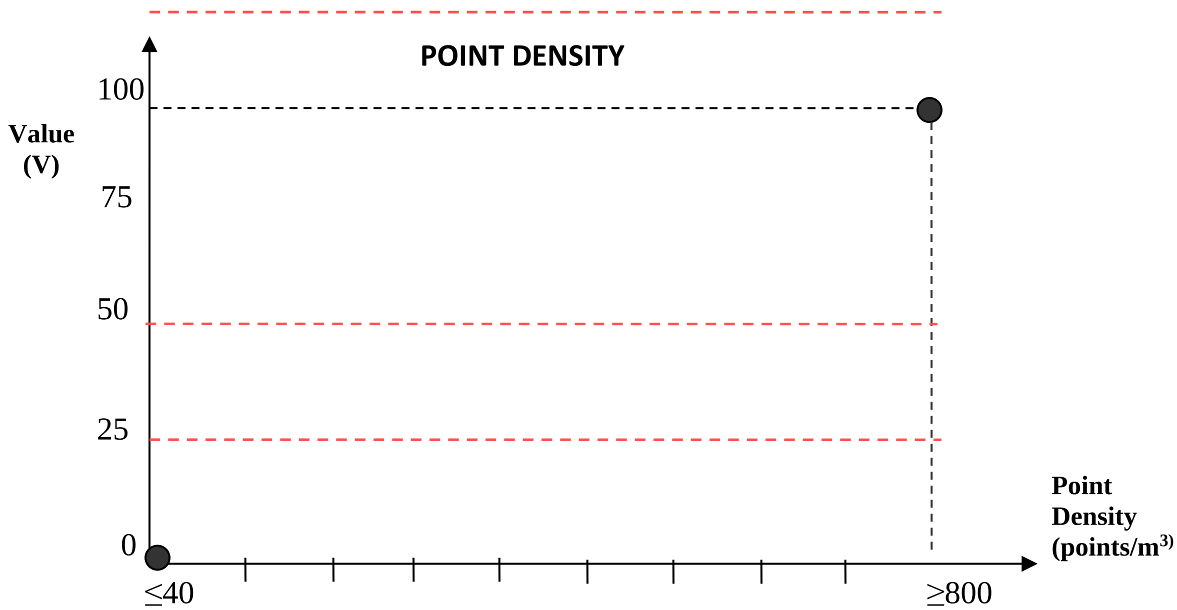
POINT DENSITY
Value (V)
100
75
50
25
0
≤40
≥800
Point Density (points/m3)

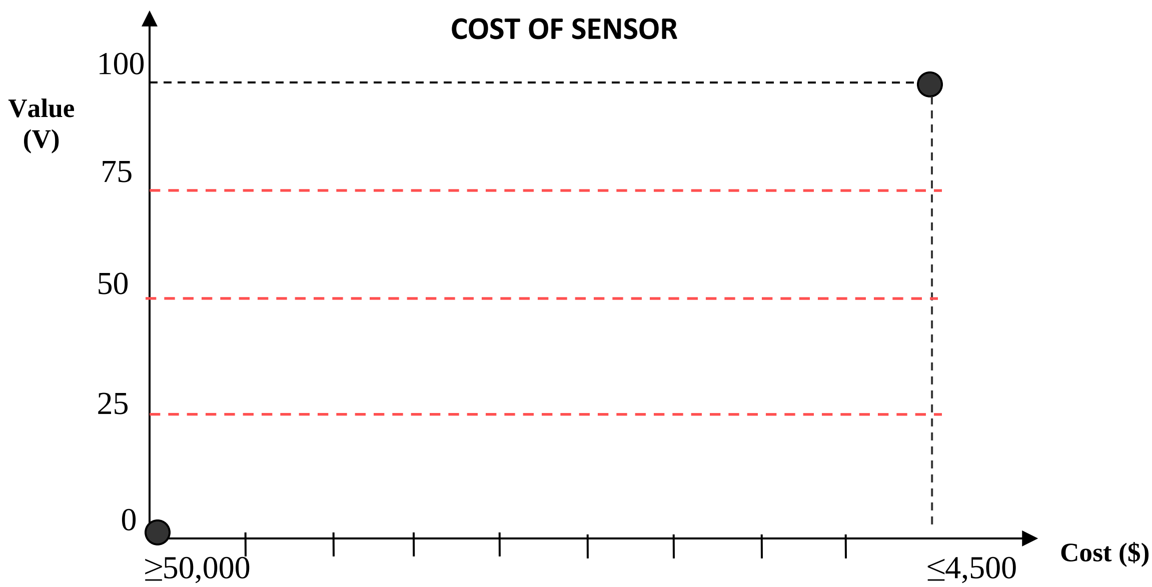
COST OF SENSOR
Value (V)
100
75
50
25
0
≥50,000
≤4,500
Cost ($)

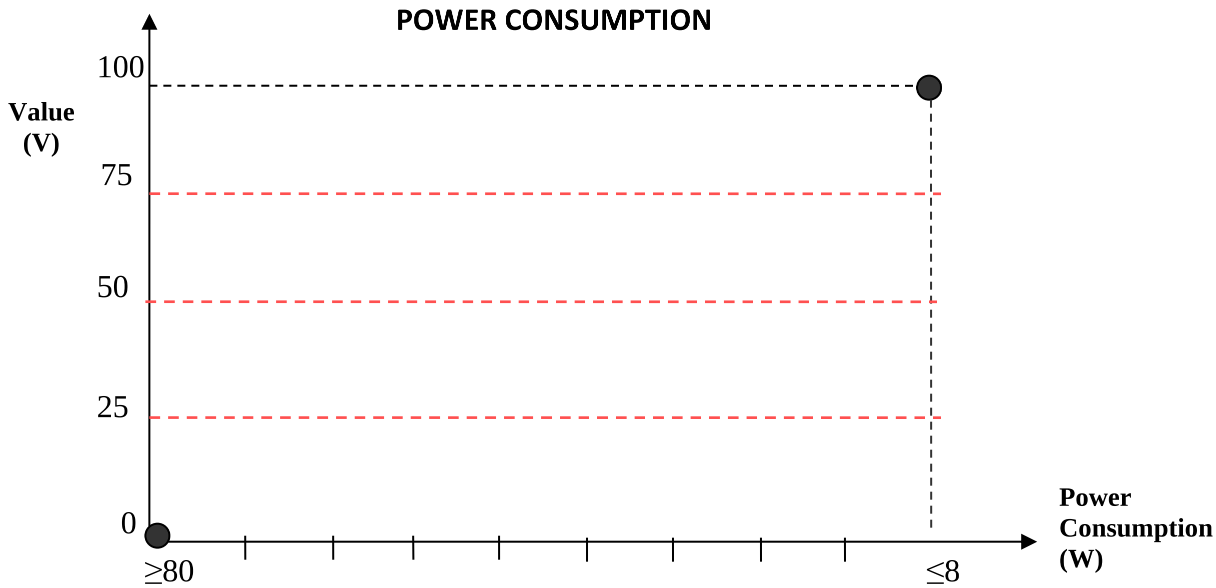
POWER CONSUMPTION
Value
(V)
100
75
50
25
0
≥80
≤8
Power
Consumption
(W)

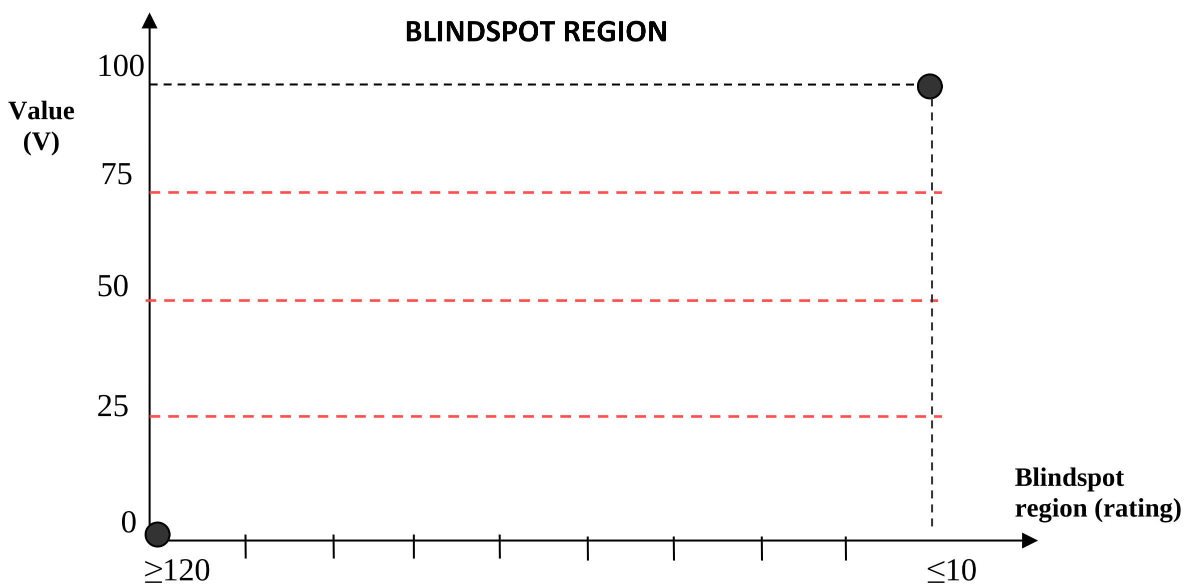
BLINDSPOT REGION
Value
(V)
100
75
50
25
0
≥120
≤10
Blindspot
region (rating)

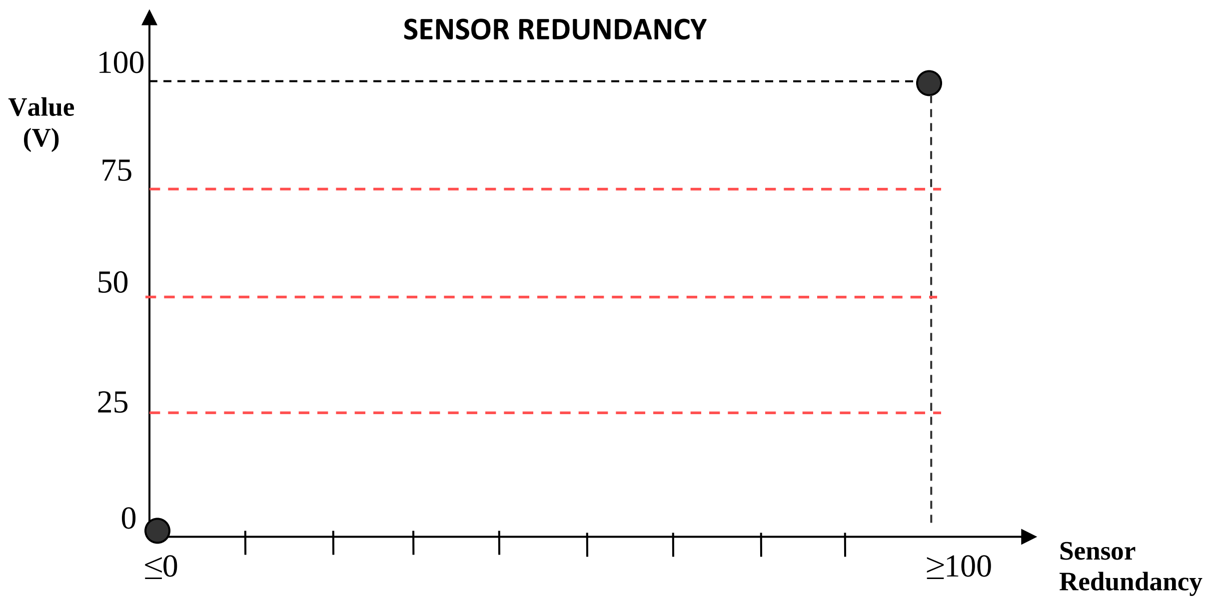
SENSOR REDUNDANCY
Value
(V)
100
75
50
25
0
≤0
≥100
Sensor
Redundancy

AESTHETICS

Because Aesthetics is subjective, please assign values of 0, 25, 50, 75 and 100 for each of them with 100 signifying your most favorable and 0 your least desirable.

Set V (A =) = 0 and V (A =) = 100

Aesthetics (SR)	Value
No Sensors	
1-2 sensors elevated low on the roof	
1-2 sensors elevated high on the roof	
3-4 sensors elevated low on the roof	
3-4 sensors elevated high on the roof	

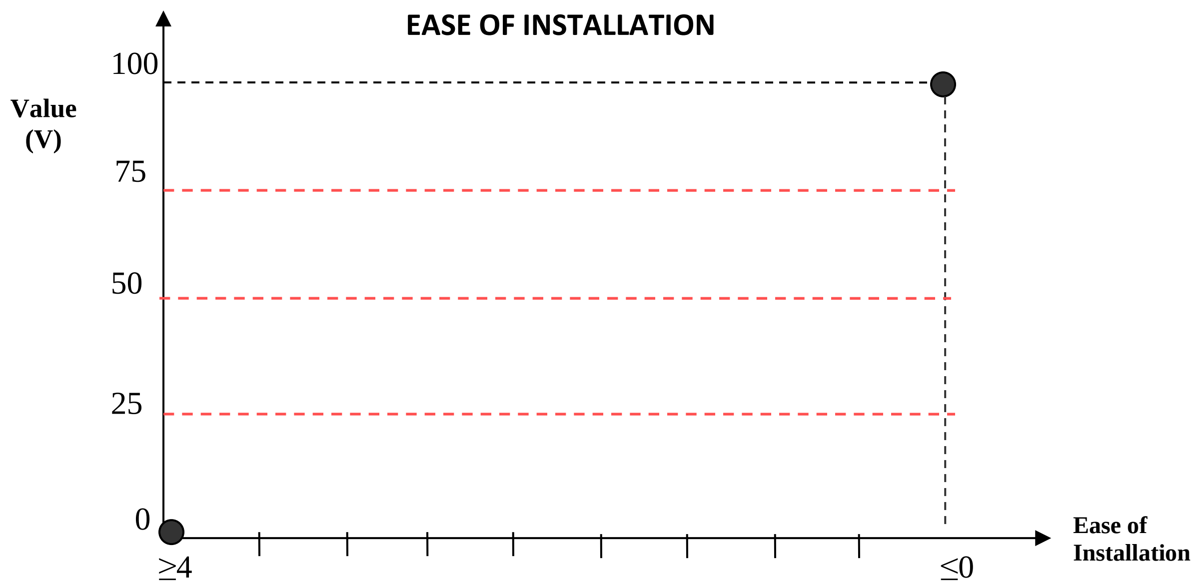

Thank you for your time!

APPENDIX B. RECRUITMENT LETTER

LiDAR Placement Optimization using a Multi-Criteria Approach

Zainab Saka (Graduate Student) / zsaka@purdue.edu
Professor Samuel Labi (Principal Investigator) / labi@purdue.edu

Subject: Requesting Your Participation in LiDAR Placement Research using a Multi Criteria Analysis Approach.

IRB Protocol Number: #IRB-2023-1570

Dear Student,
I am reaching out to invite you to participate in my research. This study focuses on LiDAR placement analysis and your input is highly valuable in helping us address our study objectives.

Brief Description:
Most road crashes and fatalities result from human error. Consequently, companies are turning to Advanced Driver Assistance Systems (ADAS) and Autonomous Vehicles (AVs) to enhance safety. For this, the placement of the LIDAR sensor (which is integral to ADAS and AVs), must be analyzed carefully. This research has developed and implemented a methodology for optimal LiDAR placement using a multi-criteria analysis approach. In this approach, the issues of relative weighting and scaling of the placement criteria (performance measures) are critical. This survey is intended to generate user perspectives that will help address these issues.

Survey Objectives:
- To collect road users' perspectives to determine the weighting of LiDAR placement criteria (performance measures).
- To collect road users' perspectives to determine the scaling of LiDAR placement criteria (performance measures).

Estimated Completion Time:
10-15 minutes

Your Privacy and Voluntary Participation:

We would like to reassure you that your participation in this research is entirely voluntary. You are under no obligation to take part, and you have the freedom to choose whether or not to participate. Should you decide to participate, you are welcome to withdraw from the study at any point without any consequences. This survey is conducted under protocol #IRB-2023-1570 and adheres to stringent ethical standards. It does not collect any personal or identifiable information from respondents. The insights gained will be instrumental in LiDAR placement analysis for Autonomous Vehicles, and this will ultimately benefit road users, industry, and society at large.

Please feel free to contact us if you have any questions or suggestions. Thank you!

REFERENCES

Adeyemo, A., Wimmer, H., & Powell, L. M. (2019). Effects of Normalization Techniques on Logistic Regression in Data Science. Journal of Information Systems Applied Research, 12(2), 37.

Ahrabian, A., Emambakhsh, M., Sheeny, M., & Wallace, A. (2019). Efficient Multi-Sensor Extended Target Tracking using GM-PHD Filter. 2019 IEEE Intelligent Vehicles Symposium (IV), 1731–1738. https://doi.org/10.1109/IVS.2019.8814257

AlAli, A. M., Salih, A., & Hassaballa, A. (2023). Geospatial-Based Analytical Hierarchy Process (AHP) and Weighted Product Model (WPM) Techniques for Mapping and Assessing Flood Susceptibility in the Wadi Hanifah Drainage Basin, Riyadh Region, Saudi Arabia. Water, 15(10), Article 10. https://doi.org/10.3390/w15101943

Amaran, S., Sahinidis, N. V., Sharda, B., & Bury, S. J. (2016). Simulation optimization: A review of algorithms and applications. Annals of Operations Research, 240(1), 351–380. https://doi.org/10.1007/s10479-015-2019-x

Anastasiadou, K., Gavanas, N., Pitsiava-Latinopoulou, M., & Bekiaris, E. (2021). Infrastructure Planning for Autonomous Electric Vehicles, Integrating Safety and Sustainability Aspects: A Multi-Criteria Analysis Approach. Energies, 14(17), Article 17. https://doi.org/10.3390/en14175269

Anderson, E. S., Thompson, J. A., Crouse, D. A., & Austin, R. E. (2006). Horizontal resolution and data density effects on remotely sensed LIDAR-based DEM. Geoderma, 132(3), 406–415. https://doi.org/10.1016/j.geoderma.2005.06.004

Aria, E., Olstam, J., & Schwietering, C. (2016). Investigation of Automated Vehicle Effects on Driver's Behavior and Traffic Performance. Transportation Research Procedia, 15, 761–770. https://doi.org/10.1016/j.trpro.2016.06.063

Arikumar, K. S., Deepak Kumar, A., Gadekallu, T. R., Prathiba, S. B., & Tamilarasi, K. (2022). Real-Time 3D Object Detection and Classification in Autonomous Driving Environment Using 3D LiDAR and Camera Sensors. Electronics, 11(24), Article 24. https://doi.org/10.3390/electronics11244203

Awange, J., & Kiema, J. (2019). The Global Positioning System. In J. Awange & J. Kiema (Eds.), Environmental Geoinformatics: Extreme Hydro-Climatic and Food Security Challenges: Exploiting the Big Data (pp. 55–73). Springer International Publishing. https://doi.org/10.1007/978-3-030-03017-9_5

Azim, A., & Aycard, O. (2012). Detection, classification and tracking of moving objects in a 3D environment. 2012 IEEE Intelligent Vehicles Symposium, 802–807. https://doi.org/10.1109/IVS.2012.6232303

Babaei, P., Riahinia, N., Ebadati E., O. M., & Azimi, A. (2023). Autonomous vehicles' object detection architectures ranking based on multi-criteria decision-making techniques. International Journal of Information Technology. https://doi.org/10.1007/s41870-023-01517-y

Bai, L., Zhao, Y., & Huang, X. (2022). Enabling 3-D Object Detection With a Low-Resolution LiDAR. IEEE Embedded Systems Letters, 14(4), 163–166. https://doi.org/10.1109/LES.2022.3170298

Bai, Q., Labi, S., & Li, Z. (2008). Trade-off Analysis Methodology for Asset Management (FHWA/IN/JTRP-2008/31, 3110; p. FHWA/IN/JTRP-2008/31, 3110). Purdue University. https://doi.org/10.5703/1288284314305

Barclay, C., & Osei-Bryson, K.-M. (2010). Project performance development framework: An approach for developing performance criteria & measures for information systems (IS) projects. International Journal of Production Economics, 124(1), 272–292. https://doi.org/10.1016/j.ijpe.2009.11.025

Behzadian, M., Khanmohammadi Otaghsara, S., Yazdani, M., & Ignatius, J. (2012). A state-of the-art survey of TOPSIS applications. Expert Systems with Applications, 39(17), 13051–13069. https://doi.org/10.1016/j.eswa.2012.05.056

Bell, M. L., Hobbs, B. F., & Ellis, H. (2003). The use of multi-criteria decision-making methods in the integrated assessment of climate change: Implications for IA practitioners. Socio-Economic Planning Sciences, 37(4), 289–316. https://doi.org/10.1016/S0038-0121(02)00047-2

Bendaña, R., del Caño, A., & Pilar de la Cruz, M. (2008). Contractor selection: Fuzzy-control approach. Canadian Journal of Civil Engineering, 35(5), 473–486. https://doi.org/10.1139/L07-127

Benedek, C., Majdik, A., Nagy, B., Rozsa, Z., & Sziranyi, T. (2021). Positioning and perception in LIDAR point clouds. Digital Signal Processing, 119, 103193. https://doi.org/10.1016/j.dsp.2021.103193

Berens, F., Elser, S., & Reischl, M. (2022). Genetic Algorithm for the Optimal LiDAR Sensor Configuration on a Vehicle. IEEE Sensors Journal, 22(3), 2735–2743. https://doi.org/10.1109/JSEN.2021.3136362

Bilik, I. (2023). Comparative Analysis of Radar and Lidar Technologies for Automotive Applications. IEEE Intelligent Transportation Systems Magazine, 15(1), 244–269. https://doi.org/10.1109/MITS.2022.3162886

Bilik, I., Longman, O., Villeval, S., & Tabrikian, J. (2019). The Rise of Radar for Autonomous Vehicles: Signal Processing Solutions and Future Research Directions. IEEE Signal Processing Magazine, 36(5), 20–31. https://doi.org/10.1109/MSP.2019.2926573

Branke, J. (2008). Multiobjective Optimization: Interactive and Evolutionary Approaches. Springer Science & Business Media.

Bridgman, P. W. (1922). Dimensional Analysis. Yale University Press; London, Humphrey Milford.). *The Mathematical Gazette, 11*(166), 393-393. doi:10.2307/3604432

Bukhsh, Z. A., Stipanović Oslaković, I., Klanker, G., Hoj, N. P., Imam, B., & Xenidis, Y. (2017). Multi-criteria decision making: AHP method applied for network bridge prioritization. Proceedings of the Joint COST TU1402 - COST TU1406 - IABSE WC1 Workshop: The Value of Structural Health Monitoring for the Reliable Bridge Management, 3.2-1-3.2-9. https://doi.org/10.5592/CO/BSHM2017.3.2

Cai, X., Jiang, W., Xu, R., Zhao, W., Ma, J., Liu, S., & Li, Y. (2023). Analyzing Infrastructure LiDAR Placement with Realistic LiDAR Simulation Library (arXiv:2211.15975). arXiv. https://doi.org/10.48550/arXiv.2211.15975

Campbell, S., O'Mahony, N., Krpalcova, L., Riordan, D., Walsh, J., Murphy, A., & Ryan, C. (2018). Sensor Technology in Autonomous Vehicles: A review. 2018 29th Irish Signals and Systems Conference (ISSC), 1–4. https://doi.org/10.1109/ISSC.2018.8585340

Castro-Gutierrez, J., Landa-Silva, D., & Pérez, J. M. (2010). Improved Dynamic Lexicographic Ordering for Multi-Objective Optimisation. In R. Schaefer, C. Cotta, J. Kołodziej, & G. Rudolph (Eds.), Parallel Problem Solving from Nature, PPSN XI (pp. 31–40). Springer. https://doi.org/10.1007/978-3-642-15871-1_4

Catapang, A. N., & Ramos, M. (2016). Obstacle detection using a 2D LIDAR system for an Autonomous Vehicle. 2016 6th IEEE International Conference on Control System, Computing and Engineering (ICCSCE), 441–445. https://doi.org/10.1109/ICCSCE.2016.7893614

Cavalli-Sforza, V., & Ortolano, L. (1984). Delphi Forecasts of Land Use: Transportation Interactions. Journal of Transportation Engineering, 110(3), 324–339. https://doi.org/10.1061/(ASCE)0733-947X(1984)110:3(324)

Cazzato, D., Cimarelli, C., Sanchez-Lopez, J. L., Voos, H., & Leo, M. (2020). A Survey of Computer Vision Methods for 2D Object Detection from Unmanned Aerial Vehicles. Journal of Imaging, 6(8), Article 8. https://doi.org/10.3390/jimaging6080078

Chen, Q., Xie, Y., Guo, S., Bai, J., & Shu, Q. (2021). Sensing system of environmental perception technologies for driverless vehicle: A review of state of the art and challenges. Sensors and Actuators A: Physical, 319, 112566. https://doi.org/10.1016/j.sna.2021.112566

Chen, S.-J., & Hwang, C.-L. (1992). Fuzzy Multiple Attribute Decision Making Methods. In S.-J. Chen & C.-L. Hwang (Eds.), Fuzzy Multiple Attribute Decision Making: Methods and Applications (pp. 289–486). Springer. https://doi.org/10.1007/978-3-642-46768-4_5

Chen, X., Ma, H., Wan, J., Li, B., & Xia, T. (2017). Multi-View 3D Object Detection Network for Autonomous Driving. 1907–1915. https://openaccess.thecvf.com/content_cvpr_2017/html/Chen_Multi-View_3D_Object_CVPR_2017_paper.html

Choi, H., & Kim, W.-C. (2020). Optical system design for light detection and ranging sensor with an ultra-wide field-of-view using a micro actuator. Microsystem Technologies, 26(11), 3561–3567. https://doi.org/10.1007/s00542-020-04997-1

Choi, J. (2016). Range Sensors: Ultrasonic Sensors, Kinect, and LiDAR. In A. Goswami & P. Vadakkepat (Eds.), Humanoid Robotics: A Reference (pp. 1–19). Springer Netherlands. https://doi.org/10.1007/978-94-007-7194-9_108-1

Claussmann, L. (2019). Motion Planning for Autonomous Highway Driving: A Unified Architecture for Decision-Maker and Trajectory Generator. https://www.researchgate.net/publication/340479318_Motion_Planning_for_Autonomous_Highway_Driving_A_Unified_Architecture_for_Decision-Maker_and_Trajectory_Generator

Cochrane, J. L., & Zeleny, M. (1973). Multiple criteria decision making ([1st ed.]). University of South Carolina Press.

Combs, T. S., Sandt, L. S., Clamann, M. P., & McDonald, N. C. (2019). Automated Vehicles and Pedestrian Safety: Exploring the Promise and Limits of Pedestrian Detection. American Journal of Preventive Medicine, 56(1), 1–7. https://doi.org/10.1016/j.amepre.2018.06.024

Cristóbal, J. R. S. (2012). Multi Criteria Analysis in the Renewable Energy Industry. Springer Science & Business Media.

Curto, S., Severino, A., Trubia, S., Arena, F., & Puleo, L. (2021). The effects of autonomous vehicles on safety. 110013. https://doi.org/10.1063/5.0047883

Dalkey, N., & Helmer, O. (1963). An Experimental Application of the DELPHI Method to the Use of Experts. Management Science, 9(3), 458–467. https://doi.org/10.1287/mnsc.9.3.458

De Almeida, A. T., & Morais, D. C. (Eds.). (2020). Innovation for Systems Information and Decision: Second International Meeting, INSID 2020, Recife, Brazil, December 2–4, 2020, Proceedings (Vol. 405). Springer International Publishing. https://doi.org/10.1007/978-3-030-64399-7

De la Cruz, M. P., del Caño, A., & de la Cruz, E. (2008). New paradigms for public procurement of construction projects in the United Kingdom—Potential applicability in Spain. Canadian Journal of Civil Engineering, 35(3), 276–286. https://doi.org/10.1139/L07-100

Deng, J., Shi, S., Li, P., Zhou, W., Zhang, Y., & Li, H. (2021). Voxel R-CNN: Towards High Performance Voxel-based 3D Object Detection. Proceedings of the AAAI Conference on Artificial Intelligence, 35(2), Article 2. https://doi.org/10.1609/aaai.v35i2.16207

Dombi, J. (2009). The Generalized Dombi Operator Family and the Multiplicative Utility Function. In V. E. Balas, J. Fodor, & A. R. Várkonyi-Kóczy (Eds.), Soft Computing Based Modeling in Intelligent Systems (Vol. 196, pp. 115–131). Springer Berlin Heidelberg. https://doi.org/10.1007/978-3-642-00448-3_6

Domínguez, R., Onieva, E., Alonso, J., Villagra, J., & González, C. (2011). LIDAR based perception solution for autonomous vehicles. 2011 11th International Conference on Intelligent Systems Design and Applications, 790–795. https://doi.org/10.1109/ISDA.2011.6121753

Dong, J., Chen, S., Li, Y., Du, R., Steinfeld, A., Labi, S. (2021). Space-weighted information fusion using deep reinforcement learning: The context of tactical control of lane-changing autonomous vehicles and connectivity range assessment, Transportation Research Part C: Emerging Technologies 128, 103192, https://doi.org/10.1016/j.trc.2021.103192

Dosovitskiy, A., Ros, G., Codevilla, F., Lopez, A., & Koltun, V. (2017). CARLA: An Open Urban Driving Simulator. Proceedings of the 1st Annual Conference on Robot Learning, 1–16. https://proceedings.mlr.press/v78/Movitskiy17a.html

Du, R., Chen, S., Dong, J., Chen, T., Fu, X., & Labi, S. (2023). Dynamic urban traffic rerouting with fog-cloud reinforcement learning. Computer-Aided Civil and Infrastructure Engineering, https://doi.org/10.1111/mice.13115

Du, R. (2023). Safety and Mobility Improvement of Mixed Traffic Using Optimization- and Learning-Based Methods, Ph.D. Thesis, Purdue University, West Lafayette, IN.

Du, R., Chen, S., Li, Y., Ha, P.Y.J., Dong, J., Anastasopoulos, P., Labi, S. (2021). A cooperative crash avoidance framework for autonomous vehicle under collision-imminent situations in mixed traffic stream, 2021 IEEE International Intelligent Transportation Systems Conference (ITSC), 1997-2002. https://doi.org/10.1109/ITSC48978.2021.9564937

Du, R., Ha, P.Y.J., Dong, J., Chen, S., Labi, S. (2022). Large network multi-level control for CAV and Smart Infrastructure: AI-based Fog-Cloud collaboration, CCAT Report #55, The Center for Connected and Automated Transportation, Purdue University, West Lafayette, IN. https://doi.org/10.5703/1288284317465

Duan, X., Jiang, H., Tian, D., Zou, T., Zhou, J., & Cao, Y. (2021). V2I based environment perception for autonomous vehicles at intersections. China Communications, 18(7), 1–12. https://doi.org/10.23919/JCC.2021.07.001

Dubljevic, V., List, G., Milojevich, J., Ajmeri, N., Bauer, W. A., Singh, M. P., Bardaka, E., Birkland, T. A., Edwards, C. H. W., Mayer, R. C., Muntean, I., Powers, T. M., Rakha, H. A., Ricks, V. A., & Samandar, M. S. (2021). Toward a rational and ethical sociotechnical system of autonomous vehicles: A novel application of multi-criteria decision analysis. PLOS ONE, 16(8), e0256224. https://doi.org/10.1371/journal.pone.0256224

Dybedal, J., & Hovland, G. (2017). Optimal placement of 3D sensors considering range and field of view. 2017 IEEE International Conference on Advanced Intelligent Mechatronics (AIM), 1588–1593. https://doi.org/10.1109/AIM.2017.8014245

Elhousni, M., & Huang, X. (2020). A Survey on 3D LiDAR Localization for Autonomous Vehicles. 2020 IEEE Intelligent Vehicles Symposium (IV), 1879–1884. https://doi.org/10.1109/IV47402.2020.9304812

Fagnant, D. J., & Kockelman, K. (2015). Preparing a nation for autonomous vehicles: Opportunities, barriers and policy recommendations. Transportation Research Part A: Policy and Practice, 77, 167–181. https://doi.org/10.1016/j.tra.2015.04.003

Fang, J., Yan, F., Zhao, T., Zhang, F., Zhou, D., Yang, R., Ma, Y., & Wang, L. (2018). Simulating LIDAR Point Cloud for Autonomous Driving using Real-world Scenes and Traffic Flows. ArXiv, abs/1811.07112.

Feng, S., Yan, X., Sun, H. et al. Intelligent driving intelligence test for autonomous vehicles with naturalistic and adversarial environment. Nat Commun **12**, 748 (2021). https://doi.org/10.1038/s41467-021-21007-8

FHWA. (2005). Traffic Congestion and Reliability: Trends and Advanced Strategies for Congestion Mitigation: Executive Summary. https://ops.fhwa.dot.gov/congestion_report/executive_summary.htm

Figueira, J. R., Mousseau, V., & Roy, B. (2016). ELECTRE Methods. In S. Greco, M. Ehrgott, & J. R. Figueira (Eds.), Multiple Criteria Decision Analysis: State of the Art Surveys (pp. 155–185). Springer. https://doi.org/10.1007/978-1-4939-3094-4_5

Fishburn, P. C. (1974). Exceptional Paper—Lexicographic Orders, Utilities and Decision Rules: A Survey. Management Science, 20(11), 1442–1471. https://doi.org/10.1287/mnsc.20.11.1442

Gal, T., Stewart, T., & Hanne, T. (2013). Multicriteria Decision Making: Advances in MCDM Models, Algorithms, Theory, and Applications. Springer Science & Business Media.

Goicoechea, A. (1982). Multiobjective decision analysis with engineering and business applications. (No Title). https://cir.nii.ac.jp/crid/1130000796933928576

Gómez-Huélamo, C., Del Egido, J., Bergasa, L. M., Barea, R., López-Guillén, E., Arango, F., Araluce, J., & López, J. (2021). Train Here, Drive There: Simulating Real-World Use Cases with Fully-Autonomous Driving Architecture in CARLA Simulator. In L. M. Bergasa, M. Ocaña, R. Barea, E. López-Guillén, & P. Revenga (Eds.), Advances in Physical Agents II (pp. 44–59). Springer International Publishing. https://doi.org/10.1007/978-3-030-62579-5_4

Goswami, S. S., Behera, D. K., & Mitra, D. S. (2020). A Comprehensive Study of Weighted Product Model for Selecting the Best Product in Our Daily Life. Brazilian Journal of Operations & Production Management, 17(2), Article 2. https://doi.org/10.14488/BJOPM.2020.017

Gross, M., & Webster, J. (2021). Autonomous Transport Innovation: A review of enabling technologies. Engineer Research and Development Center (U.S.). https://doi.org/10.21079/11681/42028

Gunantara, N. (2018). A review of multi-objective optimization: Methods and its applications. Cogent Engineering, 5(1), 1502242. https://doi.org/10.1080/23311916.2018.1502242

Guo, Y., Souders, D., Labi, S., Peeta, S., Benedyk, I., & Li, Y. (2021). Paving the way for autonomous Vehicles: Understanding autonomous vehicle adoption and vehicle fuel choice under user heterogeneity. Transportation Research Part A: Policy and Practice, 154, 364–398. https://doi.org/10.1016/j.tra.2021.10.018

Hassan, K. (2023). Lidar vs. Radar: Comprehensive Comparison and Analysis. https://www.wevolver.com/article/lidar-vs-radar-detection-tracking-and-imaging

Hazelrigg, G. A. (2019). A Note on the Weighted Sum Method. Journal of Mechanical Design, 141(100301). https://doi.org/10.1115/1.4044326

He, M., Zhao, H., Cui, J., & Zha, H. (2014). Calibration method for multiple 2D LIDARs system. 2014 IEEE International Conference on Robotics and Automation (ICRA), 3034–3041. https://doi.org/10.1109/ICRA.2014.6907296

Hobbs, B. F., & Meier, P. (2000). Resolving Differences (Step 10). In B. F. Hobbs & P. Meier (Eds.), Energy Decisions and the Environment: A Guide to the Use of Multicriteria Methods (pp. 99–109). Springer US. https://doi.org/10.1007/978-1-4615-4477-7_5

Hu, H., Liu, Z., Chitlangia, S., Agnihotri, A., & Zhao, D. (2022). Investigating the Impact of Multi-LiDAR Placement on Object Detection for Autonomous Driving. 2550–2559. https://openaccess.thecvf.com/content/CVPR2022/html/Hu_Investigating_the_Impact_of_Multi-LiDAR_Placement_on_Object_Detection_for_CVPR_2022_paper.html

Hussain, A., Akhtar, F., Khand, Z., Ali, A., & Shaukat, Z. (2021). Complexity and Limitations of GNSS Signal Reception in Highly Obstructed Enviroments. Engineering, Technology & Applied Science Research, 11, 6864–6868. https://doi.org/10.48084/etasr.3908

Hwang, C.-L., & Yoon, K. (1981). Methods for Multiple Attribute Decision Making. In C.-L. Hwang & K. Yoon (Eds.), Multiple Attribute Decision Making: Methods and Applications A State-of-the-Art Survey (pp. 58–191). Springer. https://doi.org/10.1007/978-3-642-48318-9_3

Ignatious, H. A., Sayed, H.-E.-, & Khan, M. (2022). An overview of sensors in Autonomous Vehicles. Procedia Computer Science, 198, 736–741. https://doi.org/10.1016/j.procs.2021.12.315

Imad, M., Doukhi, O., & Lee, D.-J. (2021). Transfer Learning Based Semantic Segmentation for 3D Object Detection from Point Cloud. Sensors, 21(12), 3964. https://doi.org/10.3390/s21123964

Project Management Institute, (2008). A Guide to the Project Management Body of Knowledge: PMBOK Guide. Project Management Institute.

Jain, A., Nandakumar, K., & Ross, A. (2005). Score normalization in multimodal biometric systems. Pattern Recognition, 38(12), 2270–2285. https://doi.org/10.1016/j.patcog.2005.01.012

Javaid, M., Haleem, A., Rab, S., Pratap Singh, R., & Suman, R. (2021). Sensors for daily life: A review. Sensors International, 2, 100121. https://doi.org/10.1016/j.sintl.2021.100121

Jin, S., Gao, Y., Hui, F., Zhao, X., Wei, C., Ma, T., & Gan, W. (2022). A Novel Information Theory-Based Metric for Evaluating Roadside LiDAR Placement. IEEE Sensors Journal, 22(21), 21009–21023. https://doi.org/10.1109/JSEN.2022.3204836

Josselin, J.-M., & Le Maux, B. (2017). Multi-criteria Decision Analysis. In J.-M. Josselin & B. Le Maux (Eds.), Statistical Tools for Program Evaluation: Methods and Applications to Economic Policy, Public Health, and Education (pp. 385–416). Springer International Publishing. https://doi.org/10.1007/978-3-319-52827-4_11

Kappal, S. (2019). Data Normalization Using Median & Median Absolute Deviation (MMAD) based Z-Score for Robust Predictions vs. Min-Max Normalization. https://doi.org/10.13140/RG.2.2.32799.82088

Keeney, R. L., & Raiffa, H. (1976). Decisions with multiple objectives: Preferences and value tradeoffs (pp. xix, 569). Cambridge University Press.

Keeney, R. L., & Raiffa, H. (1993). Decisions with Multiple Objectives: Preferences and Value Trade-Offs. Cambridge University Press.

Kelly, J., & Sukhatme, G. S. (2014). A General Framework for Temporal Calibration of Multiple Proprioceptive and Exteroceptive Sensors. In O. Khatib, V. Kumar, & G. Sukhatme (Eds.), Experimental Robotics: The 12th International Symposium on Experimental Robotics (pp. 195–209). Springer. https://doi.org/10.1007/978-3-642-28572-1_14

Khayyam, H., Javadi, B., Jalili, M., & Jazar, R. N. (2020). Artificial Intelligence and Internet of Things for Autonomous Vehicles. In R. N. Jazar & L. Dai (Eds.), Nonlinear Approaches in Engineering Applications: Automotive Applications of Engineering Problems (pp. 39–68). Springer International Publishing. https://doi.org/10.1007/978-3-030-18963-1_2

Kibii, J. E., Dreher, A., Wormser, P. L., & Gimpel, H. (2022). Design and Calibration of Plane Mirror Setups for Mobile Robots with a 2D-Lidar. Sensors, 22(20), 7830. https://doi.org/10.3390/s22207830

Kim, J. H., Kim, D.-H., & Choi, M.-R. (2019). Radar data processing for detecting the front vehicle. 2019 8th Asia-Pacific Conference on Antennas and Propagation (APCAP), 191–192. https://doi.org/10.1109/APCAP47827.2019.9472171

Kim, M., Stoker, J., Irwin, J., Danielson, J., & Park, S. (2022). Absolute Accuracy Assessment of Lidar Point Cloud Using Amorphous Objects. Remote Sensing, 14(19), Article 19. https://doi.org/10.3390/rs14194767

Kim, S. U., Lee, J., Yoon, J., Ko, S.-K., & Kim, J. (2021). Robust methods for estimating the orientation and position of IMU and MARG sensors. Electronics Letters, 57(21), 816–818. https://doi.org/10.1049/ell2.12263

Kim, T.-H., & Park, T.-H. (2020). Placement Optimization of Multiple Lidar Sensors for Autonomous Vehicles. IEEE Transactions on Intelligent Transportation Systems, 21(5), 2139–2145. https://doi.org/10.1109/TITS.2019.2915087

Kini, R. R. (2020). Sensor Position Optimization for Multiple LiDARs in Autonomous Vehicles. http://urn.kb.se/resolve?urn=urn:nbn:se:kth:diva-289597

Kocić, J., Jovičić, N., & Drndarević, V. (2018). Sensors and Sensor Fusion in Autonomous Vehicles. 2018 26th Telecommunications Forum (TELFOR), 420–425. https://doi.org/10.1109/TELFOR.2018.8612054

Kos, T., Markezic, I., & Pokrajcic, J. (2010). Effects of multipath reception on GPS positioning performance. Proceedings ELMAR-2010, 399–402. https://ieeexplore.ieee.org/abstract/document/5606130

Kukkala, V. K., Tunnell, J., Pasricha, S., & Bradley, T. (2018). Advanced Driver-Assistance Systems: A Path Toward Autonomous Vehicles. IEEE Consumer Electronics Magazine, 7(5), 18–25. https://doi.org/10.1109/MCE.2018.2828440

Kuutti, S., Fallah, S., Katsaros, K., Dianati, M., Mccullough, F., & Mouzakitis, A. (2018). A Survey of the State-of-the-Art Localization Techniques and Their Potentials for Autonomous Vehicle Applications. IEEE Internet of Things Journal, 5(2), 829–846. https://doi.org/10.1109/JIOT.2018.2812300

Labi, S. (2014). Introduction to Civil Engineering Systems: A Systems Perspective to the Development of Civil Engineering Facilities. John Wiley & Sons.

Labi, S., & Sinha, K. C. (2022). Emerging transportation innovations: Promises and pitfalls. Innovation and Emerging Technologies, 09, 2240001. https://doi.org/10.1142/S2737599422400011

Lamptey, G., Ahmad, M., & Labi, S. (2005). Life Cycle Cost Analysis for INDOT Pavement Design Procedures (FHWA/IN/JTRP-2004/28, 2712; p. FHWA/IN/JTRP-2004/28, 2712). Purdue University. https://doi.org/10.5703/1288284313261

Li, N., Ho, C. P., Xue, J., Lim, L. W., Chen, G., Fu, Y. H., & Lee, L. Y. T. (2022). A Progress Review on Solid-State LiDAR and Nanophotonics-Based LiDAR Sensors. Laser & Photonics Reviews, 16(11), 2100511. https://doi.org/10.1002/lpor.202100511

Li, Z. (2003). Multicriteria highway programming incorporating risk and uncertainty: A methodology for highway asset management system [Ph.D., Purdue University]. https://www.proquest.com/docview/305309703/abstract/65DAD7C7E3A7473CPQ/1Saat

Li, Z., & Sinha, K. (2000). A Methodology to Estimate Load and Non-Load Shares of Highway Pavement Routine Maintenance and Rehabilitation Expenditures. JTRP Technical Reports. https://doi.org/10.5703/1288284313129

Li, Z., & Sinha, K. C. (2004). Methodology for Multicriteria Decision Making in Highway Asset Management—Zongzhi Li, Kumares C. Sinha, 2004. https://journals.sagepub.com/doi/abs/10.3141/1885-12

Lin, Y., Wang, Y., Wang, S., Li, S., Wang, M., Cai, H., & Teng, F. (2022). Noise Point Detection From Airborne LiDAR Point Cloud Based on Spatial Hierarchical Directional Relationship. IEEE Access, 10, 82076–82091. https://doi.org/10.1109/ACCESS.2022.3196388

Liu, Z., Arief, M., & Zhao, D. (2019). Where Should We Place LiDARs on the Autonomous Vehicle? - An Optimal Design Approach. 2019 International Conference on Robotics and Automation (ICRA), 2793–2799. https://doi.org/10.1109/ICRA.2019.8793619

Lucic, M. C., Ghazzai, H., & Massoud, Y. (2020). Elevated LiDAR Placement under Energy and Throughput Capacity Constraints. 2020 IEEE 63rd International Midwest Symposium on Circuits and Systems (MWSCAS), 897–900. https://doi.org/10.1109/MWSCAS48704.2020.9184579

Malik, S., Khan, M. A., & El-Sayed, H. (2022). CARLA: Car Learning to Act — An Inside Out. Procedia Computer Science, 198, 742–749. https://doi.org/10.1016/j.procs.2021.12.316

Marler, R. T., & Arora, J. S. (2010). The weighted sum method for multi-objective optimization: New insights. Structural and Multidisciplinary Optimization, 41(6), 853–862. https://doi.org/10.1007/s00158-009-0460-7

Martel, J.-M., Khoury, N. T., & Bergeron, M. (1988). An Application of a Multicriteria Approach to Portfolio Comparisons. Journal of the Operational Research Society, 39(7), 617–628. https://doi.org/10.1057/jors.1988.107

Mateo, J. R. S. C. (2012). Weighted Sum Method and Weighted Product Method. In J. R. San Cristóbal Mateo (Ed.), Multi Criteria Analysis in the Renewable Energy Industry (pp. 19–22). Springer. https://doi.org/10.1007/978-1-4471-2346-0_4

Meadows, W., Hudson, C., Goodin, C., Dabbiru, L., Powell, B., Doude, M., Carruth, D., Islam, M., Ball, J. E., & Tang, B. (2019). Multi-LiDAR placement, calibration, co-registration, and processing on a Subaru Forester for off-road autonomous vehicles operations. In M. C. Dudzik & J. C. Ricklin (Eds.), Autonomous Systems: Sensors, Processing, and Security for Vehicles and Infrastructure 2019 (p. 7). SPIE. https://doi.org/10.1117/12.2518915

Miettinen, K. (1998). Nonlinear Multiobjective Optimization (Vol. 12). Springer US. https://doi.org/10.1007/978-1-4615-5563-6

Milakis, D., van Arem, B., & van Wee, B. (2017). Policy and society related implications of automated driving: A review of literature and directions for future research. Journal of Intelligent Transportation Systems, 21(4), 324–348. https://doi.org/10.1080/15472450.2017.1291351

Morency, P., Gauvin, L., Plante, C., Fournier, M., & Morency, C. (2012). Neighborhood Social Inequalities in Road Traffic Injuries: The Influence of Traffic Volume and Road Design. American Journal of Public Health, 102(6), 1112–1119. https://doi.org/10.2105/AJPH.2011.300528

Mou, S., Chang, Y., Wang, W., & Zhao, D. (2018b). An Optimal LiDAR Configuration Approach for Self-Driving Cars (arXiv:1805.07843). arXiv. https://doi.org/10.48550/arXiv.1805.07843

Mullen, P. M. (2003). Delphi: Myths and reality. Journal of Health Organization and Management, 17(1), 37–52. https://doi.org/10.1108/14777260310469319

Ng, T. S. (2021). ADAS in Autonomous Driving. In T. S. Ng (Ed.), Robotic Vehicles: Systems and Technology (pp. 87–93). Springer. https://doi.org/10.1007/978-981-33-6687-9_12

NHTSA. (2021). Automated Vehicles for Safety. NHTSA.

Nobis, F., Geisslinger, M., Weber, M., Betz, J., & Lienkamp, M. (2019). A Deep Learning-based Radar and Camera Sensor Fusion Architecture for Object Detection. 2019 Sensor Data Fusion: Trends, Solutions, Applications (SDF), 1–7. https://doi.org/10.1109/SDF.2019.8916629

Odu, G. O. (2019). Weighting methods for multi-criteria decision making technique. Journal of Applied Sciences and Environmental Management, 23(8), Article 8. https://doi.org/10.4314/jasem.v23i8.7

Ortiz Arteaga, A., Scott, D., & Boehm, J. (2019). Initial Investigation of a Low-Cost Automotive LIDAR System. The International Archives of the Photogrammetry, Remote Sensing and Spatial Information Sciences, XLII-2-W17, 233–240. https://doi.org/10.5194/isprs-archives-XLII-2-W17-233-2019

Ortiz, F. M., Sammarco, M., Costa, L. H. M. K., & Detyniecki, M. (2023). Applications and Services Using Vehicular Exteroceptive Sensors: A Survey. IEEE Transactions on Intelligent Vehicles, 8(1), 949–969. https://doi.org/10.1109/TIV.2022.3182218

Ortiz-Barrios, M., Cabarcas-Reyes, J., Ishizaka, A., Barbati, M., Jaramillo-Rueda, N., & de Jesús Carrascal-Zambrano, G. (2021). A hybrid fuzzy multi-criteria decision making model for selecting a sustainable supplier of forklift filters: A case study from the mining industry. Annals of Operations Research, 307(1), 443–481. https://doi.org/10.1007/s10479-020-03737-y

OS0 Ultra-wide field-of-view lidar sensor for autonomous vehicles and robotics. (n.d.). Ouster. Retrieved April 18, 2023, from https://ouster.com/products/scanning-lidar/os0-sensor

Pamučar, D., Stević, Ž., & Sremac, S. (2018). A New Model for Determining Weight Coefficients of Criteria in MCDM Models: Full Consistency Method (FUCOM). Symmetry, 10(9), Article 9. https://doi.org/10.3390/sym10090393

Papathanasiou, J., & Ploskas, N. (2018). TOPSIS. In J. Papathanasiou & N. Ploskas (Eds.), Multiple Criteria Decision Aid: Methods, Examples and Python Implementations (pp. 1–30). Springer International Publishing. https://doi.org/10.1007/978-3-319-91648-4_1

Parekh, D., Poddar, N., Rajpurkar, A., Chahal, M., Kumar, N., Joshi, G. P., & Cho, W. (2022). A Review on Autonomous Vehicles: Progress, Methods and Challenges. Electronics, 11(14), Article 14. https://doi.org/10.3390/electronics11142162

Patel, B. C., Sinha, G. R., & Goel, N. (2020). Introduction to sensors. In Advances in Modern Sensors: Physics, design, simulation and applications. IOP Publishing. https://doi.org/10.1088/978-0-7503-2707-7ch1

Patidar, V., Labi, S. A., Sinha, K. C., & Thompson, P. D. (2007). Multi-Objective Optimization for Bridge Management Systems. NCHRP Report, 590, Article Project 12-67. https://trid.trb.org/view/838856

Patro, S. G. K., & Sahu, K. K. (2015, March 19). Normalization: A Preprocessing Stage. arXiv.Org. https://arxiv.org/abs/1503.06462v1

Pavitha, P. P., Rekha, K. B., & Safinaz, S. (2021). Perception system in Autonomous Vehicle: A study on contemporary and forthcoming technologies for object detection in autonomous vehicles. 2021 International Conference on Forensics, Analytics, Big Data, Security (FABS), 1, 1–6. https://doi.org/10.1109/FABS52071.2021.9702569

Pereira, F., Correia, R., & Carvalho, N. B. (2018). Comparison of active and passive sensors for IoT applications. 2018 IEEE Wireless Power Transfer Conference (WPTC), 1–3. https://doi.org/10.1109/WPT.2018.8639445

Pereira, M., Silva, D., Santos, V., & Dias, P. (2016). Self calibration of multiple LIDARs and cameras on autonomous vehicles. Robotics and Autonomous Systems, 83, 326–337. https://doi.org/10.1016/j.robot.2016.05.010

Peterson, D. E. (1985). Life-Cycle Cost Analysis of Pavements. NCHRP Synthesis of Highway Practice, 122. https://trid.trb.org/view/271441

Photonics, S. (n.d.). Sense Photonics Introduces Osprey, the First Modular FLASH LiDAR for Autonomous Vehicles. Retrieved April 5, 2023, from https://www.prnewswire.com/news-releases/sense-photonics-introduces-osprey-the-first-modular-flash-lidar-for-autonomous-vehicles-300981523.html

Rablau, C. (2019). LIDAR – A new (self-driving) vehicle for introducing optics to broader engineering and non-engineering audiences. Fifteenth Conference on Education and Training in Optics and Photonics: ETOP 2019 (2019), Paper 11143_138, 11143_138. https://opg.optica.org/abstract.cfm?uri=ETOP-2019-11143_138

Raj, A., Kumar, J. A., & Bansal, P. (2020). A multicriteria decision making approach to study barriers to the adoption of autonomous vehicles. Transportation Research Part A: Policy and Practice, 133, 122–137. https://doi.org/10.1016/j.tra.2020.01.013

Raj, T., Hashim, F. H., Huddin, A. B., Ibrahim, M. F., & Hussain, A. (2020). A Survey on LiDAR Scanning Mechanisms. Electronics, 9(5), 741. https://doi.org/10.3390/electronics9050741

Reddy Cenkeramaddi, L., Bhatia, J., Jha, A., Kumar Vishkarma, S., & Soumya, J. (2020). A Survey on Sensors for Autonomous Systems. 2020 15th IEEE Conference on Industrial Electronics and Applications (ICIEA), 1182–1187. https://doi.org/10.1109/ICIEA48937.2020.9248282

Roriz, R., Cabral, J., & Gomes, T. (2022). Automotive LiDAR Technology: A Survey. IEEE Transactions on Intelligent Transportation Systems, 23(7), 6282–6297. https://doi.org/10.1109/TITS.2021.3086804

Rosique, F., Navarro, P. J., Fernández, C., & Padilla, A. (2019). A Systematic Review of Perception System and Simulators for Autonomous Vehicles Research. Sensors, 19(3), Article 3. https://doi.org/10.3390/s19030648

Russell, P. (2015). How Autonomous Vehicles Will Profoundly Change The World. https://doi.org/10.13140/RG.2.2.36272.10249

Saaty, T. L. (1977). A scaling method for priorities in hierarchical structures. Journal of Mathematical Psychology, 15(3), 234–281. https://doi.org/10.1016/0022-2496(77)90033-5

SAE, 2021. (2021). J3016_202104: Taxonomy and Definitions for Terms Related to Driving Automation Systems for On-Road Motor Vehicles - SAE International. https://www.sae.org/standards/content/j3016_202104/

Saraf, N. M., Hamid, J. R. A., & Kamaruddin, M. H. (2012). Verification Of 3-D Lidar Data For Use In Monte Carlo Ray Tracing Method. 11.

Serifoglu Yilmaz, C., & Gungor, O. (2018). Comparison of the performances of ground filtering algorithms and DTM generation from a UAV-based point cloud. Geocarto International, 33(5), 522–537. https://doi.org/10.1080/10106049.2016.1265599

Setämaa-Kärkkäinen, A., Miettinen, K., & Vuori, J. (2006). Best compromise solution for a new multiobjective scheduling problem. Computers & Operations Research, 33(8), 2353–2368. https://doi.org/10.1016/j.cor.2005.02.006

Shetty, A., Yu, M., Kurzhanskiy, A., Grembek, O., Tavafoghi, H., & Varaiya, P. (2021). Safety challenges for autonomous vehicles in the absence of connectivity. Transportation Research Part C: Emerging Technologies, 128, 103133. https://doi.org/10.1016/j.trc.2021.103133

Shi, S., Wang, X., & Li, H. (2019). PointRCNN: 3D Object Proposal Generation and Detection From Point Cloud. 770–779. https://openaccess.thecvf.com/content_CVPR_2019/html/Shi_PointRCNN_3D_Object_Proposal_Generation_and_Detection_From_Point_Cloud_CVPR_2019_paper.html

Singh, M., & Pant, M. (2021). A review of selected weighing methods in MCDM with a case study. International Journal of System Assurance Engineering and Management, 12(1), 126–144. https://doi.org/10.1007/s13198-020-01033-3

Sinha, K. C., & Labi, S. (2007). Transportation Decision Making: Principles of Project Evaluation and Programming (1st ed.). Wiley. https://doi.org/10.1002/9780470168073

Sinha, K. C., Patidar, V., Li, Z., Labi, S., & Thompson, P. D. (2009). Establishing the Weights of Performance Criteria: Case Studies in Transportation Facility Management. Journal of Transportation Engineering, 135(9), 619–631. https://doi.org/10.1061/(ASCE)TE.1943-5436.0000039

Sinha, G. (2017). Introduction and Classification of Sensors. https://www.researchgate.net/publication/321625555_Introduction_and_Classification_of_Sensors. December 6, 2017, Accessed August 31, 2023.

Sinsomboonthong, S. (2022). Performance Comparison of New Adjusted Min-Max with Decimal Scaling and Statistical Column Normalization Methods for Artificial Neural Network Classification. International Journal of Mathematics and Mathematical Sciences, 2022, e3584406. https://doi.org/10.1155/2022/3584406

Sourani, A., & Sohail, M. (2015). The Delphi Method: Review and Use in Construction Management Research. International Journal of Construction Education and Research, 11(1), 54–76. https://doi.org/10.1080/15578771.2014.917132

Sundararajan, S., Yousuf, M., Omay, M., Steinfeld, A., & Owens, J. M. (2019). Automated Vehicles (AVs) for People with Disabilities. In G. Meyer & S. Beiker (Eds.), Road Vehicle Automation 5 (pp. 85–90). Springer International Publishing. https://doi.org/10.1007/978-3-319-94896-6_8

Supriyono, H., & Sari, C. P. (2018). Developing decision support systems using the weighted product method for house selection. AIP Conference Proceedings, 1977(1), 020049. https://doi.org/10.1063/1.5042905

Szűcs, H., & Hézer, J. (2022). Road Safety Analysis of Autonomous Vehicles: An Overview. Periodica Polytechnica Transportation Engineering, 50(4), Article 4. https://doi.org/10.3311/PPtr.19605

Taherdoost, H., & Madanchian, M. (2023). A Comprehensive Overview of the ELECTRE Method in Multi Criteria Decision-Making. Journal of Management Science & Engineering Research, 6. https://doi.org/10.30564/jmser.v6i2.5637

Triantaphyllou, E., & Mann, S. H. (1989). An examination of the effectiveness of multi-dimensional decision-making methods: A decision-making paradox. Decision Support Systems, 5(3), 303–312. https://doi.org/10.1016/0167-9236(89)90037-7

US EPA, O. (2015, August 25). Fast Facts on Transportation Greenhouse Gas Emissions [Overviews and Factsheets]. https://www.epa.gov/greenvehicles/fast-facts-transportation-greenhouse-gas-emissions

US EPA, O. (2022, October 19). Climate Change Impacts on Transportation [Overviews and Factsheets]. https://www.epa.gov/climateimpacts/climate-change-impacts-transportation

USDOT. (2022). Transportation Statistics Annual Report 2022. https://doi.org/10.21949/1528354

Vargas, J., Alsweiss, S., Toker, O., Razdan, R., & Santos, J. (2021). An Overview of Autonomous Vehicles Sensors and Their Vulnerability to Weather Conditions. Sensors, 21(16), Article 16. https://doi.org/10.3390/s21165397

Vavra, C. (2022, January 6). Precise positioning for autonomous vehicles. Control Engineering. https://www.controleng.com/articles/precise-positioning-for-autonomous-vehicles/

Velodyne Lidar Unveils Solid State Lidar Sensor. (2020.). Velodyne Lidar. Retrieved March 10, 2023, from https://velodynelidar.com/press-release/velodyne-lidar-unveils-breakthrough-solid-state-lidar-sensor/

Velodyne Ultra Puck VLP-32C Long-Range LiDAR Sensor—Clearpath Robotics. (n.d.). Retrieved November 2, 2023, from https://store.clearpathrobotics.com/products/ultra-puck

Wang, Z., & Menenti, M. (2021). Challenges and Opportunities in Lidar Remote Sensing. Frontiers in Remote Sensing, 2. https://www.frontiersin.org/articles/10.3389/frsen.2021.641723

Warren, M. E. (2019). Automotive LIDAR Technology. 2019 Symposium on VLSI Circuits, C254–C255. https://doi.org/10.23919/VLSIC.2019.8777993

Winston, W. L. (1999). Decision Making Under Uncertainty With RISKOptimizer: A Step-To-Step Guide Using Palisade's RISKOptimizer for Excel (Pap/Cdr edition). Palisade Corporation.

Wojtanowski, J., Zygmunt, M., Kaszczuk, M., Mierczyk, Z., & Muzal, M. (2014). Comparison of 905 nm and 1550 nm semiconductor laser rangefinders' performance deterioration due to adverse environmental conditions. Opto-Electronics Review, 22(3), 183–190. https://doi.org/10.2478/s11772-014-0190-2

Woo, A., Fidan, B., & Melek, W. W. (2018). Localization for Autonomous Driving. In Handbook of Position Location (pp. 1051–1087). John Wiley & Sons, Ltd. https://doi.org/10.1002/9781119434610.ch29

Wu, X., Cao, J., & Douma, F. (2021). The impacts of vehicle automation on transport-disadvantaged people. Transportation Research Interdisciplinary Perspectives, 11, 100447. https://doi.org/10.1016/j.trip.2021.100447

Yan, D., Wang, C., Feng, X., & Dong, B. (2018). Validation and Ground Truths. In A. Wagner, W. O'Brien, & B. Dong (Eds.), Exploring Occupant Behavior in Buildings: Methods and Challenges (pp. 239–260). Springer International Publishing. https://doi.org/10.1007/978-3-319-61464-9_9

Yang, D., Liu, Y., Chen, Q., Chen, M., Zhan, S., Cheung, N., Chan, H.-Y., Wang, Z., & Li, W. J. (2023). Development of the high angular resolution 360° LiDAR based on scanning MEMS mirror. Scientific Reports, 13(1), Article 1. https://doi.org/10.1038/s41598-022-26394-6

Yeong, D. J., Velasco-Hernandez, G., Barry, J., & Walsh, J. (2021). Sensor and Sensor Fusion Technology in Autonomous Vehicles: A Review. Sensors, 21(6), Article 6. https://doi.org/10.3390/s21062140

Yu, P. L. (1973). A Class of Solutions for Group Decision Problems. Management Science, 19(8), 936–946. https://doi.org/10.1287/mnsc.19.8.936

Zhang, J., & Singh, S. (2014, July 12). LOAM: Lidar Odometry and Mapping in Real-time. Robotics: Science and Systems X. Robotics: Science and Systems 2014. https://doi.org/10.15607/RSS.2014.X.007

Zhang, Y., Carballo, A., Yang, H., & Takeda, K. (2023). Perception and sensing for autonomous vehicles under adverse weather conditions: A survey. ISPRS Journal of Photogrammetry and Remote Sensing, 196, 146–177. https://doi.org/10.1016/j.isprsjprs.2022.12.021

Zhao, F., Jiang, H., & Liu, Z. (2019). Recent development of automotive LiDAR technology, industry and trends. Eleventh International Conference on Digital Image Processing (ICDIP 2019), 11179, 1132–1139. https://doi.org/10.1117/12.254027

Zhong, H., Li, W., Burris, M. W., Talebpour, A., & Sinha, K. C. (2020). Will autonomous vehicles change auto commuters' value of travel time? Transportation Research Part D: Transport and Environment, 83, 102303. https://doi.org/10.1016/j.trd.2020.102303